Review and Assessment of Current Modeling Techniques in Support of Next-Generation Rollover Research—Phase I

U.S. Department of Transportation
Federal Highway Administration

FOREWORD

This report, *Review and Assessment of Current Modeling Techniques in Support of Next-Generation Rollover Research—Phase I*, provides a comprehensive review of previous research related to rollovers and a plan to support the next generation of rollover modeling, including improved roadway design guidance to mitigate the rollover problem. The plan recommends using multirigid-body vehicle dynamics codes to investigate the influence of key roadway and roadside design variables on rollover probability. The research highlights several notable enhancements to improve the predictive accuracy of outcomes of roadside-encroachment simulations. This report may be useful to researchers and funding agencies interested in performing research to mitigate rollover risk through roadway and roadside design.

<div align="center">

Brian P. Cronin, P.E.
Director, Office of Safety
Research and Development

</div>

Front cover image: © 2016 TTI.

TECHNICAL DOCUMENTATION PAGE

1. Report No. FHWA-HRT-21-045	2. Government Accession No.	3. Recipient's Catalog No.	
4. Title and Subtitle Review and Assessment of Current Modeling Techniques in Support of Next-Generation Rollover Research—Phase I		5. Report Date April 2021	
		6. Performing Organization Code	
7. Author(s) R. Bligh (ORCID: 0000-0001-5699-070X), N. Sheikh (ORCID: 0000-0003-1718-4881), A. Abu-Odeh (ORCID: 0000-0002-1277-1895), and M. Kiani (ORCID: 0000-0001-9123-7895)		8. Performing Organization Report No. Report 607921-1	
9. Performing Organization Name and Address Texas A&M Transportation Institute The Texas A&M University System College Station, TX 77843-3135		10. Work Unit No.	
		11. Contract or Grant No. DTFH61-14-D-00055; TOPR HRDS421016018	
12. Sponsoring Agency Name and Address Office of Safety Research and Development Federal Highway Administration 6300 Georgetown Pike McLean, VA 22101-2296		13. Type of Report and Period Covered Final Report; September 2016–September 2018	
		14. Sponsoring Agency Code HRDS-20	
15. Supplementary Notes Ana Maria Eigen, D.Sc. (ORCID: 0000-0003-4056-361X; HDRS-20), Research Highway Safety Specialist with the Federal Highway Administration (FHWA) Office of Safety Research and Development, was the Task Manager for this research.			

16. Abstract
The overall goal of this research was to develop guidelines that relate different roadway and roadside design variables to rollover risk. Specific objectives included harmonizing FHWA and National Highway Traffic Safety Administration rollover modeling efforts, evaluating potential countermeasures, and mitigating rollover crashes by executing the research plan and implementing the results into new design guidelines. In phase I, the research team conducted an extensive review of past rollover studies and developed a plan for achieving the research objectives. The plan incorporated the selection of preferred modeling methodologies based on the reliability and availability of state-of-the-art modeling technologies. The research team considered the benefits, capabilities, sophistication, and robustness of different technologies versus their cost, including factors such as level of effort and time required. Based on this investigation, the research team developed a proposed simulation matrix for a phase II research effort that will incorporate key roadway and roadside design variables with a particular emphasis on horizontal curvature. The research team recommends several notable enhancements as part of this plan to support the development of a next-generation vehicle dynamics modeling tool that aims to improve the predictive accuracy of outcomes of roadside-encroachment simulations.

17. Key Words Rollover, rollover modeling, rollover mitigation, vehicle dynamics, simulation	18. Distribution Statement No restrictions. This document is available to the public through the National Technical Information Service, Springfield, VA 22161. http://www.ntis.gov		
19. Security Classif. (of this report) Unclassified	20. Security Classif. (of this page) Unclassified	21. No. of Pages 135	22. Price N/A

Form DOT F 1700.7 (8-72)   Reproduction of completed page authorized.

SI* (MODERN METRIC) CONVERSION FACTORS

APPROXIMATE CONVERSIONS TO SI UNITS

Symbol	When You Know	Multiply By	To Find	Symbol
LENGTH				
in	inches	25.4	millimeters	mm
ft	feet	0.305	meters	m
yd	yards	0.914	meters	m
mi	miles	1.61	kilometers	km
AREA				
in^2	square inches	645.2	square millimeters	mm^2
ft^2	square feet	0.093	square meters	m^2
yd^2	square yard	0.836	square meters	m^2
ac	acres	0.405	hectares	ha
mi^2	square miles	2.59	square kilometers	km^2
VOLUME				
fl oz	fluid ounces	29.57	milliliters	mL
gal	gallons	3.785	liters	L
ft^3	cubic feet	0.028	cubic meters	m^3
yd^3	cubic yards	0.765	cubic meters	m^3
NOTE: volumes greater than 1,000 L shall be shown in m^3				
MASS				
oz	ounces	28.35	grams	g
lb	pounds	0.454	kilograms	kg
T	short tons (2,000 lb)	0.907	megagrams (or "metric ton")	Mg (or "t")
TEMPERATURE (exact degrees)				
°F	Fahrenheit	5 (F-32)/9 or (F-32)/1.8	Celsius	°C
ILLUMINATION				
fc	foot-candles	10.76	lux	lx
fl	foot-Lamberts	3.426	candela/m^2	cd/m^2
FORCE and PRESSURE or STRESS				
lbf	poundforce	4.45	newtons	N
lbf/in^2	poundforce per square inch	6.89	kilopascals	kPa

APPROXIMATE CONVERSIONS FROM SI UNITS

Symbol	When You Know	Multiply By	To Find	Symbol
LENGTH				
mm	millimeters	0.039	inches	in
m	meters	3.28	feet	ft
m	meters	1.09	yards	yd
km	kilometers	0.621	miles	mi
AREA				
mm^2	square millimeters	0.0016	square inches	in^2
m^2	square meters	10.764	square feet	ft^2
m^2	square meters	1.195	square yards	yd^2
ha	hectares	2.47	acres	ac
km^2	square kilometers	0.386	square miles	mi^2
VOLUME				
mL	milliliters	0.034	fluid ounces	fl oz
L	liters	0.264	gallons	gal
m^3	cubic meters	35.314	cubic feet	ft^3
m^3	cubic meters	1.307	cubic yards	yd^3
MASS				
g	grams	0.035	ounces	oz
kg	kilograms	2.202	pounds	lb
Mg (or "t")	megagrams (or "metric ton")	1.103	short tons (2,000 lb)	T
TEMPERATURE (exact degrees)				
°C	Celsius	1.8C+32	Fahrenheit	°F
ILLUMINATION				
lx	lux	0.0929	foot-candles	fc
cd/m^2	candela/m2	0.2919	foot-Lamberts	fl
FORCE and PRESSURE or STRESS				
N	newtons	2.225	poundforce	lbf
kPa	kilopascals	0.145	poundforce per square inch	lbf/in^2

*SI is the symbol for International System of Units. Appropriate rounding should be made to comply with Section 4 of ASTM E380. (Revised March 2003)

TABLE OF CONTENTS

LIST OF FIGURES

LIST OF TABLES

LIST OF ACRONYMS

AASHTO	American Association of State Highway and Transportation Officials
ABS	antilock brake system
Adams	Automated Dynamic Analysis of Mechanical Systems
ANOVA	analysis of variance
CCW	counterclockwise
CDS	Crashworthiness Data System
CG	center of gravity
CMC	cross-median crash
CMF	crash modification factor
CW	clockwise
D2R	deformable-to-rigid
EB	empirical Bayes
ESC	electronic stability control
FARS	Fatality Analysis Reporting System
FHE	first harmful event
FHWA	Federal Highway Administration
HVE	Human Vehicle Environment
HVOSM	Highway-Vehicle-Object Simulation Model
MADYMO	Mathematical Dynamic Models
MASH	*Manual for Assessing Safety Hardware*
MC	Monte Carlo
MHE	most harmful event
MVM	million vehicle miles
NASS	National Automotive Sampling System
NCHRP	National Cooperative Highway Research Program
NHTSA	National Highway Traffic Safety Administration
NN	neural network
PC	point of curvature
POD	point of departure
ROR	run-off-road
RSAP	Roadside Safety Analysis Program
SIM	Simulation Interface Manager
SPF	safety performance function
STD	standard deviation
SUV	sport utility vehicle
SVROR	single-vehicle run-off-road

CHAPTER 1. BACKGROUND, OBJECTIVES, AND APPROACH

BACKGROUND

Rollovers are the leading cause of fatalities in single-vehicle run-off-road (SVROR) crashes. Analysis of 6 yr of data from the National Automotive Sampling System (NASS) Crashworthiness Data System (CDS) indicated that 31 percent of SVROR crashes result in a rollover.[1] Approximately 75 percent of these rollover crashes were initiated by vehicles digging into the ground on embankments or in ditches after encroaching onto the roadside.

Several factors influence the probability of rollover, including vehicle type, encroachment speed, driver input during encroachment, and roadway and roadside characteristics. Compared to passenger cars, light trucks (e.g., pickup trucks, sport utility vehicles [SUVs], vans) have higher centers of gravity, making them inherently less stable. Numerous crash data studies have documented that light trucks are overrepresented in rollover crashes. For example, the previously referenced analysis from the NASS CDS indicated that the risk of an SUV rolling over in an SVROR crash on a high-speed roadway is 2.2 times that of a passenger car. Light truck sales currently outpace passenger car sales, accounting for more than 69 percent of all new passenger vehicles sold.[2] Thus, it is important to update roadside safety guidelines and practices to accommodate the current vehicle fleet.

Lack of detailed roadside data in most crash databases limits the usefulness of crash data when investigating the causes and probability of rollovers during roadside encroachments. Even the detailed NASS CDS data lack roadway and roadside data elements such as roadway curvature and grade, shoulder width, and embankment slope. In 1995, Viner analyzed national crash data from the Fatality Analysis Reporting System (FARS) and NASS General Estimates System to define the nature and importance of rollover crashes on slopes, including ditches and embankments.[3] Slope rollovers were identified as the leading cause of run-off-road (ROR) fatalities. Horizontal curves were found to be especially problematic. On rural two-lane roads, about one-third of all slope rollover crashes and one-half of all slope rollover fatalities took place on curves. Viner also found that most vehicles that rolled over on side slopes and ditches were skidding (or nontracking) as they left the roadway.[3]

Glennon et al. compared crashes on rural two-lane highway curved and straight segments.[4] They used crash data analyses, encroachment simulations using the Highway-Vehicle-Object Simulation Model (HVOSM), field studies, and analytical studies to evaluate the safety and operational characteristics of two-lane rural highway curves. Safety on highway curves was found to be influenced by elements of the cross section, such as shoulder width, cross-slope break, embankment slope, and clear zone. Results suggested that different roadside slope and clear-zone width may be needed for highway curves than for highway tangent sections.

Glennon et al. developed an equation to define the maximum recommended roadside foreslope for different degrees of roadway curvature.[4] To maintain the same level of safety provided by a given foreslope on a straight roadway, flatter roadside foreslopes were needed as roadway curvature increased. Additionally, any roadside foreslope was considered unsafe when the roadway curvature was 4 degrees or more.

1

Little information is available on the probability of rollover for different side-slope ratios. According to the *Roadside Design Guide*, roadside foreslopes can be categorized as recoverable, nonrecoverable, or critical.[5] Foreslopes steeper than 3H:1V have historically been considered critical. The *Roadside Design Guide* indicates that such slopes can cause vehicles to roll over and should be flattened or shielded with a barrier if they occur within the clear-zone distance of the roadway.[5] This guidance is largely based on studies conducted in the late 1960s and early 1970s that included a limited number of full-scale embankment tests and computer simulations with passenger cars.

National Cooperative Highway Research Program (NCHRP) Project 17-11 suggested that some roadside slope conditions that have for many years been considered traversable for passenger cars may not be traversable for light trucks (i.e., pickup trucks, SUVs, vans).[6] Results from a comprehensive computer simulation study were weighted with real-world data derived from reconstructed SVROR crashes and used to compute rollover probability as a function of side-slope ratio. Researchers observed a dramatic increase in rollovers and decrease in stable vehicle encroachments between side-slope ratios of 4H:1V and 3H:1V. This effect was much more pronounced for light trucks than for passenger cars.

Because of the high percentage of light trucks in the vehicle fleet and changes in vehicle technology, such as antilock brake systems (ABSs) and electronic stability control (ESC), research is needed to reassess the probability of rollover associated with different roadway and roadside design elements. Proper assessment of rollover probability can inform roadside design and help reduce the number of rollover crashes and associated fatalities.

For decades, researchers have used vehicle dynamics codes such as HVOSM, CarSim®, Automated Dynamic Analysis of Mechanical Systems (Adams), and others in studies sponsored by the Federal Highway Administration (FHWA), NCHRP, and various State agencies.[7–9] These studies involved safety evaluation of various roadway and roadside conditions, including embankments, ditches, driveways, culverts, slope rounding, and clear zones. Most recently, members of the current research team have led NCHRP projects on clear-zone requirements (17-11), safe treatment of roadside ditches (16-05), placement of barriers on roadside and median slopes and ditches (22-22), and traversability of roadside slopes (17-55).[6,10–12] Encroachment simulations using both vehicle dynamics and finite-element codes were a primary tool in these analyses. These studies helped define the state of the knowledge in vehicular behavior (i.e., lateral extent of encroachment, stability, and severity) when traversing various roadside features.

GOAL AND OBJECTIVES

The overarching goal of this research was to develop guidelines that relate different roadway and roadside design variables to rollover risk. There were three stated objectives for accomplishing this goal. The near-term objective was to review previous research and develop a plan to support the next generation of rollover modeling. The mid-term objective was to develop a research plan to harmonize FHWA and National Highway Traffic Safety Administration (NHTSA) rollover modeling and evaluate potential countermeasures. Finally, the long-term objective was to help mitigate rollover crashes by executing the research plan and implementing the results in new design guidelines.

RESEARCH APPROACH

In phase I, the research team conducted an extensive review of past rollover studies and developed a detailed plan for achieving the goals of this research. The plan incorporated selection of preferred modeling methodologies based on the reliability and availability of state-of-the-art modeling technologies. The research team considered the benefits, capabilities, sophistication, and robustness of different technologies versus their cost, including factors such as level of effort and time required. Based on this investigation, the research team developed a proposed simulation matrix for a phase II effort that will focus on implementing the simulation plan developed in phase I. The research team recommends several key enhancements as part of this plan to support the development of a next-generation vehicle dynamics modeling tool that will improve the predictive accuracy of outcomes of roadside-encroachment simulations.

OVERVIEW

Chapters 2 and 3 present an extensive review of key past research efforts on vehicle rollovers and rollover modeling. Chapter 4 summarizes the available simulation analysis methods and discusses their capabilities and limitations. Several key enhancements that promise to significantly improve the ability to model rollover mechanisms associated with roadside encroachments are described in chapter 5. The simulation variable evaluation and selection analyses presented in chapter 6 are used to support the development of a comprehensive simulation matrix to study the influence of various roadway and roadside variables on vehicle rollover possibility. Chapter 7 describes a data analytics approach to support analysis of the proposed massive simulation dataset. Researchers can use this advanced analysis method to perform probabilistic analyses to understand variable sensitivities, trends, and relationships to rollover probability. Finally, chapter 8 provides a summary of key conclusions from the research performed and recommendations for using vehicle dynamics simulation and data analytics in future research to develop roadside design guidance to mitigate rollover probability associated with curved roadway segments.

CHAPTER 2. ASSESSMENT OF PREVIOUS RESEARCH

The first steps of the research plan were recreating and updating the research performed and guidance developed by Glennon et al. related to safety on horizontal curves.[4] Special emphasis was placed on reviewing simulation-based research findings and results that might relate roadway and roadside design elements to rollover probability.

SAFETY AND OPERATIONAL CONSIDERATIONS FOR DESIGN OF RURAL HIGHWAY CURVES

In 1983, Glennon et al. performed a study throughout four States (Florida, Illinois, Ohio, and Texas) to compare crashes on rural two-lane curved and straight segments.[4] Crash analyses, vehicle and driver operation simulations using HVOSM, field studies, and analytical studies were used to evaluate the safety and operational characteristics of two-lane rural highway curves. The Glennon et al. study demonstrated that highway curves have higher crash rates than highway tangents and highway curve design involves the geometry of the curve itself and design of the alignment before the curve. Primary elements of the cross section, such as roadway width, shoulder width, superelevation, and roadside character, were found to influence the safety of highway curves.[4]

Glennon et al. developed recommendations that related the safety of highway curves to 16 operational characteristics of two-lane rural highway curves:[4]

- Maximum lateral acceleration.
- Driver–vehicle curve transition behavior.
- Spiral transitions.
- Tradeoff between highway curve radius and superelevation.
- Tradeoff between highway curve radius and length.
- Driver–vehicle speed behavior.
- Underdesigned highway curves.
- Short highway curves.
- Superelevation runoff.
- Highway grade.
- Roadside slopes.
- Roadside clear zones.
- Roadside safety improvements.
- Pavement irregularities.
- Stopping sight distance.
- Cross-slope break.

The researchers then evaluated the safety of highway curves for a given range of these characteristics as well as the relationships of the characteristics with each other. The research by Glennon et al. indicated that highway curves affect the dynamics of a vehicle given the complexity of vehicle operations on highways.[4]

Simulation Studies by Glennon et al.

One of the initial objectives of the current research was to recreate the modeling and simulation efforts of Glennon et al. related to safety on curves to verify results and determine the current relevance of any specific design guidance.[4] Consequently, particular emphasis was placed on reviewing the simulation studies performed by Glennon et al. during the literature review.

Glennon et al. conducted vehicle dynamics simulations using HVOSM and a midsize vehicle model.[4] As discussed in the following sections, the number of simulations performed was limited, even considering the available technology at the time.

Horizontal Curve Study

Table 1 summarizes the 12 simulation runs performed on unspiraled highway curves with American Association of State Highway and Transportation Officials (AASHTO) superelevation runoff lengths. Lateral vehicle accelerations from the simulations were compared to those predicted from a centripetal force equation to validate the use of HVOSM.

Table 1. HVOSM initial curve validation simulations.

Speed (mph)	Roadway Radius (ft)	Superelevation (%)	Lateral Acceleration (g)*	Tire Friction*	Maximum Lateral Acceleration (g)**	Maximum Tire Friction (g)**	Maximum Driver Discomfort Factor (g)**
20	108	8	0.25	0.17	0.25	0.17	0.20
20	128	4	0.21	0.17	0.20	0.14	0.18
31	230	10	0.26	0.16	0.26	0.17	0.20
31	272	6	0.22	0.16	0.22	0.17	0.20
42	469	8	0.23	0.15	0.23	0.16	0.18
42	574	4	0.19	0.15	0.19	0.16	0.19
52	650	10	0.26	0.16	0.27	0.17	0.21
52	850	6	0.20	0.14	0.20	0.14	0.18
62	1,207	8	0.20	0.12	0.22	0.10	0.15
62	1,529	4	0.16	0.12	0.18	0.12	0.16
73	1,637	10	0.20	0.10	0.20	0.11	0.12
73	2,083	6	0.16	0.10	0.16	0.11	0.13

*Calculated results.
**HVOSM results.
Note: Data from Glennon et al.[4]

After achieving what they considered an acceptable level of validation of the HVOSM vehicle dynamics simulation code, Glennon et al. performed a second series of simulations to evaluate various curve design parameters.[4] Table 2 summarizes the simulations performed to study the sensitivity of vehicle dynamics to various curve and operational factors. The researchers performed 24 simulation runs using 6 different curve geometries to determine the tire friction demand required to negotiate the curves. The researchers performed simulations with the vehicle traveling both at and 12 mph above the design speed. The following variables were investigated:

- Vehicle speed.
- Superelevation runoff length.

- Superelevation runoff distribution.
- Spiral presence.
- Spiral length.
- Downgrade presence.
- Curve length.

Table 2. HVOSM curve design simulations.

Curve Radius (ft)	Maximum Superelevation (%)	Curve Design Speed (mph)	Length of Superelevation Runoff (ft)	Percent of Maximum Superelevation on Tangent	Presence and Length of Spiral	Grade (%)	Test Vehicle Operating Speed (mph)	AASHTO Design Friction	HVOSM Friction
2,461	6	75	200	70	None	0	87	0.092	0.190
2,461	6	75	200	70	None	0	75	0.092	0.150
1,968	10	75	302	70	None	0	87	0.092	0.230
1,968	10	75	302	70	None	0	75	0.092	0.160
1,968	10	75	302	20	None	0	75	0.092	0.190
1,968	10	75	164	70	None	0	75	0.092	0.120
1,345	8	62	216	70	None	0	75	0.116	0.260
1,345	8	62	216	70	None	0	62	0.116	0.170
1,345	8	62	108	70	None	0	62	0.116	0.140
1,345	8	62	216	NA	AASHTO	0	62	0.116	0.100
689	10	50	236	70	None	0	62	0.140	0.390
689	10	50	236	70	None	0	50	0.140	0.240
689	10	50	236	20	None	0	50	0.140	0.260
689	10	50	236	70	None	5	50	0.140	0.240
689	10	50	236	NA	AASHTO	0	50	0.140	0.120
689	10	50	236	70	None	0	50	0.140	0.200
689	10	50	236	20	None	5	62	0.140	0.430
426	8	37	164	70	None	0	50	0.152	0.400
426	8	37	164	70	None	0	37	0.152	0.200
426	8	37	164	70	None	5	37	0.152	0.210
426	8	37	164	NA	AASHTO	0	37	0.152	0.120
164	10	25	164	70	None	0	37	0.164	0.520
164	10	25	164	70	None	0	25	0.164	0.200
164	10	25	164	70	None	5	25	0.164	0.200

NA = not applicable.
Note: Data from Glennon et al.[4]

The researchers drew the following conclusions from the curve runs:

- Tire friction was most sensitive for lower design speed curves.

- An existing highway curve that is underdesigned for the prevailing operating speed could present a severe roadway hazard.

- Shorter superelevation runoff length yielded slightly smaller friction demands because of the higher superelevation in the beginning of the curve.

- Presence of a spiral reduces the friction demand to below the design limit.

- Driver correction was much less dramatic on spirals than on regular curves.

- No difference in friction demand was found between a level curve and a curve on a 5-percent downgrade.

- Shorter curves resulted in lower friction values because the driver spirals in and then directly out without turning sharper than the curve.

The researchers evaluated numerous design variables using only 24 simulation runs. Some variables, such as vertical grade, were evaluated with as few as four simulations. For comparison, some current research analyzes roadway and roadside design variables based on tens and even hundreds of thousands of encroachment simulations.

Moreover, this analysis was related to driver comfort negotiating various curve configurations and not rollover propensity. The study was concerned with evaluating the friction demand required to negotiate a curve and comparing that demand to the AASHTO design guidelines. The simulation analysis did not address mitigating the outcome of a roadside encroachment. Other simulation efforts performed by Glennon et al. related to other roadway and roadside design parameters are described in the following sections.

Cross-Slope Break Analysis

Cross-slope break is defined as the difference between the slope of the pavement and the shoulder. Glennon et al. performed an analysis to determine the effects of cross-slope break on the safety of curved roadway segments and verify the adequacy of the AASHTO requirement.[4] A moderate departure was selected, defined as the vehicle having the ability to steer back to the pavement if the shoulder was wide enough and the cross-slope break and shoulder slope did not cause the vehicle to exceed available skid resistance. The selected design departure path was a circular path with a radius smaller than the curvature of the road and tangent to a concentric arc 1.64 ft inside the outside edge of the shoulder. The driver was assumed to be driving at the highway design speed at the cross-slope break, and then a 0.1-g deceleration was applied.

Researchers selected a skid resistance limit of 0.25 to represent a wet turf shoulder. A lateral acceleration limit of 0.3 was selected for use in the driver discomfort factor, which was calculated using the equation in figure 1.

$$Discomfort\ Factor = - (Lateral\ Acceleration) + 1.0 \times \sin (Roll\ Angle)$$

Figure 1. Equation. Discomfort factor.

A full-width 8.85-ft shoulder with negative cross slopes of 2, 4, and 6 percent was considered in the analysis. The researchers made preliminary runs to study the differences between four-wheel and two-wheel traversals and entry to and exit from the shoulder. Results showed that four-wheel traversals and entry to the cross-slope break produced the highest dynamic responses. Therefore, subsequent HVOSM design simulations included full four-wheel traversals over 4 s of real time. Of the 63 potential variable combinations, only 14 cross-slope configurations were simulated. The results are summarized in table 3.

Researchers drew the following conclusions from the cross-slope break analysis:

- Driver discomfort level mainly increased with the shoulder slope and not the cross-slope break.

- Shoulder slopes should always be the minimum that is consistent with drainage requirements.

- Wet turf shoulders are not safe if they have a negative slope.

- Roadside slopes should be designed flatter than normal on highway curves.

- There is a greater need for guardrails on highway curves because of certain embankment configurations.

- Clear zones on highway curves should be wider than normal.

- Modifying the shoulder cross slope to carry the superelevation across the shoulder may be a worthwhile crash countermeasure.

Critical review of this simulation study determined that these broad-ranging conclusions are not adequately supported. The simulation analysis evaluated four design variables (radius of curvature, superelevation, shoulder slope, and cross-break slope) in 14 simulations that used one vehicle and two encroachment conditions (speed and path radius). The maximum roll angles achieved in the simulations varied from 3.6 to 7.8 degrees. Although the roadside was not explicitly evaluated in these simulations, the results were used to draw general conclusions about roadside slope rate, guardrail need, and clear-zone requirements. Clearly, a more comprehensive evaluation is needed to understand the influence and interaction of roadway and roadside variables on vehicle stability and rollover probability.

Table 3. Cross-slope HVOSM tests.

Speed (mph)	Highway Design Curve Radius (ft)	Path Radius (ft)	Superelevation (%)	Shoulder Slope (%)	Cross-Slope Break (%)	Maximum Discomfort Factor (g)	Maximum Friction Demand (g)	Maximum Roll Angle (°)
75	3,346	1,923	2	−2	4	0.24	0.20	3.6
75	3,346	1,923	2	−6	8	0.30	0.25	6.6
75	2,854	1,722	4	−4	8	0.32	0.27	5.8
75	2,198	1,427	8	−4	12	0.35	0.29	6.0
75	1,968	1,312	10	−2	12	0.37	0.30	5.0
75	1,968	1,312	10	−6	16	0.43	0.36	7.8
62	1,673	1,152	4	−2	6	0.29	0.25	4.2
62	1,673	1,152	4	−6	10	0.35	0.34	7.2
62	1,476	1,043	6	−4	10	0.38	0.31	6.3
62	1,214	886	10	−4	14	0.38	0.31	6.3
50	919	696	4	−4	8	0.31	0.26	5.5
50	853	650	6	−2	8	0.28	0.24	4.0
50	853	650	6	−6	12	0.36	0.30	7.1
50	689	538	10	−4	14	0.41	0.38	6.6

Side-Slope Study

Based on the cross-slope break analysis, a small study was performed to evaluate vehicle stability on roadside slopes. The researchers performed four HVOSM simulation runs to study vehicle dynamic response on 4H:1V and 6H:1V roadside slopes. The objective was to determine whether roadside slope design and embankment guardrail warrants should vary as a function of highway curvature. A −2-percent shoulder slope was modeled in advance of the roadside slope. The roadside was modeled as hard and flat. The results of the encroachment simulations are summarized in table 4.

Table 4. HVOSM roadside slope simulations.

Side-Slope Ratio	Side-Slope Angle (°)	Curve Design Speed (mph)	Curve Radius (ft)	Path Radius (ft)	Maximum Lateral Acceleration on Tires (g)	Maximum Roll Angle (°)
6:1	9.5	50	689	538	0.47	14.5
6:1	9.5	75	1,968	1,312	0.6	15
4:1	14	50	689	538	0.6	19.5
4:1	14	75	1,968	1,312	0.78	20

The researchers drew the following conclusions from the side-slope study:

- For most well-stabilized roadside surfaces, skidding is likely.

- The roll tendencies in combination with tire plowing or side impact produce a high expectation of rollover.

Once again, broad conclusions were drawn from a small set of encroachment simulations. The researchers evaluated each roadside slope with only two simulations. For the 6H:1V slope, the maximum roll angle was 15 degrees. The maximum roll angle for the 4H:1V slope was 20 degrees. It is worth noting that a 6H:1V slope has an angle of 9.5 degrees from horizontal and a 4H:1V slope has an angle of 14 degrees from horizontal. Thus, the maximum roll angles obtained in the side-slope simulations were only 5 to 6 degrees beyond the angle of the actual slope, yet these results were used to conclude that a high expectation of rollover exists on these slopes when tire plowing (which was not modeled) is considered. Clearly, a more comprehensive evaluation is needed to understand the effect of side slope on vehicle stability and rollover probability on both straight and curved roadways.

Passing Maneuver Studies

Glennon et al. performed a simulation study to investigate the effects of cross-slope break at the center or crown of the road on vehicle dynamics.[4] HVOSM was used to simulate two different passenger cars (compact and midsize), and PHASE 4 was used to model a tractor-trailer (empty and loaded).[13] A single-unit truck was modeled in both HVOSM and PHASE 4.

The simulation matrix included 2- and 4-percent cross slopes on each side of the roadway centerline and four different speeds ranging from 50 to 87 mph. A passing maneuver path was

defined for each speed, and a path-following driver model was used. Fourteen simulations were performed, and table 5 summarizes the results of the study.

Table 5. Comparison of speed effects on dynamics of passing maneuvers.

Vehicle Type	Speed (mph)	Cross Slope (%)	Tire Friction Demand (g)	Driver Discomfort (g)	Vehicle Roll Angle (°)
Midsize auto	87	2	0.33	0.36	4.6
Midsize auto	74	2	0.34	0.38	4.9
Midsize auto	62	2	0.28	0.32	4.0
Midsize auto	74	4	0.36	0.40	6.2
Midsize auto	62	4	0.29	0.34	5.2
Midsize auto	50	4	0.22	0.26	4.4
Compact auto	74	2	0.36	0.38	3.7
Compact auto	62	2	0.31	0.34	3.0
Single-unit truck (HVOSM)	74	2	0.23	0.32	6.3
Single-unit truck (PHASE 4)	74	2	0.22	0.31	6.3
Tractor-trailer (empty)	74	2	0.30	0.22	1.8
Tractor-trailer (loaded)	74	2	0.29	0.30	3.3
Tractor-trailer (loaded)	62	2	0.34	0.37	3.8
Tractor-trailer (loaded)	62	4	0.38	0.42	5.3

The researchers drew the following conclusions from this study:

- The passing maneuver on high-speed (>60 mph) two-lane highways is potentially severe regardless of cross slope.

- An increase in cross slope causes a marginal increase in driver discomfort and tire friction demand.

- Higher cross slopes may be permissible on highways with lower design speeds (<50 mph).

- In general, the cross slope should be kept to the minimum consistent with drainage requirements.

The results of this study pertain more to the friction demand required to execute a passing maneuver on a crowned roadway segment than to the effects of cross slope, speed, and vehicle type on vehicle dynamics. These effects were evaluated with a small simulation matrix. Although the study results provide some insight into geometric design related to passing maneuvers across a roadway cross slope, they do not pertain directly to rollover probability.

Pavement/Shoulder Dropoffs

Glennon et al. performed a small simulation study to characterize vehicle dynamics as a vehicle makes a travel lane recovery from a scrubbing condition on a pavement edge or dropoff.[4] HVOSM was modified to include tire sidewall contact, motion resistance due to tire soil sinkage,

an emergency-maneuver driver-control model used to accelerate and decelerate change in the front wheel steer angle, and a variable-torque path-following driver model.

Initial steer angles of 3 and 5 degrees were considered for 2- and 3-inch pavement edge dropoffs, respectively. The researchers used a 0.7-s driver perception/reaction time with a 20-degree/s maximum front wheel steering rate and a 175-degree/s^2 maximum front wheel steering acceleration rate. The driver began to reduce steering rate after 0.3-g lateral acceleration.

Table 6 shows the results of the four simulations performed to investigate the dynamic effects of a vehicle climbing pavement/shoulder edge dropoffs. The researchers concluded that both lateral excursion distance and maximum lateral acceleration increase as speed and dropoff height increase. Although attempting to recover from a scrubbing condition can lead to roadway departure under certain conditions, the results of this small simulation study do not directly relate to vehicle rollover probability from a roadway or roadside design standpoint.

Table 6. Results of HVOSM scrubbing reentry tests.

Run No.	Input: Auto Type	Input: Vehicle Speed (mph)	Input: Dropoff Height (Inch)	Output: Maximum Lateral Excursion (ft)	Output: Maximum Heading Angle (°)	Output: Maximum Lateral Acceleration (g)
1	Midsize	45	3	>30	25	0.8
2	Midsize	45	2	2	15	0.6
3	Midsize	30	2	12.5	11	0.3
4	Compact	45	2	23	17	0.6

Conclusions From Glennon et al.: Operational Characteristics of Two-Lane Rural Highway Curves

Glennon et al. drew several conclusions from their research on the safety and operational characteristics of two-lane rural highway curves.[4] These conclusions, which were based on crash analyses, vehicle and driver operation simulations using HVOSM, field studies, and analytical studies, are summarized in the following sections.

Maximum Lateral Acceleration

When a car is traversing a highway curve, a significant number of driver path radii are less than the highway curve radius, regardless of the car's speed. (This is termed "path overshoot.") Therefore, many drivers traveling at design speed or faster will exceed the lateral tire acceleration implied by the AASHTO design friction factor. Considering the high lateral tire friction generated by the 95th-percentile path at design speed, the effective safety margin is considerably less than that implied by AASHTO criteria.

Driver–Vehicle Curve Transition Behavior

All vehicles effect a spiral path transition when proceeding from tangent to circular curve alignment. This path behavior generally occurs over the full lane width and is centered about the point of curvature (PC). Although the severity or length of spiraling path behavior varies among

drivers, it is independent of vehicle speed. Drivers with more severe spiraling rates tend to produce greater path overshoot and, therefore, higher levels of lateral acceleration.

Spiral Transitions

Adding spiral transitions to the design of highway curves dramatically reduces the severity of path behavior and associated lateral tire acceleration. Because path overshoot increases with the severity of spiraling behavior on unspiraled highway curves, adding a spiral transition to the highway curve lessens both the severity of the spiraling behavior and the amount of path overshoot. These conclusions about the effectiveness of spirals are supported by the HVOSM simulations, which showed a significant reduction in lateral tire acceleration when a spiral transition was added to the highway curve.

Tradeoff Between Highway Curve Radius and Superelevation

A driver control tradeoff exists between highway curve radius and superelevation rate. When comparing two different controlling highway curves with the same design speed, the highway curve with the larger radius and lower superelevation rate provides a slightly greater safety margin against loss of control than the highway curve with the smaller radius and higher superelevation rate.

Tradeoff Between Highway Curve Radius and Length

A safety tradeoff exists between highway curve radius and length. For a given curve radius, the probability of a crash increases with length of highway curve. Conversely, when comparing highway curves of a given length, the probability of a crash decreases as the highway curve radius increases. For any central angle, therefore, the benefit of choosing a larger radius may be partially offset by the disadvantage of a longer curve.

Driver–Vehicle Speed Behavior

Higher speed drivers approaching sharper highway curves do not adjust their open highway speeds to a safe or comfortable speed for the curve until the curve is imminent. Speed reduction begins about 200 to 300 ft before the PC and continues in the initial portion of the curve. Mean speeds reached in the curve are strongly related to highway curvature.

Underdesigned Highway Curves

Existing highway curves that are significantly underdesigned for prevailing highway speeds pose considerable safety problems. Drivers who do not reduce their open highway speeds to the safe speed of an underdesigned highway curve tend to generate high lateral tire accelerations.

Short Highway Curves

The amount of path overshoot on highway curves 300 ft in length is considerably less than that on longer curves. On curves of all lengths, drivers effect a spiral path transition roughly centered about the PC. Drivers do not significantly adjust either the location or the length of their spiral

paths on short curves. Therefore, when traversing short highway curves, most drivers spiral in and out of the curve without generating a large path overshoot.

Superelevation Runoff

Full superelevation should be provided on the curve within 150 ft of the PC, by which point most drivers are tracking their maximum path curvature. This is consistent with the AASHTO design policy for superelevation runoff length and distribution.

Highway Grade

Vehicle dynamics are not sensitive to downgrades as high as 5 percent when traversing highway curves. However, this conclusion does not consider the effect of downgrade on drivers' ability to properly control their speed.

Roadside Slopes

Roadside slope traversals on highway curves are more severe than those on highway tangents. Severity is defined by the effective path angle to the slope, which is a function of highway curvature. More severe traversals lead to both higher vertical accelerations and higher potential for rollover. These results suggest that for comparable safety levels, roadside slopes on highway curves may need to be flatter than those on highway tangents. Also, further investigation on determining variable guardrail warrants for roadside slopes on highway curves is needed.

Roadside Clear Zones

Roadsides on the outside of flat highway curves may require less clear-zone width than highway tangents, and roadsides on the outside of sharp highway curves may require more. The converse is apparently true for roadsides on the inside of highway curves. For comparable safety levels, roadside clear-zone requirements for highway curves may need to differ from requirements for highway tangents.

Roadside Safety Improvements

A limited cost-effectiveness analysis used discriminant analysis results to generate broad effectiveness measures. This analysis indicated that roadside safety measures are the most (and, at some locations, the only) cost-effective means of altering the roadway to reduce crashes at existing high crash highway curves.

Pavement Irregularities

Vehicular control stability on highway curves is sensitive to pavement washboard and short pavement humps.

Stopping Sight Distance

Glennon et al. concluded that AASHTO stopping sight distance requirements are inconsistent when applied to highway curves because of the higher resultant pavement friction demands

created when a vehicle is both cornering and braking. Also, when the sight restriction is a vertical rock cut, wall, or line of trees, truck drivers lose their eye height advantage, which AASHTO policy assumes always compensates for the longer braking distances of trucks.[4]

Cross-Slope Break

When a vehicle is on the outside shoulder of highway curves, the driver's control is sensitive to the shoulder slope and not the cross-slope break (difference between superelevation and shoulder cross slope).

ASSESSMENT OF RESEARCH BY GLENNON ET AL.

The research by Glennon et al. covered a breadth of topics.[4] Most of the simulation-based research dealt with operational and geometric design elements of the roadway, including various horizontal curve design parameters. The simulations primarily addressed friction demand and driver discomfort as a means of assessing the adequacy of the design parameters against AASHTO design criteria.[4] These factors assess the ability of a driver to comfortably and safely negotiate a particular curve configuration. Although this is an important element of roadway design and can certainly be considered an element of highway safety, it does not address causation or mitigation of rollover.

Other simulation efforts performed by Glennon et al. related to the influence of roadway and roadside design parameters on vehicle dynamic response were limited in size and scope.[4] These simulations were based on a single 1971 vehicle model, few roadway and roadside variables and configurations, and extremely limited encroachment conditions. The resulting conclusions were general and not adequately supported. For example, one simulation analysis evaluated four design variables (radius of curvature, superelevation, shoulder slope, and cross-break slope) in only 14 simulations that used only one vehicle model and two encroachment conditions (speed and path radius). The maximum roll angles achieved in the simulations ranged from 3.6 to 7.8 degrees. Although the roadside was not explicitly evaluated in these simulations, the results were used to make broad, general conclusions about roadside slope rate, guardrail need, and clear-zone requirements related to horizontal curves.

In another example, researchers performed only four HVOSM simulation runs to study vehicle dynamic response on 4H:1V and 6H:1V roadside slopes. The maximum roll angles obtained in these side-slope simulations were only 5 to 6 degrees beyond the angle of the actual slope, but these results were used to conclude that a high expectation of rollover exists on these slopes when the roll tendencies are combined with tire plowing (which was not modeled).

Several aspects of the research by Glennon et al. were limited in scope and did not account for many variables that can be considered using current simulation technologies and computational capabilities.[4] Some variables were evaluated with as few as two simulations. For comparison, some current research analyzing roadway and roadside design variables is based on tens and even hundreds of thousands of encroachment simulations.

It became evident that a more comprehensive evaluation of the influence of roadway and roadside variables on vehicle stability and rollover probability on curved roadways is needed. The research team concluded that using currently available state-of-the-art simulation tools and

analysis technologies would enable a far more comprehensive study to be performed that would provide more specific design guidance for a much broader range of design variables. Such a study would offer a better opportunity to achieve a meaningful reduction in rollover crashes than simply recreating and updating the simulations performed by Glennon et al.

Although Glennon et al. used the best tools available at the time, the vehicle dynamics code (HVOSM) and vehicle model (1971 Dodge® Coronet) used in their now three-decades-old research are greatly outdated.[4] Current vehicle dynamics codes have many enhancements that enable them to surpass HVOSM in terms of modeling technology, accuracy, number of degrees of freedom, graphical output, and many others. This is mainly because HVOSM is a public-domain code that is not routinely updated and enhanced like commercial vehicle dynamics codes. An example of one such enhancement is the tire model. The tire model incorporated into HVOSM was a simple radial spring concept. Newer tire models included in state-of-the-art vehicle dynamics codes, such as CarSim, incorporate detailed stiffness articulation and multiple contact segments.[8]

In addition, current vehicle dynamics codes can capture more vehicular characteristics, including enhanced suspension, and can model advanced vehicle technologies, such as ABS and ESC. These improvements permit researchers to perform more realistic encroachment simulations and obtain more accurate vehicle response.

Presently, different vehicle classes can be easily modeled, and a massive number of analyses can be performed in a reasonable amount of time. This massive amount of simulation data can be combined with data analytics to give researchers a powerful tool for conducting tradeoff, sensitivity, and trend studies. The ample data also reduce biases that are inherent when limited data are analyzed.

Consequently, after an in-depth review of the research performed by Glennon et al.,[4] the research team decided to forgo recreating and updating this simulation-based research and instead use some of the findings of Glennon et al. to propose a new simulation methodology based on more current simulation technology and data analytics. As discussed in subsequent chapters of this report, the research team proposes developing relationships between rollover probability and various roadway and roadside design elements using state-of-the-art simulation technology and vehicle models that reflect current vehicle platforms and technologies. These relationships will form the basis for developing design guidance that offers the potential for mitigating rollover probability associated with roadside encroachments.

CHAPTER 3. LITERATURE REVIEW

The research team reviewed domestic and international literature related to vehicle rollovers. The search included literature published after the publication of the research related to highway curves by Glennon et al. in 1985.[4] The literature was searched using Google Scholar, Engineering Village, and Transport Research International Documentation databases for documents concerning the effect of roadway and roadside geometry on rollover crashes.[14–16] A keyword search yielded 136 different research documents. The abstracts of these documents were used to categorize the documents and assess their relevance to research objectives. The research team used the literature with the highest relevance to prepare the following review. Variables influencing rollover initiation and causation, including various roadside, roadway, and vehicle factors, were mined as part of the review process and subsequently considered in formulating a recommended simulation-based approach for developing design guidance to mitigate rollover crashes.

EFFECT OF ROADWAY AND ROADSIDE DESIGN VARIABLES ON ROLLOVER CRASHES

In 1994, Zegeer et al. quantified the effects of lane width, shoulder width, and shoulder type on crashes for various traffic and roadway conditions for rural roads with no more than two lanes with traffic volumes of 2,000 vehicles per day or fewer.[17] Crash data were collected from various State and local databases; a sample of these data that conformed to the desired evaluation conditions was used for analysis. The researchers analyzed data using the covariance method to evaluate crash relationships on these low-volume roads. The following are the major research conclusions of the study:

- Crash rates decreased when roadway width increased. Crash rates dropped from 2.5 crashes/million vehicle miles (MVM) to 1.25 crashes/MVM when the roadway width increased from 20 to 42 ft.

- Crash rates decreased when lane width increased. Crash rates dropped from 2.41 crashes/MVM to 1.57 crashes/MVM when the lane width increased from 10 to 13 ft.

- The effect of shoulder width varied with lane width. When the lane width was 10 ft, the crash rate for shoulders 4-ft wide or less was 2.41 crashes/MVM. For shoulders 5-ft wide or more, the crash rate was 1.43 crashes/MVM. For lane widths of 11 to 12 ft, the crash rate for shoulders 4-ft wide or less was 1.87 crashes/MVM. For shoulders 5-ft wide or more, the crash rate was 1.31 crashes/MVM.

- The percentage of rollover crashes was 13.4 percent for the rural roads that had fewer than 2,000 vehicles per day, whereas the roads with higher volume had a percentage of 6.8 percent.

In 2011, Lord et al. performed an extensive review of crash data from the Texas Department of Transportation to evaluate the factors affecting ROR crashes and determine how to prevent them.[18] They collected and combined information from four different databases to see which

sites had the most frequent crashes and the characteristics of these sites. The data collected were restricted to two-lane, rural, undivided roads. Next, they gathered data from the field to provide more complete information about the sites. Then, regression models were calculated based on the data collected to determine which variables affected crash rates and to what extent. They performed this modeling for all segments and for curves.

After the large-scale crash data analysis, Lord et al. studied several crashes in more detail through police reports.[18] They analyzed the statistics of this dataset to look for contributing factors that may not have been picked up in the databases. The following conclusions were drawn from their study:

- Increasing shoulder width decreased ROR crash rate. Regression models showed a decrease from 1.25 crashes/MVM to 0.2 crashes/MVM when the shoulder width increased from 0.5 to 10 ft.

- Increasing lane width decreased ROR crash rate. Regression models showed a decrease from 1.55 crashes/MVM to 0.4 crashes/MVM when the lane width increased from 10 to 12.25 ft.

- Increasing clear zone decreased ROR crash rate. Regression models showed a decrease from 1.2 crashes/MVM to 0.1 crashes/MVM when the clear zone increased from 16 to 54 ft.

- Increasing side slope increased ROR crash rate. Regression models showed an increase from 0.25 crashes/MVM to 2.0 crashes/MVM when the side-slope rating increased from 1.5 to 3.8 ft.

- Changing the shoulder type from an earth shoulder to a stabilized surfaced shoulder decreased the fatal crash rate from 65 to 2 percent.

Using CarSim to evaluate the effects of median geometry on vehicle crashes, Stine et al. investigated the safety of earth-divided, traversable rural highway medians without longitudinal median barriers by simulating median encroachments for several different vehicle classes, initial speeds, and encroachment angles.[8,19] Seven vehicles, seven initial speeds, seven encroachment angles, three steering inputs, and two braking inputs were considered for each simulated median cross section. The researchers assigned weight factors to the outputs based on the likelihood of each encroachment and the probability of the vehicle appearing on the highway. These weight factors were taken from previous studies and the *Roadside Safety Analysis Program (RSAP)— Engineer's Manual*.[20] The researchers concluded that the shallower sloped medians resulted in fewer rollover scenarios.

In 2012, Peng et al. collected field data on 501 rural two-lane segments in four districts of Texas to investigate the relationship of SVROR crash frequency and severity to roadside features, such as clear-zone distance and side-slope conditions.[21] The researchers first selected the sections of road to study. Next, they drove an instrumented vehicle along those sections of road to collect data about the roadside conditions. After the data were collected, researchers performed both negative binomial regression and multinomial logit regression models and concluded that

increasing shoulder width and lateral clearance and improving side-slope conditions decreased crash frequency and severity.

Sabbaghian et al. used CarSim to evaluate the effects of shoulder width and edge dropoff on vehicle rollover and shoulder crossover.[8,22] A number of shoulder width and dropoff conditions were defined and modeled. The model also included details such as the type of vehicle (an SUV) and driver behavior. The simulations were run, and the location where the vehicle came to a stop was recorded. The study concluded that crash frequency decreased as shoulder width increased. Additionally, crash severity increased in the presence of edge dropoff.

Lee and Mannering performed a statistical analysis using roadside and crash data collected from the Washington State crash database and the Washington State roadway geometric/traffic database.[23] To analyze crash frequency, Poisson, negative binomial, zero-inflated Poisson, and zero-inflated negative binomial models were created and compared to see which model was the best fit to the data. To analyze crash severity, a nested logit model was used. The researchers drew the following conclusions from the study:

- A median width increase of 1 percent caused a 0.526-percent reduction in ROR crash frequencies.

- A vertical curve length increase of 1 percent caused a 0.379-percent reduction in ROR crash frequencies.

- The presence of a cut side slope increased the crash rate by 67.6 percent.

- A clear zone increase of 1 percent caused a 0.055-percent reduction in ROR crash frequencies.

Molan and Kordani used CarSim to investigate the impact of horizontal curve combined with longitudinal grade on safety factors (such as the side friction factor and lateral acceleration) to determine the stability of various vehicles against skidding and rollover.[8,24] The following were the main outcomes of their study:

- The beginning of a horizontal curve was the most dangerous.

- Traction forces affected the side friction of heavy vehicles but had no effect on passenger cars.

- Side friction factor increased as downgrade increased.

- Longitudinal grade had a significant effect on only heavy vehicles; side friction demand increased as the grade decreased.

- Braking significantly increased the side friction demand.

- As vertical grade decreased from 9 to −9 percent, the side friction factor increased by 5 percent.

- As curve radius increased from 134 to 2,730 ft, the side friction factor decreased by 43 percent.

- As vertical grade decreased from 9 to −9 percent, the lateral acceleration increased by 3 percent.

- As curve radius increased from 134 to 2,730 ft, the lateral acceleration decreased by 32 percent.

Hildebrand et al. studied crash data from the New Brunswick enforcement agencies from 1993 to 2003.[25] The data collected included the number and types of vehicles involved, crash severity, nature of each collision, clear zone, speed limit, and traffic volumes. The data were restricted to SVROR crashes, and the clear zone was analyzed categorically rather than numerically. The study showed that 555 SVROR crashes per billion vehicle miles occurred when the clear zone was less than 19.7 ft and 217 crashes per billion vehicle miles occurred when the clear zone was greater than 33 ft. Furthermore, crash rates among the clear-zone categories were not dependent on the posted speed limit.

Gross et al. determined the safety effectiveness of combinations of lane and shoulder width on two-lane, rural, undivided roads for a fixed pavement width.[26] They used a matched case-control study with conditional logistic regression of crash data from several States' databases. The model was created for a general case and a handful of target events. They concluded that for a lane width of 12 ft, the crash rate increased by 84.5 percent when the shoulder width decreased from 6 to 1 ft. Additionally, for a shoulder width of 6 ft, the crash rate decreased by 25.3 percent when the lane width decreased from 12 to 10 ft. Finally, for a shoulder width of 3 ft, the crash rate increased by 1.2 percent when the lane width decreased from 12 to 10 ft.

Hu and Donnell performed an exploratory analysis of the roadway, roadside, environmental, and driver-related factors associated with cross-median crashes (CMCs) and median rollover crash severity outcomes.[27] Data were collected from a database of CMCs and median rollover crashes occurring on rural highways with earth-divided, traversable medians with no barrier in Pennsylvania. Binary logit and multinomial logit models were created to predict the severity outcomes of these types of crashes. The key variables of their study were median foreslope, backslope, and width. The researchers drew the following conclusions from the binary model:

- The probability of being severely injured or killed in a CMC increased by 32.9 percent when the median width was less than 60 ft and the backslope was flatter than 10:1 when compared to steeper backslopes.

- The probability of being severely injured or killed in a CMC increased by 27.3 percent when the median width was greater than 60 ft and the backslope was flatter than 10:1 when compared to steeper backslopes.

- The probability of having a severe CMC outcome increased by 13.8 percent when the foreslope was flatter than 10:1.

The following conclusions were drawn from the multinomial model:

- A median foreslope steeper than 7:1 increased the chances of minor, moderate, and severe injuries by 6.2, 7.4, and 4.3 percent, respectively, in rollover crashes.

- A median backslope steeper than 7:1 decreased the chances of minor and moderate injuries by 1.2 and 0.6 percent, respectively, and increased the probability of severe injuries by 3.0 percent in rollover crashes.

- A road curved to the left decreased the chances of minor and moderate injuries by 1.8 and 0.9 percent, respectively, and increased the probability of severe injuries by 4.6 percent in rollover crashes.

- A median of less than 70 ft increased the chances of minor, moderate, and severe injuries by 1.2, 7.4, and 7.6 percent, respectively, in rollover crashes.

Miaou identified the limitations of the predictive models in the current *Highway Safety Manual*–estimated SVROR crashes for roadside safety analyses and suggested the need for changes and development efforts.[28] The *Highway Safety Manual* assumes that the proportion of certain crash types to total crashes remains constant for the annual average daily traffic.[29] However, this is inconsistent with the data, as shown by the proportion of SVROR crashes. Miaou showed that factors such as speed, vehicle type, and large truck volume were not considered in the *Highway Safety Manual*, and a significant statistical bias is created if some of the interacting variables are left out of the analysis.[28]

SIMULATION-BASED RESEARCH

Chou et al. performed an extensive literature review of test methods that have been used to provide data for development of rollover occupant protection systems, including rollover sensor algorithms, test methodologies, and restraint-system performance.[30] Test methods reviewed were SAE J2114, side-curb trip, corkscrew ramp, critical sliding velocity, deceleration rollover sled, ditch/embankment, soil trip, and various misuse tests. According to the data Chou et al. extracted from the NASS CDS database, rollovers were classified into two main categories: untripped and tripped. The researchers concluded that nearly half of all rollovers are initiated by some kind of vehicle tripping mechanism, such as a tire or wheel digging into the ground, or by the vehicle striking a curb or other obstacle.

Chou et al. reviewed match-based computer-aided engineering tools for rollover simulations.[31] They reviewed both rigid-body- and deformable-body-based (or finite-element-based) models. The rigid-body-based models included Adams, CarSim/TruckSim, and Mathematical Dynamic Models (MADYMO).[7,8,32] The deformable-body-based models required the use of nonlinear crash analysis codes, such as LS-DYNA®.[33] The researchers simulated the SAE J2114 rollover test procedure using both types of models. The following are the findings from the study:

- When a vehicle leaves the ground, its airborne trajectory could be computed by assuming it to be rigid body.

- Most tire models were still incapable of predicting tire debeading or tire blowout.

- No dummy has been developed specifically for rollover testing.

- Test variability could not be easily established because in general practice only a limited number of rollover tests of identical vehicles was available.

- Interaction characteristics were divided into two categories: dummy interaction with interiors and interaction of vehicular structure with the ground.

The following are the conclusions from the study:

- Rigid-body-based MADYMO models were easier to run than finite-element models. They were useful in predicting roll and nonroll conditions for setting up laboratory tests.

- The capability of vehicular dynamics and Adams-like models needs to be extended to cope with highly nonlinear response for rollover crash analysis.

- Finite-element-based models can be continuously improved by correlation with future experimental data.

Shu-ju et al. evaluated the crashworthiness of a 6756-type bus modeled with finite-element simulation using LS-DYNA to analyze the dynamic numerical simulation results.[34] The simulation was validated by comparing its results with data from a full-scale crash test. The bench test was performed to evaluate the superstructure of the bus. A finite-element approach was taken based on ECE R66 for a 6756-type bus, using the LS-DYNA software, and the contact condition was set as single-surface automatic, using Coulomb's formula. The researchers concluded that 40, 30, and 15 percent of the energy absorbed was attributed to deformation of the right-side, top, and left-side walls of the vehicle, respectively. Deformation in the same window decreased from top to bottom, whereas deformation at the same height in different windows decreased from front to back. The periods of collision were plotted at 40, 80, 100, 120, and 160 ms, with 100 ms being the most severe. The simulation result was consistently lower than that of the real experiment because the simulation model was simplified. The simulation was more conservative than the crash test. Thus, if the simulation passed, then the real bus would also pass.

Parent et al. characterized crash, vehicle, and occupant parameters and their influence in a crash parameter sensitivity study.[35] They used Human Vehicle Environment (HVE) and PC-Crash[TM] to predict vehicle dynamics, Adams and MADYMO to predict rollover initiation and occupant response, and LS-DYNA and Pam-Crash to predict deformation in contact interactions, which required enormous computational resources.[7,32] A midsize SUV model developed by the National Crash Analysis Center was used in finite-element simulation, and the model was verified in a range of quasistatic roof crush conditions. After 129 simulations, Parent et al. concluded that drop height was the most important variable in predicting vehicle structural

deformation, kinematic response, roof crush, and vertical acceleration. Other important parameters included roll angle and pitch angle.[35]

Mongiardini et al. used LS-DYNA to identify critical test conditions to reduce the number of experimental tests needed.[36] The simulations were validated by two full-scale experimental crash tests. They concluded that implementation of the initial offset between the roadbed bottom skids and the ground rollers was important in the simulation and had significant influence on the impact force measured by the load cells. The axis around which the vehicle initially rolls needs to be properly defined. The simulation model can be used to test the performance and reliability of the rollover. Dynamic deformation was slightly underpredicted.

In an effort to make the rollover event repeatable, Marur and Namdeo used a deceleration rollover sled to induce rollover.[37] First, a full finite-element model of a pickup truck was simulated normally. A modified version of the truck was also simulated to take advantage of LS-DYNA's deformable-to-rigid (D2R) routine. This routine allows the user to define when certain parts should be deformable and when they should be rigid. Using this routine reduces the computational time of a simulation because rigid-body calculations take much less time than deformable-body calculations. The results of the two models were then compared. A simple box model was used to investigate the effect of the time of the D2R switch on the model results. The study showed that different D2R switching times resulted in different roll angles because of the difference in the elastic energies of the models. The researchers performed an analysis to determine the best time to make the D2R switches and then tested the vehicle model again. The original model took 25.5 h on an 8-CPU high-performance computer. The model with D2R switching took 6.5 h on the same computer (75-percent reduction in computational time).

Linstromberg et al. determined the borderline between roll and nonroll events by providing sensor signals and the requested trigger time for the activation of protection devices using numerical simulations performed with Adams and MADYMO.[7,32] They performed embankment, ramp, and curb-trip rollover tests and concluded that protection is possible in rollover events.[38] However, understanding the differences between human behavior and dummy simulation is required for determining the best possible protection.

Garrott and Heydinger investigated vehicle characteristics that contribute to steering maneuver–induced rollover crashes.[39] They improved predictive accuracy by including vehicle directional response metrics to determine which one (or more) could best predict rollover propensity. The tests included 28 different steering maneuvers (such as slowly increasing maneuvers, J-turn maneuvers, single-sine maneuvers, and reversal maneuvers) for 51 vehicles. Vehicle dynamics analysis, nonlinear simulations designed by Systems Technology Inc., and a statistical analysis system were used. The researchers concluded that vehicle directional response metrics were not good predictors of observed crash rates. The most significant directional response metric was less significant than two environmental metrics and four other vehicle metrics. Static rollover characteristics (static stability factor, tilt table ratio, side pull ratio) correlated with vehicle rollover propensity. Vehicles with a higher probability of single-vehicle crashes tended to be involved in more severe crashes, thus increasing rollover propensity.

Czechowicz and Mavros used multibody simulation and the Magic Formula tire model in combination with design of experiment methodology to improve understanding of rollover

dynamics and identify tire properties affecting vehicle rollover.[40] A Newton–Euler approach in conjunction with a relative kinematics formulation for the inclusion of the effects of constraints was used to generate a high-fidelity vehicle model able to capture complex elastokinematic suspension characteristics. They concluded that road–tire friction, tire camber stiffness, and kinematics and compliance characteristics (e.g., front and rear suspension rate, front roll stiffness, front camber gain, front and rear camber compliance, and rear jacking force) played an important role in rollover propensity.

TIRE–SOIL INTERACTION MODELING

Major improvements in tire–soil interaction modeling approaches have occurred in recent years. Taheri et al. reviewed the most relevant capabilities and limitations of three categories of terramechanic models: empirical models, physics-based models, and semiempirical models.[41] They concluded that empirical models were useful in conditions similar to the test environment with similar tire properties but could not be used for extrapolating. Physics-based models generally had high computational time requirements. Finally, semiempirical models produced high-fidelity results while keeping computational efforts and the number of variables low; thus, they were good candidates for performing vehicle simulations in a multirigid-body simulation environment.

In 2014, Taheri et al. developed a hybrid lumped mass–brush type discretized model with Kelvin–Voigt elements that can be linked with multibody dynamics software packages to simulate vehicle performance on deformable terrains.[42] In the simulation, a tire initially started traveling over the terrain in a straight line. Then the tire continued along a second path perpendicular to the first path. Using the developed model, the drawbar pull coefficient was calculated at four slip ratio values and on three terrain types, which were called soft, medium, and hard soils. They concluded that the drawbar pull coefficients were mainly influenced by the terrain stiffness and shear deformation parameter.

Naranjo et al. performed an experimental study to improve understanding of the interaction between a pneumatic tire and deformable terrain.[43] They concluded that low inflation pressure had the greatest impact on improving the drawbar pull response of the tire. Also, lower inflation pressure achieved the greatest depth in tire sinkage. The experiment attributed increased sinkage depth in the higher slip range to inconsistent soil moisture content. In general, higher normal load, lower inflation pressure, and higher soil compaction improved the tire drawbar pull coefficient (however, higher normal load had a negative impact on tire performance at greater than 60-percent slip). The test setup had the following limitations that make the study not applicable to tripped rollovers:

- It was based on only longitudinal movement of a tire on soil.

- It did not account for lateral forces on tire sidewall due to soil buildup (also known as soil furrowing).

- The soft soil experiment was performed only at low speed and over limited distance.

Day proposed a method based on Bekker's study to implement a soft soil–tire model into vehicle dynamics codes.[44,45] Day's method considered tire sinkage as well as frontal and sidewall forces resulting from sinkage. Day's approach was condition specific and hard coded, which limits its usefulness as a more general model for tripped rollover scenarios.[44]

Fukushima et al. demonstrated the difficulties in soil-trip rollover tests, including proper maintenance of soil under fluctuating humidity and homogeneity of soil in the pool.[46] They proposed using sled test methods to simulate a soil-trip rollover. Sled test methods typically do not use a soil pool to simulate the interaction between a vehicle and the soil. Various sled test methods for curb-trip rollover tests were used to simulate a soil-trip rollover test with a soil pool and results were compared with results of simulations of actual soil-trip rollovers using a soil pool. Sled lateral deceleration, curb depth and tilting, and curb material used in the sled test methods were evaluated using time histories of the vehicle roll angle and roll rate and pressure distribution on the tires. Time histories of the roll angle and roll rate were used to design deployment algorithms. The pressure distribution on the tires indicated the tripping force and its loading position. The researchers concluded that using a sled test method for simulating soil-trip rollover tests is one conceivable way of ensuring repeatability of the test results and protecting the measurement instruments from possible soil damage.

KEY SIMULATION-BASED ROADSIDE ENCROACHMENT STUDIES

The research team thoroughly studied NCHRP reports to gain a better understanding of the current capabilities of simulation packages and identify possible rollover causation factors. The following subsections present key studies.

NCHRP Project 22-21

The objective of NCHRP Project 22-21, "Median Cross-Section Design for Rural Divided Highways," was to develop improved guidelines for designing typical median cross sections (i.e., width, slope, and barrier) on new and existing rural divided highways.[47] A literature review was performed to understand current median design guidelines and review studies on the safety of median designs, State highway agency median safety, and median barrier effectiveness. The researchers performed the following safety analyses (considering roadway and crash data) on rural divided highways:

- Analysis of traversable medians to determine the effects of median cross-section design features and roadway characteristics on vehicle encroachment trajectory and stability.

- Analysis of medians with barriers to develop a methodology for predicting the safety performance of barrier-shielded medians.

The simulation matrix included 2,058 different cases and considered the following variables: roadway cross sections, vehicle parameters, initial parameters, and driver inputs.

The following roadway cross sections were included in the simulation matrix:

- A 60-ft-wide V-shaped median with 1V:6H slopes.
- A 40-ft-wide V-shaped median with 1V:6H slopes.

- A 60-ft-wide V-shaped median with 1V:5H slopes.
- A 60-ft-wide trapezoidal-shaped median with 1V:5H slopes.
- A 60-ft-wide V-shaped median with 1V:10H slopes.

The vehicle parameters were obtained by averaging data (including sprung mass, wheelbase, track width, center of gravity [CG] location, and inertial properties) collected in the 1998 New Car Assessment Program.

The following initial parameters were included in the simulation matrix:

- Initial speed ranged from 5 to 55 mph in 10-mph increments, also including 70 mph.

- Departure angle upon encroachment varied from 2.5 to 32.5 degrees in 5-degree increments.

- All other vehicle states, including roll, pitch, and sideslip, were set to zero.

The following driver inputs were included in the simulation matrix:

- In the first scenario, the driver steers the vehicle to the center of the median.

- In the second scenario, the driver attempts a return to the roadway by steering to the edge of the pavement on the original travel lane shoulder.

- In the third scenario (the no-steer condition), the driver takes their hands completely off the steering wheel.

- Braking was defined as either light braking (5 MPa of pressure at the cylinder) or hard braking (15 MPa), both with an ABS onboard.[1]

A weighting method from the *RSAP Engineer's Manual* was used to better represent the likelihood of each specific encroachment in real-life crash scenarios. The probability of each vehicle class appearing on the highway was extracted from the 2001 National Household Travel Survey.[48] Because no prior study had incorporated the probability of the driver's actions, the steering and braking inputs were weighted evenly across all runs. The following presents the results, their interpretation, and the proposed design guidelines.

---

[1]For ease of understanding, metric units are used; 5 MPa = 725.189 psi and 15 MPa = 2,175.57 psi.

The following are the results regarding median width:

- CMCs decreased with wider medians, whereas rollover crashes generally increased.

- The research results suggested that in general, wider medians should be preferred.

- The crash analysis results indicated that wider medians would generally cause more crashes; however, fewer severe crashes would occur as the median got wider.

The following are the results regarding median slope:

- The vehicle dynamics simulation results indicated an interaction between median slope and median width not evident in the crash analysis results.

- High-severity CMCs were of greatest concern for median widths less than 60 ft and median slopes steeper than 1V:8H.

- The vehicle dynamics simulation results suggested that the likelihood of CMCs does not continue increasing as the median slope becomes flatter than 1V:8H.

- The most favorable median shape from the standpoint of roadside safety was a trapezoidal shape.

The following are the results regarding median barriers:

- The analysis results showed that flexible barriers (i.e., cables), semirigid barriers (i.e., steel guardrail), and rigid barriers (i.e., concrete) can all be cost effective in reducing crashes under appropriate conditions.

- Each of these barrier types reduced the more severe CMCs while increasing less severe hit-fixed-object crashes (including hit-barrier crashes).

The following are the proposed design guidelines based on this project:[47]

- AASHTO's *A Policy on Geometric Design of Highways and Streets*, commonly known as the Green Book, recommends 1V:6H slopes within medians, with 1V:4H slopes considered adequate in some cases.[49] Based on the research results, it was recommended that the Green Book be changed to recommend 1V:8H slopes within medians, with 1V:6H slopes considered adequate in some cases. The researchers also recommended that slopes flatter than 1V:8H be considered near the center of the median, where practical.

- The researchers recommended that the median barrier warrants in the AASHTO *Roadside Design Guide* be changed to recommend that a barrier be considered for median widths up to 60 ft where the median slope is less than 1V:8H.[5]

- The researchers recommended that the crash modification factors (CMFs) for median barriers developed under NCHRP Project 22-21 be considered for inclusion in the AASHTO *Highway Safety Manual*, potentially in conjunction with the safety performance functions (SPFs) for median-related crashes.[29] The researchers considered the developed CMFs suitable for planning roadside design policies that could be applied over many sites or for analyses conducted with a combination of an SPF for median-related crashes and the application of the empirical Bayes (EB) method. They did not consider the CMFs suitable for application to individual sites without use of an SPF and the EB method because individual sites are unlikely to have experienced enough CMCs to make application of the CMFs accurate.

- Cost–benefit analysis suggested that flexible median barriers may be cost effective even at lower traffic volumes than those suggested in AASHTO median barrier warrants.

NCHRP Project 22-22

The objective of NCHRP Project 22-22, "Placement of Traffic Barriers on Roadside and Median Slopes," was to make comprehensive recommendations for the placement of barriers on roadside and median slopes.[11] Researchers performed a literature review to study current crash testing guidelines, current placement of barriers guidelines, and key research studies.

For terrain configurations, the median width was defined as the total width of the ditch (excluding the shoulder of either road) with the following parameters:

- Ditch side slopes of 1V:6H and 1V:8H.
- Ditch widths of 32, 42, 52, and 62 ft.
- Ditch depths of 3, 4, and 6 ft.

The researchers created 15 unique median profiles using CarSim software.[8] The median profiles included both trapezoidal and V-shaped ditches.

To confirm the accuracy of the finite-element models, each selected barrier system underwent a validation procedure. To obtain the override and underride limit for each barrier, the researchers performed simulations with AASHTO *Manual for Assessing Safety Hardware* (MASH) design vehicles (pickup truck or passenger car) impacting the barrier at different heights.[50] The vehicles were raised or lowered in 1-inch increments and evaluated for override or underride. The pickup truck was used to assess override, and the passenger car was used to evaluate underride.

The researchers performed 120 vehicle dynamics runs based on the 15 unique median profiles and MASH vehicle (5,000-lb pickup truck or 2,425-lb passenger car), design speed (49.7 or 62.1 mph), and entrance angle (15 or 25 degrees).

The project report presented the final barrier placement guidelines for each of the studied barrier systems, and the following are the conclusions and recommendations:

- The vehicle trajectory plots from CarSim were more conservative representations of the bumper heights of the vehicles.[8]

- Researchers were unable to perform finite-element analysis to refine the placement on the backslope of the ditch because the vehicle suspension models resulted in unrealistic behavior.

- Crash testing of the barriers at the edge of the placement ranges was recommended to verify the final barrier placement guidelines.

NCHRP Project 22-25

The objective of NCHRP Project 22-25, "Development of Guidance for the Selection, Use, and Maintenance of Cable Barrier Systems," was to develop guidelines for the selection, use, and maintenance of cable barrier systems.[51] A literature review of recent studies, including international studies, relating to cable barrier systems was conducted. Additionally, a questionnaire was designed to acquire information about the use of cable barriers in the States and the guidelines, if any, used in the design and construction process.

Analyses, including finite-element impact simulations, were performed to investigate the effects of several factors and address identified cable barrier issues. The researchers then proposed cable barrier placement guidelines. The following were the investigated factors:

- Cable barrier lateral placement.
- Cable barrier deflection.
- End-anchoring and post-anchoring systems.
- Interconnection with other systems.
- Horizontal curvature.
- Installation costs.
- Cable barrier maintenance.

The proposed cable barrier guidelines included the following sections:

- Lateral barrier placement.
- Cable barrier deflection.
- End anchors and post embedment.
- Interconnection with other systems.
- Cable barrier tolerances.
- Placement along horizontal curves.
- Placement on vertical curves.
- Installation and maintenance costs.

NCHRP Project 17-11

The objective of NCHRP Project 17-11, "Determination of Safe/Cost-Effective Roadside Slopes and Associated Clear Distances," was to determine relationships between recovery-area distance and roadway and roadside features, vehicle factors, encroachment parameters, and traffic conditions for the full range of highway functional classes and design speeds that can be used to establish clear-zone guidelines.[6]

The use of crash data for determining the statistics on the extent of lateral movement of vehicles encroaching onto the roadside is often limited by a vehicle striking a fixed object or rolling over. Therefore, any lateral extent of encroachment distribution derived from crash data is a truncated distribution, and the full effect of side slopes and other variables on the lateral extent of encroachments is only partially observed.

The researchers developed a research approach that combined crash data analyses with computer simulation results to overcome this limitation. Use of computer simulation permitted a detailed analysis of vehicle trajectory and resulting vehicle kinematics for a wide range of variables for which data were not otherwise available. When combined with real-world crash data, the simulation results can be used to develop relationships between various encroachment parameters.

NASS CDS data were clinically reconstructed and analyzed to investigate key encroachment parameters for ROR crashes, including encroachment speed, encroachment angle, vehicle orientation at encroachment (i.e., tracking, nontracking), and driver control input (i.e., steering, braking, or both). The researchers considered NASS CDS crash cases from 1997 to 1999. A total of 559 cases were selected for the study based on an adopted set of criteria. A supplemental data collection effort was planned and executed to obtain desired roadway and roadside characteristics associated with the crash sites.

The weighted crash data were used to develop probability distributions for the key encroachment parameters for nine highway functional classes. The functional classes were defined in terms of roadway type, land use, and posted speed limit. The researchers then segmented the distributions into prescribed value categories to develop probability input matrices to apply to the simulation data.

The computer simulation study was performed using the HVOSM computer simulation program. The variables included were vehicle type, encroachment speed and angle, vehicle orientation, driver input, horizontal curvature, vertical grade, shoulder width, foreslope ratio, foreslope width, ditch width, backslope ratio, backslope width, and tire–terrain friction. A simulation matrix of all possible combinations of these variables would consist of millions of simulations, which was not practical. A selective simulation matrix was prepared by categorizing the variables into two groups: baseline variables and adjustment variables.[52]

The baseline variables were control variables from which a basic set of lateral extent of encroachment relationships could be obtained. The adjustment variables were additional variables evaluated independently with additional simulation runs to provide information on the effects of specific roadway or roadside factors on lateral extent of encroachment or vehicle

stability. For example, the effect of horizontal curvature can be quantified by comparing the lateral extent of encroachment obtained for a curved section of roadway with that for a tangent section of roadway having similar roadside characteristics. The effects of these adjustment variables can be presented as factors that can be applied to a basic set of relationships (i.e., developing numerous sets of relationships is not required).

The following were baseline variables and their selected values:

- Vehicle type (1,800-lb passenger car, 3,000-lb passenger sedan, 4,400-lb pickup truck, and small SUV).

- Encroachment speed (30, 45, 55, and 68 mph).

- Encroachment angle (5, 15, and 25 degrees).

- Driver control response (steering and combined steering and braking).

- Foreslope ratio (flat, 10:1, 6:1, 4:1, and 3:1).

- Roadside coefficient of friction (longitudinal/lateral is 0.5/1.2).

- Vehicle orientation (tracking and nontracking with yaw rate of 15 degree/s).

Under the baseline conditions, the roadway was assumed to be straight and level and the foreslope was assumed to extend indefinitely (i.e., no ditch or backslope).

The researchers analyzed each adjustment variable individually (not in combination with other adjustment variables). Selected values for each adjustment variable were evaluated with the same set of encroachment parameters used for the baseline simulations. This permitted a more direct comparison of the baseline and adjustment variable simulation results and the use of the same probability distributions.

The adjustment variables and their values were the following:

- Horizontal curvature (3, 6, and 9 degrees).
- Vertical grade (3 and 6 percent downgrade; 3 and 6 percent upgrade).
- Shoulder width (2, 6, and 12 ft).
- Ditch foreslope width (13, 26, and 40 ft).
- Ditch width (3 and 10 ft).
- Ditch backslope ratio (6:1, 4:1, and 2.5:1).
- Ditch backslope width (20 and 40 ft).

The ranges used for these variables were generally intended to encompass current design practice for the classes of roadways being investigated.

The magnitude of the simulation effort conducted for this project was unprecedented (>45,000 runs). To establish functional relationships from the discrete simulation data points, the

probability distributions developed from the weighted NASS CDS data were applied to each encroachment parameter to obtain a probability for each value category of that parameter used in the simulation matrix.

The combined probability for a given simulation with a unique set of encroachment conditions was determined by multiplying the individual probabilities assigned to the value of each encroachment parameter. The probability that a vehicle encroaching onto the roadside will have a lateral extent of movement within a specified range is simply the sum of the probabilities of the simulated encroachments that have a maximum extent of lateral movement within that range. In this way, exceedance curves were developed and used to create lateral extent of movement relationships that combine simulation and real-world crash data such that they are a function of multiple encroachment parameters.

Following this procedure, relationships for lateral extent of movement were developed for each functional class in terms of foreslope ratio. For a given functional class and foreslope ratio, the exceedance curves can be used to determine the percentage of encroachments that will exceed a certain lateral distance.

The simulation runs conducted for the adjustment variables were analyzed in the same manner as the baseline runs. The exceedance curves developed for each value of the adjustment variables were compared to those of the baseline simulations to develop adjustment factors. The adjustment factors can be applied to the baseline exceedance curves to account for the effect of an adjustment variable on lateral extent of encroachment.

The researchers also analyzed the simulation results to develop encroachment severity relationships for the different roadway and roadside variables of interest. Such relationships can be used for determining crash costs associated with roadside encroachments. Vehicular resultant accelerations and angular displacements were captured as outputs from the simulations and used to help assess encroachment severity. The simulation results were used to compute rollover probability as a function of side-slope ratio. The injury severity for the rollover encroachments was estimated using 6 yr of NASS CDS data. Nonrollover encroachments were treated separately as a function of maximum resultant vehicle accelerations obtained from the computer simulations.

Recovery-area guidelines were developed for selected highway functional classes based on the data and relationships in this study. Researchers recommended that the future guideline development process include cost-effectiveness procedures or use a cost–benefit analysis program such as RSAP. The lateral extent of encroachment relationships developed in this study can be used to establish clear-zone guidance as a function of recovery distance and side slope. The severity relationships can be used to update crash severity in the RSAP model expressed in terms of injury probability and vehicle stability (i.e., rollover probability).

The approach described in this section for developing guidelines for roadside clear zones is currently being used by members of the NCHRP Project 17-11(2) research team. The research work plan is organized into two phases with a total of 12 tasks. The first phase primarily involves the development of relationships, analysis tools, and data for subsequent use in phase II. Phase II of the project focuses on development of clear recovery-area guidelines.

NCHRP Project 16-05

The objective of NCHRP Project 16-05, "Guidelines for Cost-Effective Safety Treatment of Roadside Ditches," was to develop guidelines for cost-effective treatments of roadside ditches and appurtenances to reduce the severity of ditch crashes.[10] ROR traffic crashes account for almost one-third of the deaths and serious injuries each year on the Nation's highways. In 2007, 41,059 people were killed in motor vehicle crashes; 15,506 of these people (>37 percent) were known to be killed in SVROR crashes.[53] In addition, collisions with fixed objects and noncollisions (e.g., rollovers, which mainly occurred off road) accounted for about 19 percent of all crashes but were responsible for 46 percent of fatal crashes.

ROR crashes occur for various reasons, including the following:

- Driver inattention.
- Excessive speed.
- Driving under the influence of alcohol or drugs.
- Collision avoidance.
- Roadway condition (ice, snow, rain).
- Vehicle component failure.
- Poor visibility.

Inattentive driving, including distracted driving, drowsy driving, or fatigued driving, has been identified as a significant causal factor in crashes of all types.[54] Although inattentive driving is not always identifiable during crash investigations, safety experts consider such behavior to be prevalent among drivers involved in crashes. With the recent trend in cell phone talking and texting while driving, it has been suggested that inattentive driving is as serious a problem as impaired driving (i.e., driving under the influence of alcohol and drugs).[55] Inattentive driving and impaired driving have been, and will continue to be, responsible for a significant number of inadvertent roadside encroachments and thus ROR crashes.

Roadside ditches, built as part of the drainage system, are open-flow areas that generally parallel the highway embankment within the right-of-way. The drainage system should be designed, constructed, and maintained considering both hydraulic function and roadside safety. The following three design options, listed in order of preference, are applicable when considering roadside safety of drainage structures:[5]

- Eliminate nonessential drainage structures.

- Design or modify drainage structures so they are traversable or present minimal hazard to errant vehicles.

- If elimination, relocation, or redesign of drainage structures is impractical, shield structures with a traffic barrier if they are in a vulnerable location.

The AASHTO *Roadside Design Guide* provides some guidance on preferred configurations for ditches.[5] However, this guidance is based on limited testing and simulations conducted in the 1970s. Limited right-of-way often dictates the configuration of ditches, and in many cases the

preferred configurations are not practical. Enclosed drainage systems are expensive and may result in additional requirements for treatment and discharge of the runoff. Other drainage elements, such as culvert ends, inlets, headwalls, and holding basins, may themselves become roadside obstacles. Installing a barrier to shield a ditch reduces the available clear zone, may not always be cost effective, and presents maintenance and operational issues.

Fatal Crashes Involving Ditches

The NCHRP Project 16-05 researchers analyzed crash data to investigate the hazard associated with roadside ditches.[10] Figure 2 shows the number of fatal crashes and fatalities involving vehicles striking ditches as the first harmful event (FHE) from 1994 to 2008. FHE is defined as the first property-damaging or injury-producing event in the crash. These numbers are taken from the FARS of NHTSA. The numbers generally trended up from 1994 to 2006, with slight decreases in the last 2 yr. There were 761 fatal crashes involving 1,324 fatalities in 1994 and 1,198 fatal crashes involving 1,850 fatalities in 2008. Figure 3 shows that the percentage of fatal crashes involving vehicles striking ditches as the FHE has generally increased during the same period, from about 2.1 percent in 1994 to 3.5 percent in 2008.
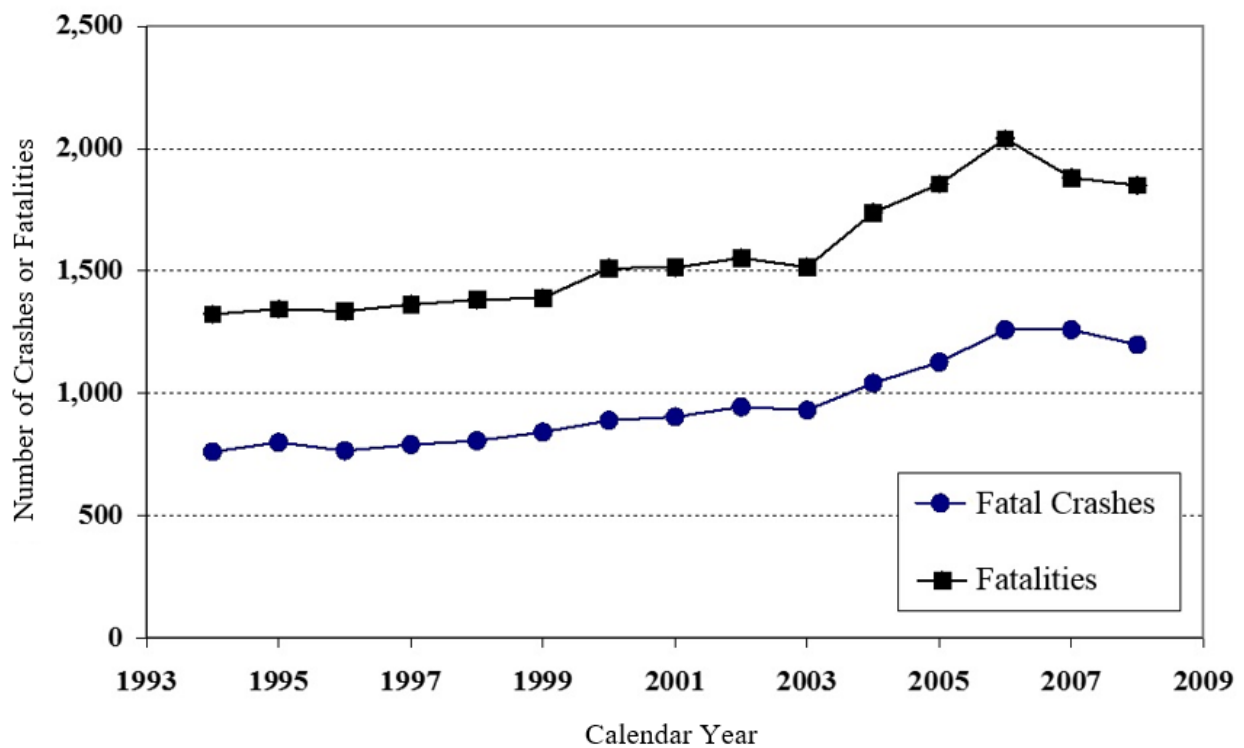
© 2010 TTI.

Figure 2. Graph. Number of fatal crashes and fatalities involving vehicles striking ditches as the FHE using FARS data from 1994 to 2008.

36
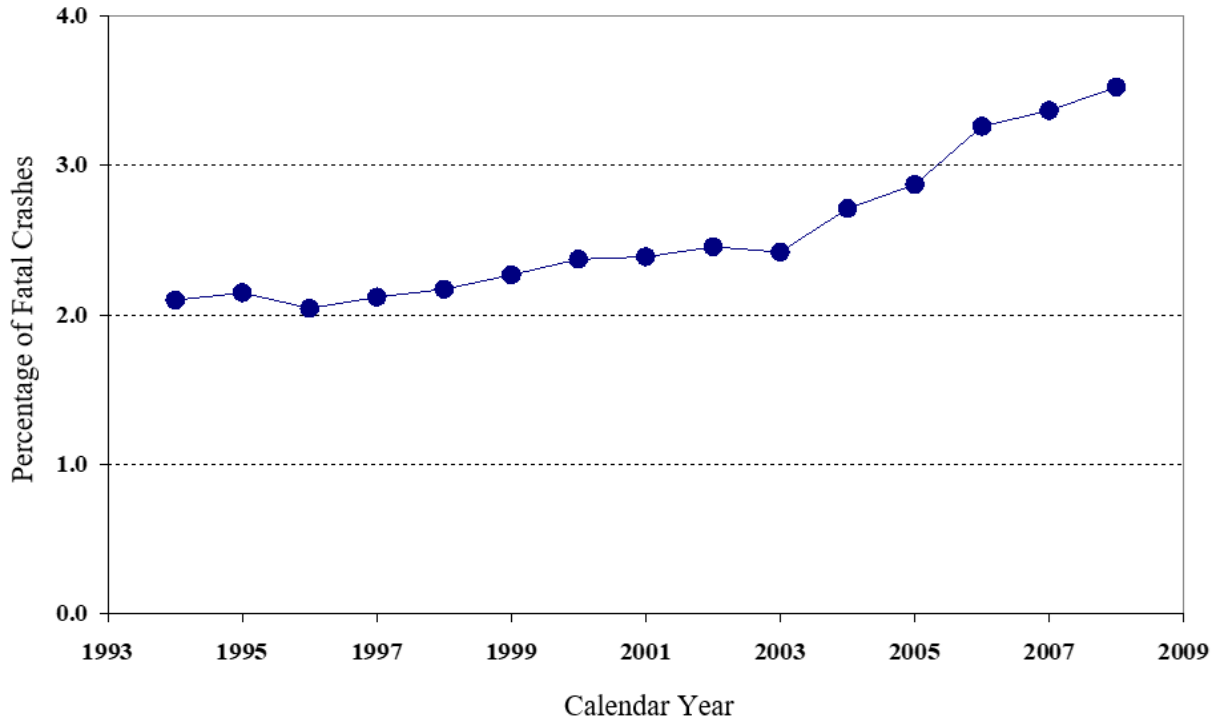
© 2010 TTI.

Figure 3. Graph. Percentage of fatal crashes involving vehicles striking ditches as the FHE using FARS data from 1994 to 2008.

After striking a ditch as the FHE, the most harmful event (MHE) for occupants involved in these fatal crashes is presented in table 7 for 2008. The MHE is the single impact that causes the greatest trauma and damage in each crash. Of the 1,198 fatal crashes that involved striking ditches as the FHE, the MHE in the crash sequence was vehicle rollover in 607 crashes, the ditch in 215 crashes, striking trees in 193 crashes, and striking utility poles in 56 crashes. Therefore, the MHE was vehicle rollover in 51 percent of the crashes, the ditch itself in about 18 percent, striking standing trees in about 16 percent, and striking utility poles in about 5 percent. Table 7 shows that rollover crashes had the most fatalities per crash (1.65 fatalities per crash). Thus, vehicle rollover is by far the deadliest event after a vehicle strikes a ditch as the FHE. Note that crashes involving hitting culverts constitute a small percentage of the MHEs (1.75 percent), which is consistent with the findings of an earlier study by Viner.[3]

Table 7. Distribution of crashes by MHE for fatal crashes involving vehicles striking ditches as the FHE in 2008.

MHE	Number of Crashes	Number of Fatalities	Fatalities per Crash	Percentage of Crashes
Rollover	607	999	1.65	50.67
Ditch	215	274	1.27	17.95
Tree (standing tree only)	193	299	1.55	16.11
Utility pole	56	81	1.45	4.67
Culvert	21	28	1.33	1.75
Fire/explosion	20	32	1.60	1.67
Embankment—material type unknown	10	13	1.30	0.83
Fell from vehicle	8	8	1.00	0.67
Other fixed object	7	11	1.57	0.58
Other post/pole/support	7	8	1.14	0.58
Immersion	7	9	1.29	0.58
Embankment—earth	5	7	1.40	0.42
Embankment—stone/rock/concrete	5	5	1.00	0.42
All others combined	37	76	3.56	3.10
Total	1,198	1,850	1.54	100.00

Note: Data from NHTSA.[56,57]

Vehicle Dynamics Simulations

To evaluate vehicle response related to a combination of ditch parameters, encroachment conditions, and vehicle and driver inputs, NCHRP Project 16-05 researchers performed an extensive matrix of simulation runs.[10]

Table 8 presents the simulation matrix used to perform simulation analyses of vehicles encroaching on roadside ditches with various encroachment conditions, ditch geometries, and other variables important to this research. The variables listed in the matrix were selected based on survey results and analysis of existing crash data while keeping the total number of simulations manageable.

Table 8. Vehicle dynamics simulation matrix.

Variable	Example Conditions
Ditch type/geometry	Foreslope ratio: 10:1, 6:1, 4:1, and 3:1 Foreslope width: 8 and 16 ft Ditch bottom width: 0, 4, and 10 ft Backslope ratio: 10:1, 6:1, 4:1, 3:1, and 2:1 Backslope width: 8 and 16 ft
Shoulder type and width	6-percent cross slope Paved (width: 2 and 6 ft) Paved + turf (width: 12 ft) (5 ft paved and 7 ft turf)
Vehicle type	2,425-lb passenger car 3,300-lb passenger sedan 5,000-lb pickup truck Small SUV
Encroachment speed	45, 55, 65, and 75 mph
Encroachment angle	10, 20, and 30 degrees
Vehicle orientation at encroachment point	Tracking Nontracking with yaw rate of 15 degree/s
Perception/reaction time	Selected based on literature review
Driver control input	Freewheeling Panic return-to-road steering Combined return-to-road steering and full ABS braking
Coefficient of frictions for tire–terrain friction (to represent soft soil conditions and various surface materials)	Selected based on literature review
Main-lane configurations	Straight and level Vertical grade: 4- and 6-percent downgrade Horizontal curvature: 0, 4.5, and 6 degrees
Impact severity and vehicle stability measures	Maximum moving 50-ms acceleration severity index for unrestrained, lap-restrained, and lap- and shoulder-restrained occupants Maximum longitudinal and lateral extent of movements Maximum angular displacements: roll, pitch, and yaw Maximum 50-ms resultant vehicular acceleration Vehicular stability: stable, sideslip, spin out, rollover

Note: Data from Sheikh et al.[10]

Because of the large number of simulation cases, the NCHRP Project 16-05 researchers decided to use the multirigid-body vehicle dynamics code CarSim.[10] During their review of commercially available codes, the researchers found that most of the newer vehicle dynamics codes can be used to build relatively sophisticated vehicle models with detailed suspensions, steering mechanisms, and braking systems. Various roadway or roadside terrain conditions can also be readily modeled to study vehicle maneuvering, handling characteristics, ride quality, and vehicle trajectory during roadside encroachments. However, one limitation of these codes is that they do not have the ability to model the contact between a vehicle's body and the terrain. Chapter 4 of this report discusses this issue and improvements that can be implemented within the codes to enhance predictive accuracy.

NCHRP Project 17-22 Database

The NCHRP Report 16-05 researchers used the database from NCHRP Project 17-22, "Identification of Vehicular Impact Conditions Associated with Serious Ran-Off-Road Crashes," to weight the simulation results.[58] The database contains 890 SVROR crashes that occurred on

highways with a posted speed limit of 45 mph or higher. These cases are a subset of the NASS CDS crashes from 1997 to 2001 (with 16 cases in 2004). The database contains additional supplemental data retrospectively collected for the roadway and roadside under NCHRP Project 17-22, NCHRP Project 17-11, and the FHWA rollover causation study.[2(6,58)]

The NCHRP Project 17-22 database also provides estimates of vehicle roadside encroachment and impact conditions (e.g., encroachment speed and angle distributions at the point of departure [POD]).[58] These conditions were clinically reconstructed using scene diagrams, narratives, photographs of the scene and vehicle, and roadway and roadside data (e.g., surface type, surface condition, and side-slope ratios).

NCHRP Project 17-55

Researchers are currently developing guidelines for traversability of roadside slopes under the ongoing NCHRP Project 17-55, "Guidelines for Slope Traversability."[12] These guidelines are being developed through extensive use of vehicle dynamics simulations. A total of 43,000 simulations were performed for 60 unique roadside slope configurations. These included five foreslopes ranging from relatively flat (1V:10H) to steep (1V:2H). Various foreslope widths were investigated to evaluate the influence of the sudden change in slope when the vehicle reaches the bottom of the slope and interacts with the flat bottom. Furthermore, researchers evaluated 2-, 6-, and 8-ft-wide shoulders.

For each of the 60 configurations, 720 unique vehicle encroachments were simulated. These encroachment conditions included a range of encroachment speeds, angles, driver inputs, and vehicle types. Six speeds (25, 35, … 75 mph), six angles (5, 10, … 30 degrees), and four vehicle types (small passenger car, large passenger car, midsize SUV, and pickup truck) were used in the simulation analyses to evaluate the rollover probability of the simulated terrains.

The NCHRP Project 17-55 researchers developed the guidelines by weighting all of the simulation outcomes according to the probability of their occurrence in the real world.[12] This weighting process enables the guidelines to be representative of real-world crash scenarios. The weighting was performed by determining the probability distributions of the encroachment variables and then applying them to the outcomes of the simulations performed.

Some of the key findings from this research are as follows:

- The 6-and 8-ft shoulders had similar rollover probabilities on the roadside slopes. The 2-ft shoulder had a slightly higher rollover probability than the 6- and 8-ft shoulders.

- For foreslopes steeper than 1V:10H, the probability of rollover increased significantly when foreslope width was increased from 8 to 16 ft. Increasing the foreslope width farther to 32 ft and the presence of an infinite slope without ditch bottom resulted in continuing decreases in rollover probability. This trend highlights the destabilizing effect

---

[2]Miaou, S.-P.E. (2004). *Rollover causation and mitigation study: Phase I report*. Prepared for Federal Highway Administration, Washington, DC.

of the ditch bottom on the vehicle. Sudden change in the terrain's slope as the vehicle goes from a steep foreslope to the flat ditch bottom results in a destabilizing effect. In some cases, the effect of this slope change was more detrimental to vehicle stability than traversing on the foreslope itself.

- The rollover probability increased with the increase in the roadside slope. A significant jump in rollover probability occurred when the foreslope was increased from 1V:3H to 1V:2H.

CHAPTER 4. SIMULATION ANALYSIS METHODS

Researchers have used numerical analysis codes to simulate vehicle handling, vehicle impacts with roadside objects, and encroachments over roadside geometric features, such as slopes, ditches, and driveways. Researchers have also used different levels of model complexity for simulated vehicles, ranging from simple lumped masses to springs and dampers to detailed finite-element models with thousands of elements.

All computer codes and models have limitations and incorporate different levels of assumptions. It was crucial that the codes and models selected for this research be capable of modeling relevant characteristics of the vehicle and terrain, and interactions between them. Vehicle dynamics codes simulate vehicular trajectory given driving conditions, roadway topology, and roadside topology, but they do not model impact events, such as impacts with barriers. Various modeling capabilities should be considered when selecting vehicle dynamics codes. Some important vehicle modeling considerations include the following:

- *Mass and mass distribution.* The inertia of the vehicle and the mass moments of inertia play a major role in the vehicle's behavior because the inertial forces are key factors in any dynamic vehicle maneuver; therefore, they must be accurately quantified and modeled.

- *Suspension system.* The suspension system of the vehicle provides the linkage between the sprung and unsprung mass. It is important to have an accurate representation of the suspension system because it affects the dynamic response of the vehicle to a given maneuver, such as traversing a slope or ditch.

- *Tires.* Tires are the linkage between the vehicle (through the suspension system) and the ground. They are the source of all disturbance forces applied to the vehicle under normal operation (except for aerodynamic forces). Although the functional description of tires is quite simple, the interaction between tires and the road is complex.

- *Steering linkages.* A simulation model must account for the steering of the vehicle to accurately capture the vehicle's motion during the slope traversal. Driver reaction is one of the most significant factors that can affect the likelihood of vehicle rollover during a slope traversal. The code selected for the simulation must have the capability to define driver reaction in terms of steering angle, braking force, and acceleration.

The selected simulation code should be capable of modeling the terrain features of interest, which may include roadway curvature and superelevation, shoulders, and side-slope or ditch configuration. Interaction between the vehicle and the ground, which includes the frictional contact between the tires and terrain features, must also be accurately modeled. Vehicle body contact with terrain can also influence vehicle dynamics for roadside encroachments. Simulation of vehicle-body-to-terrain contact is not crucial while the vehicle is traversing the foreslope. However, when a vehicle encounters a sudden change in slope, such as the bottom of a ditch, vehicle-body-to-terrain contact can be a critical aspect of the vehicle response. The ability of a simulation code to model this contact is useful in evaluating the effect of ditch depth and

backslope ratio on vehicle stability. In this type of analysis, the vehicle will encounter a sudden change in slope at the bottom of the ditch, during which vehicle-body-to-terrain contact is likely to occur.

Available simulation codes capable of modeling vehicle traversals of sloped terrains can be divided into two broad categories:

- Multirigid-body dynamics codes (e.g., CarSim, Adams, HVOSM, HVE).
- Nonlinear finite-element analysis codes (e.g., LS-DYNA, ANSYS, NASTRAN).

These two approaches are evaluated in more detail in the following section.

COMPARISON BETWEEN MULTIRIGID-BODY VEHICLE DYNAMICS CODES AND FINITE-ELEMENT CODES

Computational Time

Generally, finite-element codes require a large amount of computation time to complete a given simulation. A finite-element simulation of a sufficiently detailed vehicle model performing a driving maneuver on a foreslope for 5 s may require a few days of computation. In contrast, a similar simulation performed using a multirigid-body vehicle dynamics code typically completes in less than 5 s. The large number of degrees of freedom involved in finite-element codes like LS-DYNA require a large amount of computation time to simulate the vehicle encroachment event. In a multirigid-body vehicle dynamics code, however, fewer degrees of freedom are used, so vehicle-handling and encroachment events can be accurately captured in a small amount of computation time.

Because of their large number of degrees of freedom, finite-element codes can calculate deformations and stresses in the vehicle or safety device being impacted. This feature is not available in vehicle dynamics codes, so finite-element codes are used in crash simulations and other types of analyses requiring determination of loads and deformations. This research, however, does not require impact analysis. The simulation matrix is expected to be big to account for the many variables needed to determine the trajectory of the vehicle on slopes. Therefore, using a finite-element code like LS-DYNA is impractical because of the time needed to complete each simulation.

Accuracy

Using a finite-element code does not necessarily provide greater accuracy for the types of slope traversal simulations anticipated in this research. Researchers in a previous study compared LS-DYNA and CarSim in simulating the encroachment of a pickup and small car on a 6H:1V foreslope.[59] As shown in figure 4 and figure 5, the trajectory of the vehicles obtained from CarSim closely matched the trajectory of the vehicles obtained from LS-DYNA. A single-core processor needed 0.8 s to simulate each event in CarSim, whereas an 8-core processor needed 2 h to simulate the same event in LS-DYNA. Thus, considering the large number of parametric runs needed to address the variables of interest, using a multirigid-body dynamics code like CarSim can be more efficient.
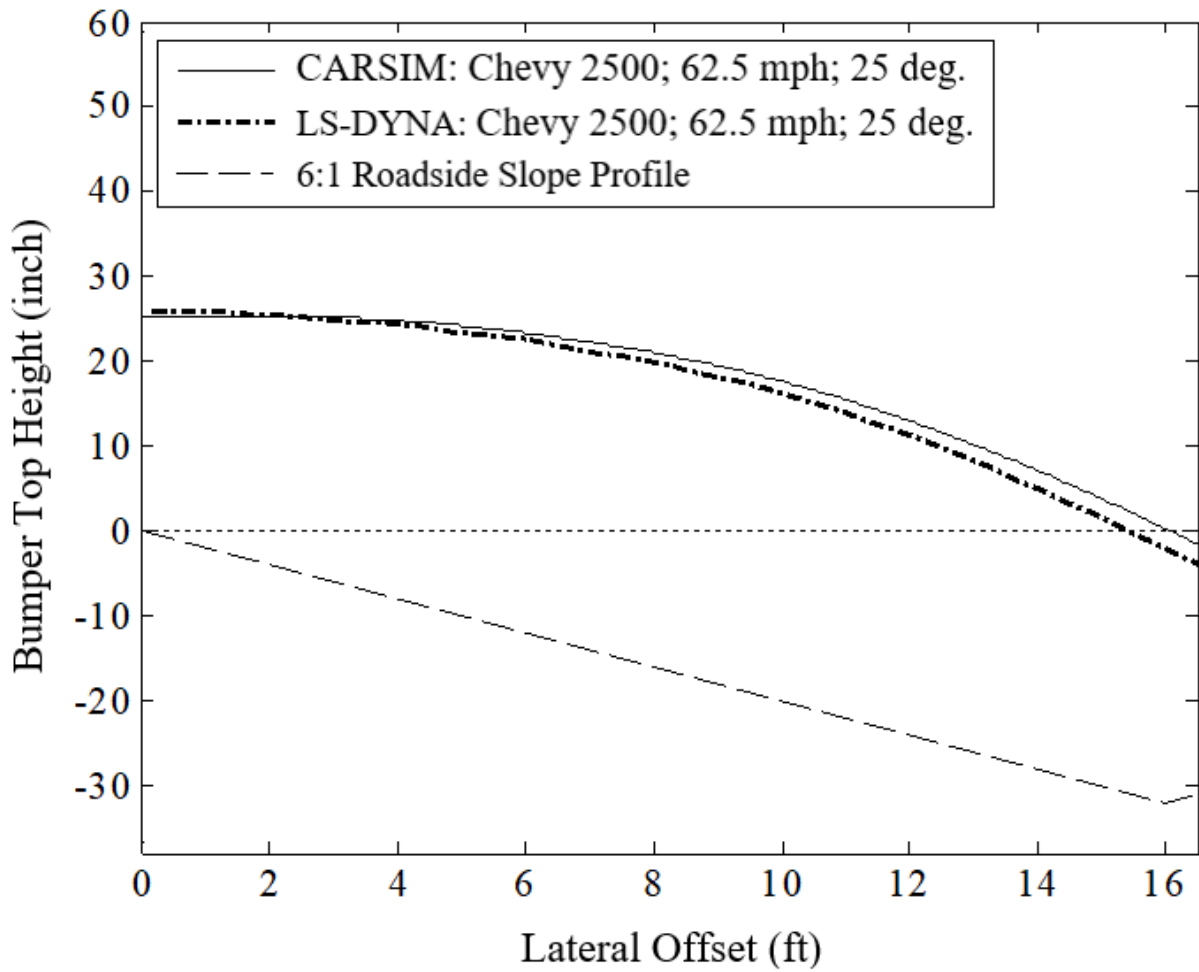
Figure 4. Graph. Comparison of CarSim and LS-DYNA simulating vehicle encroachment events on a slope (pickup truck).[59]
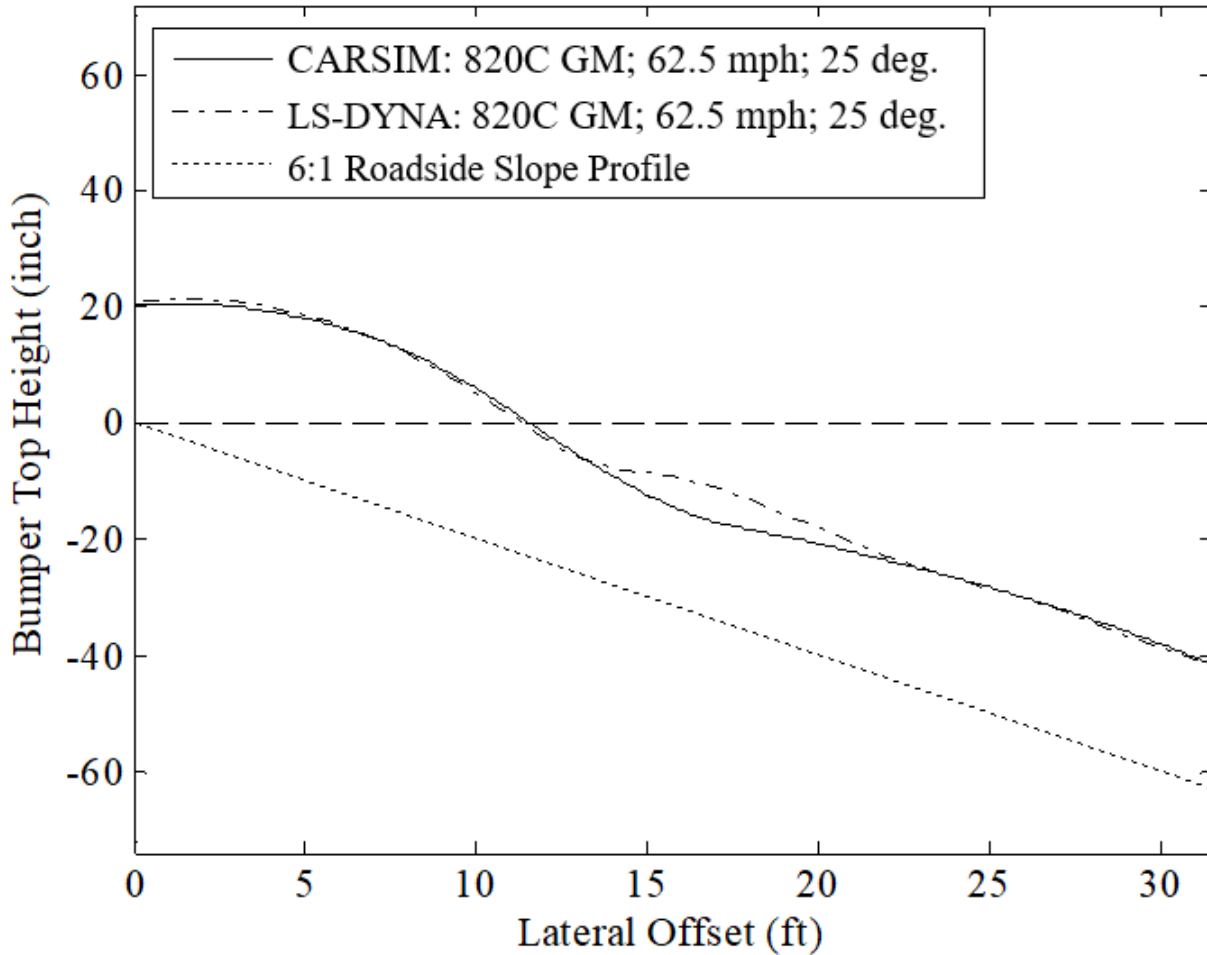
GM = Geo Metros.

Figure 5. Graph. Comparison of CarSim and LS-DYNA simulating vehicle encroachment events on a slope (passenger car).[59]

Vehicle-Model Development

The development of a vehicle model for a finite-element code like LS-DYNA requires significant resources. Currently, few finite-element vehicle models are available in the public domain. The National Crash Analysis Center has developed public-domain finite-element models of both a 5,000-lb pickup truck and a 2,425-lb small passenger car corresponding to the MASH test vehicles. Other public-domain vehicle models exist, such as a minivan and small SUV; however, these vehicle models were usually developed with a focus on frontal impact events, so their validations are limited accordingly. Using these models in a trajectory-type simulation would require enhancing and validating the modeling of steering and suspension linkages and joint, spring, and damper properties.

Conversely, CarSim has about 30 prebuilt vehicle models representing different vehicle classes. In CarSim, geometric dimensions and inertia properties of the existing vehicle models can be

easily modified to represent different vehicle makes and models. Accurate suspension properties can also be incorporated as needed. Thus, using CarSim enables researchers to simulate encroachment events for any representative vehicle type.

Advances in vehicle technology such as ABSs and ESC are incorporated into vehicle dynamics codes, but it is challenging to incorporate them into finite-element models. The effectiveness of the technologies can be readily observed by performing similar vehicle dynamics simulations with and without these technologies active in the simulation.

Although vehicle models in CarSim do not have built-in ESC, detailed ESC models can be added with an external simulation environment, such as Simulink® or LabVIEW. Another method for adding a controller to CarSim's VS math model is through VS commands.[8] Figure 6 shows an overlay of two SUVs making a challenging double-lane change, one with and the other without the ESC controller.
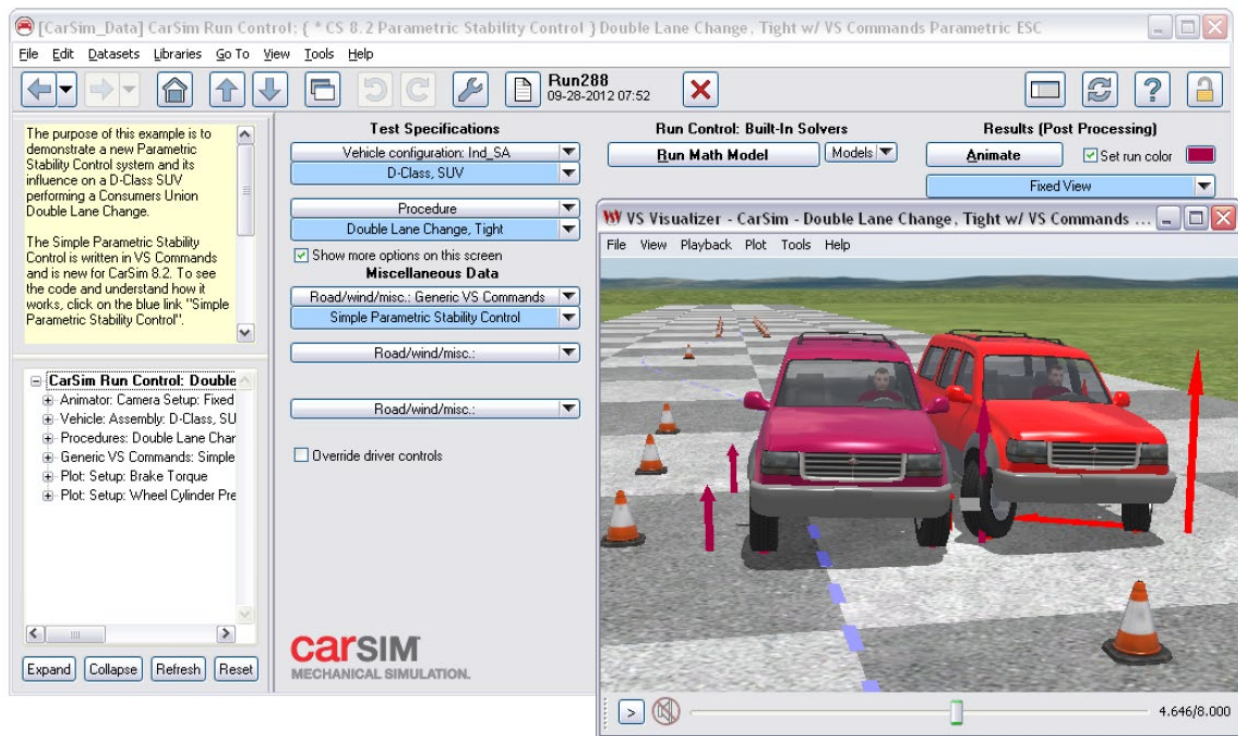
© 2012 Mechanical Simulation Corporation.

Figure 6. Illustration. Double-lane change with and without ESC.[8]

Soil Furrowing

Finite-element and multirigid-body vehicle dynamics codes have different limitations when simulating a soil-tripped rollover resulting from the tires digging into the soil as the vehicle slides laterally. The tire digging and furrowing in soil cannot be modeled explicitly in either of the codes. Although soil can be modeled explicitly in LS-DYNA, it takes a large amount of computation time, and the unavailability of reliable soil properties and limitations on mesh distortion during soil furrowing events make it difficult to accurately capture vehicle behavior.

Recent advances in methods improved the modeling of tire–soil interaction by using particle-based methods to simulate soil dispersion. Researchers typically use a high lateral coefficient of friction for tire-to-terrain contact in both CarSim and LS-DYNA as a simplistic method to represent the tire–soil interaction without expensive model development and validation.

In LS-DYNA, a single coefficient of friction is typically used for the tire–terrain interface in longitudinal and lateral tire motions. CarSim, on the other hand, can be modified to allow the user to define friction formulation with different coefficients in longitudinal and lateral tire motions. This ability allows a higher coefficient of friction in the lateral tire motion to accommodate the forces resulting from soil furrowing. This technique of modeling soil furrowing has been applied in most simulation studies employing vehicle dynamics codes that investigated using soil tripping.

Driver Input

Driver input is one of the most important parameters in rollover studies. Driver response is modeled by varying steering and braking inputs with respect to time. CarSim incorporates steering and braking input with the flexibility to modify them independently or turn off one or both. The current public-domain finite-element vehicle models have defined steering linkages; however, the steering system response has not yet been evaluated and validated. Most of these models have been developed with impact scenarios in mind, where the vehicle impacts an object almost immediately at the start of the simulation. Public-domain finite-element models lack the fidelity in the steering system needed to steer a vehicle on a terrain. Similarly, public-domain finite-element models do not have any braking systems. Although it is possible to apply certain braking inputs using torque load on the wheels, this method is significantly rudimentary for this research. Most vehicles nowadays come with an ABS. Without a well-defined braking model, using finite-element codes like LS-DYNA is not practical for considering driver input. Additionally, CarSim can model ABSs, which can have a dramatic influence on vehicle control and kinematics once brakes are applied in a panic mode.

Vehicle-Body-to-Terrain Contact

Roadside encroachments across a ditch can result in contact between the vehicle body and the terrain. The probability and severity of such contact varies with the steepness of the backslope, ditch depth, and the width of the ditch bottom. If contact between the vehicle body and the terrain occurs during an encroachment event, it can significantly change the dynamics of the vehicle.

Unlike a finite-element code like LS-DYNA, most commercially available vehicle dynamics codes cannot simulate vehicle-body-to-terrain contact. These multirigid-body dynamic analysis codes are capable of modeling only the interaction between the tire and the ground. Among the vehicle dynamics codes, HVOSM has a customized version (HVOSM V3) with a limited capability to model vehicle-body-to-terrain contact. This contact was built into the original version of HVOSM by researchers in a previous study.[9] However, HVOSM is an old public-domain code that has not been updated to incorporate changes in vehicle design features of the current vehicle fleet. In contrast to HVOSM, CarSim vehicle models have an ABS, which

is now a standard feature in the current vehicle fleet and can have dramatic influence on vehicle control and kinematics, as described previously. CarSim also has a library of more advanced tire models compared to the HVOSM tire model. In addition, CarSim has better suspension system models that account for suspension-compliance effects, which are simplified in HVOSM. Furthermore, a major advantage of using CarSim is the availability of a large number of predetermined vehicle parameters and properties representative of the current vehicle fleet. These properties can be used for building new vehicle models without performing component- and subcomponent-level testing.

The ability to develop vehicle models using available and realistic subcomponent properties and datasets in CarSim was considered a major advantage for this project. A key feature lacking in CarSim, compared to HVOSM, is vehicle-body-to-terrain contact. However, researchers have developed a subroutine for vehicle-body-to-terrain contact that can be incorporated into the CarSim package.

CONCLUSION

Based on the factors discussed in this chapter, the research team recommends multirigid-body vehicle dynamics codes (e.g., CarSim) as the simulation tool best suited for vehicle-trajectory studies, including those analyzing roadside encroachments that involve traversing ditches. The key advantages of using multirigid-body vehicle dynamics codes include the ease of developing vehicle models and their subsystems; availability of short-run durations that allow for performing a large number of simulations; availability of new vehicle features, such as ABSs and advanced suspension properties; ability to apply reliable steering and braking inputs; and ability to batch a large number of simulation cases.

CHAPTER 5. SIMULATION ANALYSIS ENHANCEMENTS

This chapter presents some of the key enhancements of standard simulation tools and techniques that can significantly benefit research into rollovers that result from roadside encroachments. These can enhance the scope of variables that can be analyzed and improve the reliability of simulation results for modeling vehicle rollovers on slopes and curves.

VEHICLE-BODY-TO-TERRAIN CONTACT ALGORITHM

When simulating vehicles traversing roadside ditches, the ability to define a contact interface between a vehicle's body and the terrain is important. As the vehicle traverses sloped ditches, its body can come into contact with the terrain because of changing slopes, which can apply significant force to the vehicle and alter its kinematics.

Enhanced Contact Features Available

Most commercial vehicle dynamics codes do not have the ability to define vehicle-body-to-terrain contact. Researchers developed and implemented a vehicle-body-to-terrain contact formulation in the old HVOSM code.[9] More recently, researchers implemented this same contact algorithm as a user-defined module that works with CarSim.[10] The ability to model this contact is considered a significant enhancement to the reliability of vehicle dynamics simulations on slopes. The contact algorithm tracks several user-defined points on the body of the vehicle and determines whether any of those points have penetrated the local terrain. If penetration is detected at a specific point, corrective forces are applied to the vehicle.

For a penetrated point (P) on the vehicle's body (figure 7), the contact algorithm calculates the terrain penetration (d) normal to the terrain. Using d, the vehicle's velocity, and penetrating velocity (PV) direction, the contact subroutine applies a normal friction force ($\mathbf{F_n}$) to remove the penetration. A tangential friction force ($\mathbf{F_f}$) is also applied tangent to the local terrain surface in the direction opposite of PV.
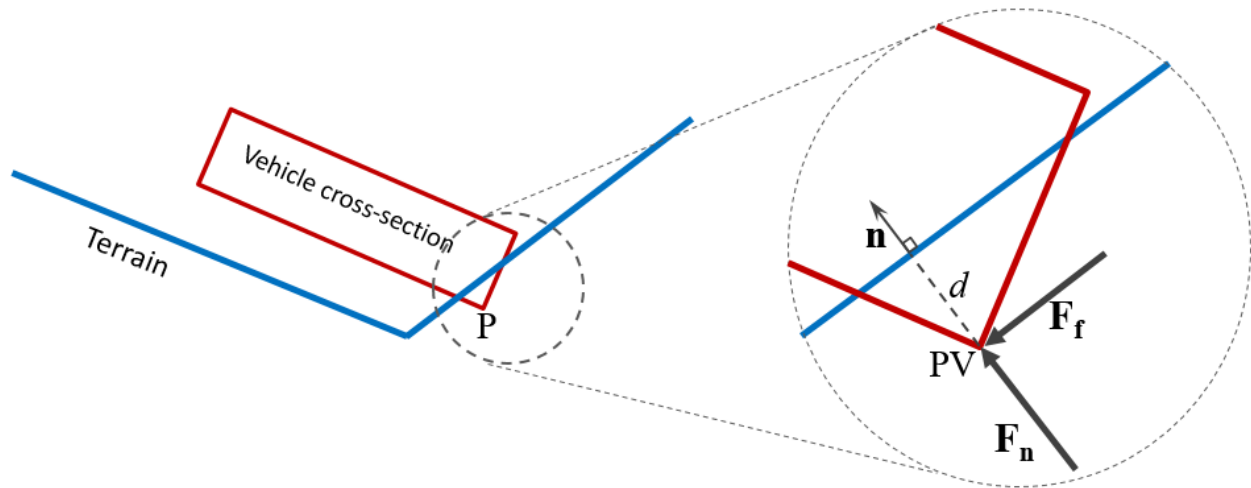
Figure 7. Illustration. Vehicle-body-to-terrain contact forces.

Terrain properties for the contact algorithm for CarSim were kept the same as those used in the HVOSM contact.[60,61] Researchers in the HVOSM study could not fully justify the use of these properties and recommended further evaluation. When implementing the contact algorithm for CarSim, researchers coded the capability to easily alter contact parameters. However, more research is needed to verify whether the currently used properties are suitable for this type of contact, and if not, to determine the appropriate set or range of properties.

Future Enhancement for Vehicle-Body-to-Terrain Contact

Researchers can improve the fidelity of the vehicle-body-to-terrain contact by determining more accurate vehicle-to-ground stiffness parameters. In lieu of full-scale crash testing, these parameters can be determined with reasonable accuracy using finite-element modeling of the vehicle interacting with a terrain at various speeds and angles.

To simplify the simulations, key stiff parts of the vehicle can be isolated from the full vehicle model. Reducing the size of the model in this manner can significantly shorten simulation durations and reduce computational resources needed for each simulation. In the simulations, a terrain comprises a block of soil material with the desired inclination representing a slope. A section of the vehicle is forced into the solid block via a displacement-controlled motion, as shown in figure 8. The contact force is calculated as a function of the prescribed displacement, resulting in the desired spring stiffness for that specific region of the vehicle. This process is repeated for the desired backslope rates and key vehicular stiff regions to determine the overall vehicle-body-to-terrain contact response for the vehicle.
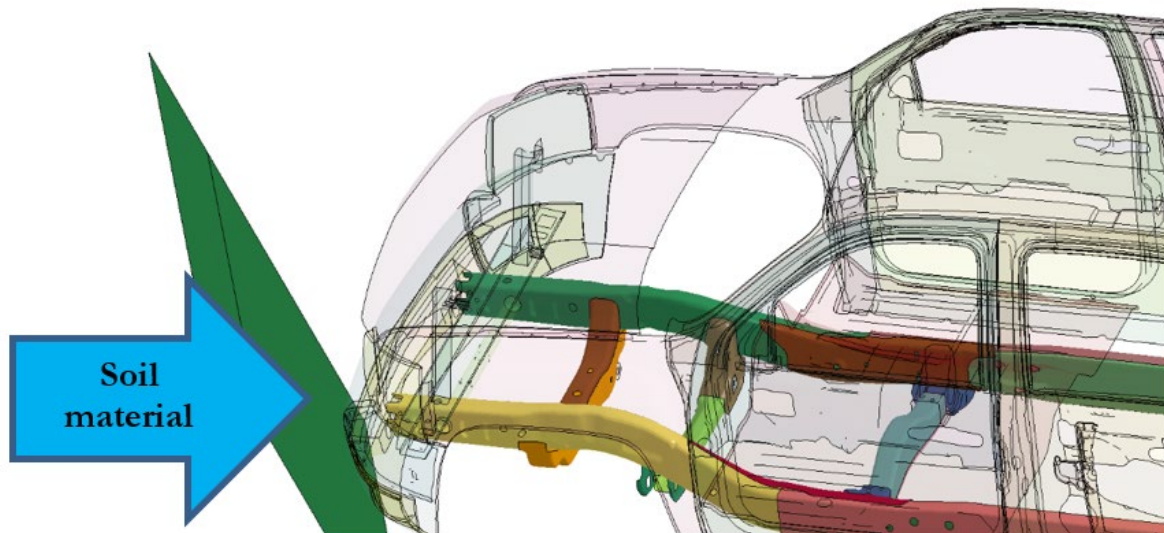
Source: FHWA.

Figure 8. Illustration. Setup of a model pickup truck impacting a slanted wall at an oblique angle.

Once these contact properties are determined, they can be included in a customized contact module for CarSim. To implement these changes, it is necessary to improve the current contact algorithm. The current algorithm uses the same contact force determination method for all the different regions of the vehicle. However, if significant differences exist between the different regions of the vehicle or if the degree of slope must be incorporated into the equation, the contact algorithm must be improved accordingly and the changes must be coded into the contact module. Doing so will significantly enhance the robustness and the validity of the vehicle-body-to-terrain contact, which is one of the key factors in many roadside vehicle encroachments on steep slopes.

SUSPENSION MODELING

Suspensions in vehicle dynamics models are formulated with a combination of springs, dampers, and mass elements. CarSim provides a range of spring and damper properties that can be used to define a vehicle's suspension. For example, when modeling a large sedan, researchers can use spring and damper properties from the software database that represent a large passenger sedan class. Furthermore, researchers can use prebuilt suspension model templates to model different suspension types, such as a MacPherson strut suspension or a twist-beam suspension.

Spring and damper properties play an important role in vehicle handling on a roadway. However, in a previous study, researchers determined that for roadside encroachments, vehicle kinematics are not greatly sensitive to the spring and damper properties of the suspension.[11] As long as these properties represent the general class of the vehicle, the vehicle's kinematics are sufficiently captured. Roadside encroachments impart severe loading on the suspension, resulting in the suspension elements (e.g., springs, dampers) going through their normal operating range quickly. Thus, the benefit of independently measuring a vehicle's spring and damper properties is not that significant for roadside safety applications. Using the default properties from a software's database is sufficient for this current research.

Although spring and damper properties can be used from the vehicle dynamics software's database, the suspension models must be enhanced by determining some key parameters for the vehicles being modeled, such as location of the suspension bump stops, maximum travel ranges of the suspension, and suspension motion ratios.

As mentioned previously, during most roadside encroachments, suspension components are expected to move through their normal roadway operating range. This expectation is because of higher loading from abruptly changing terrain slopes on the roadside or abrupt changes in the vehicle's kinematics. Suspension loading can result in the jounce (i.e., compression) and/or rebound (i.e., expansion) of the suspension, causing the springs and dampers to fully compress or elongate. Because of this behavior, it is critical that bump-stop locations of the suspension are correctly represented in the vehicle model. The location of these bump stops determines the extent of the vertical travel of the suspension. Bump stops typically prevent the compression of the springs and dampers beyond a certain travel limit. In some cases, bump stops may also be present to restrict the rebound of these suspension elements. In other cases, the limit in the jounce or rebound of the suspension may come from structural components that make up the suspension system. As part of enhancing vehicle dynamics models, it is important to determine the locations of the bump stops and maximum distances the suspension can be compressed or expanded.

Another key measurement to include in the vehicle dynamics model is the suspension's motion ratio, which is the ratio of the displacement of the suspension's spring and/or shock to the displacement of a wheel's center. This ratio significantly changes the amount of force transferred to the vehicle's chassis for a given vertical movement of a wheel and can influence the kinematics of the vehicle. Although default values are available in the vehicle dynamics software's vehicle library, this ratio should be measured from the actual vehicle being modeled.

Additionally, various standard measurements, such as the vehicle's mass, tire reactions to ensure proper weight distribution between the front and back of the vehicle, track width, and wheelbase, should be considered for proper suspension loading.

TIRE–SOIL INTERACTION

Soil tripping is a prevalent cause of vehicle rollovers on slopes. Soil-tripped rollovers occur when a vehicle starts to sideslip on soft or wet soil, resulting in the leading tire(s) of the vehicle digging into the soil, which starts building up in front of the tire's lateral motion. The soil buildup results in gradually increasing resistance force on the sideslipping tire. The soil forces are higher than the normal lateral tire forces that result from the vehicle sideslipping on a well-compacted or paved surface. Figure 9 shows the motion of a vehicle in a soil-tripped rollover and the forces applied to the tires because of the soil buildup. The lateral velocity of the vehicle (V_{lat}) decreases and the lateral force from the soil (F_{lat}) increases until a roll is initiated.
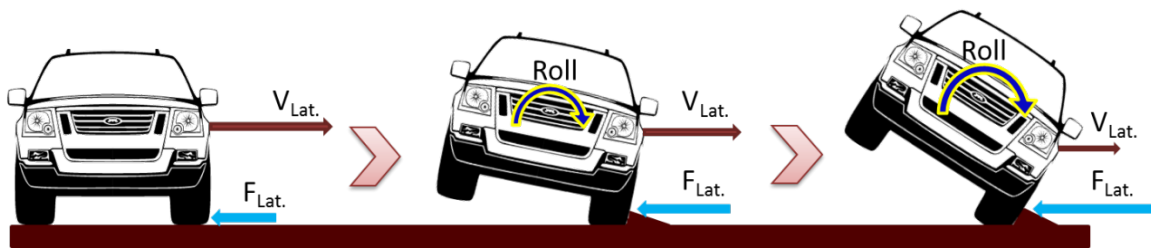
© 2014 TTI.

Figure 9. Illustration. Initiation of a soil-tripped rollover.

Soil-tripped rollovers are dependent on several factors:

- Encroachment characteristics (e.g., vehicle speed, angle of the sideslip, distance the vehicle has sideslipped).

- Vehicle characteristics (e.g., inertia, suspension, tire properties).

- Terrain characteristics (e.g., dry, wet, sandy, grassy, rocky).

As mentioned in chapter 3, vehicle dynamics models do not have the capability to model tires digging and furrowing in soil. Thus, by default, soil-tripped modeling in the vehicle dynamics simulation is not available. However, because soil tripping is the prevalent mode of vehicle rollover on slopes, it is crucial that any simulation tool used in this research be able to reasonably predict soil-tripped rollovers. To simulate soil-tripped rollovers, researchers have used increased terrain friction as a means of incorporating the extra lateral tire forces resulting from the soil buildup. This extra lateral tire force is applied to the vehicle using customized computer subroutines that interact with the vehicle dynamics software during simulation.

Although NCHRP Projects 16-05 and 17-55 have achieved reasonable success modeling soil-tripped rollovers, there are several limitations to the friction-based approach to applying soil furrowing forces. This approach is simplistic in calculating the soil furrowing forces and does not consider several key factors that influence soil-tripped rollovers, such as the speed of the vehicle, duration or distance the vehicle has sideslipped, sideslip angle, size of the vehicle's tires, nature of the soil, and so forth. Improving soil-tripped rollover modeling will significantly enhance the capability of simulation tools to predict rollover during roadside encroachments. The following sections describe the friction-based method for applying soil furrowing forces and how this method can be significantly improved using dynamic testing and finite-element analysis.

Enhanced Tire–Soil Interaction Model in CarSim

The default CarSim tire model determines lateral force on each tire using the vertical load and sideslip angle of the tire. Tire properties include a series of graphs plotting the lateral tire force as a function of the slip angle of the tire for different values of vertical load (figure 10). These plots are generated using properties provided in CarSim's database. The tire properties are determined using a known friction coefficient between the tire and the testing machine's surface. During a

simulation, the absolute lateral friction force from the test plots is adjusted based on the local terrain friction coefficient before being applied to the vehicle.
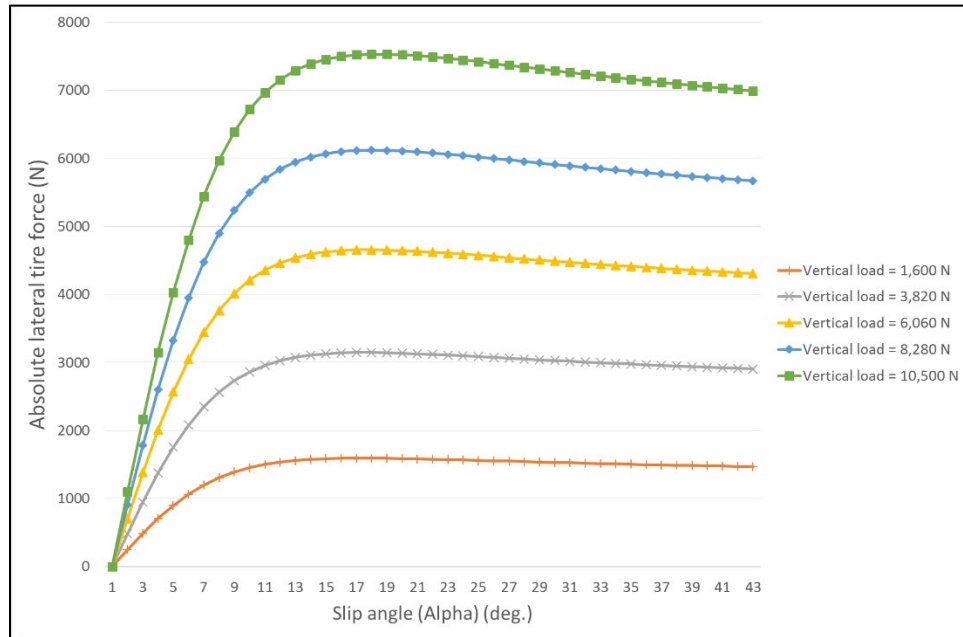
© 2012 TTI.
1 N = 0.2248 lbf.

Figure 10. Graph. Properties of tires in CarSim where the lateral force is plotted as a function of the slip angle for different vertical tire loads.

Although the default method of applying lateral forces to tires is adequate for most roadway surfaces under normal vehicle-handling conditions, this method is not adequate for applying terrain forces resulting from soil furrowing. As previously discussed, an enhancement to the tire–terrain force method is needed to improve predictive accuracy of roadside encroachment simulations. The improved method should be able to apply soil furrowing forces to the tire in addition to terrain friction forces.

Friction Ellipse Model

Researchers have developed approaches that use higher lateral friction forces as a surrogate for applying soil furrowing forces. (See references 10, 12, 52, and 62–64.) These approaches account for prolonged sideslipping of the vehicle when it is not on the roadway and therefore has potential for soil-tripped rollover due to soil furrowing.

Using an increased lateral friction coefficient as a surrogate for soil furrowing in a vehicle dynamics model is somewhat complicated. As the vehicle starts to sideslip on soil, the furrowing forces gradually build up. The amount of lateral force applied on the vehicle due to soil furrowing is a function of many factors, and the relationship between these factors and the vehicle is not completely understood at this time. Among these factors are the properties of the soil (e.g., dry or wet, well compacted or loose), mass distribution and CG of the vehicle, sideslip angle, lateral speed, duration of sideslipping, and distance the vehicle has sideslipped.

Researchers have effectively used increased lateral coefficients to model lateral tire forces due to soil furrowing. A friction ellipse model (figure 11) has been used to determine the lateral friction coefficient (μ_{soil}) as a function of the tire's lateral slip angle (α). At no lateral slip, researchers use the default terrain friction coefficient (μ_{road}), which forms the minor radius of the ellipse. As α increases, a higher μ_{soil} is used such that at a 90-degree slip, the major radius of the ellipse (μ_{limit}) is used, which is the maximum lateral friction coefficient for the terrain.
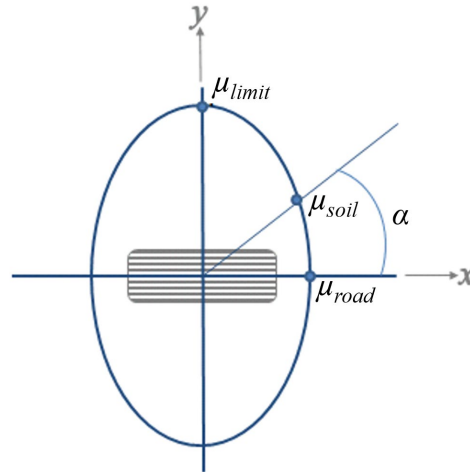
© 2013 TTI.

Figure 11. Illustration. Friction ellipse model for tire forces due to soil furrowing.

Researchers have coded the friction ellipse method into a customized terrain friction calculation module, which interacts with CarSim during run time. The module determines whether the vehicle is traversing a surface that is marked as a soil terrain, and if so, calculates the surrogate terrain friction coefficient (μ_{soil}) using the friction ellipse method and feeds it to CarSim to apply larger lateral tire force. The soil furrowing forces are applied only when the vehicle is traversing a terrain marked by the user as soil. In other words, when the vehicle is on a paved road or shoulder, the default CarSim friction formulation is used because it is more appropriate for the nonsoil terrains.

Limitations of Friction Ellipse Model

Although the friction ellipse model is a good method for applying soil furrowing forces, it has many limitations. As described previously, soil-tripped rollovers occur because of the buildup of soil in front of the tires/wheels as the vehicle slides laterally with a high slip angle. Because this soil buildup is a function of several variables, such as vehicle speed, tire loading, slip angle, and duration or distance the tire remains in sideslip mode, using only a surrogate higher terrain friction is a simplistic approach to modeling soil-tripped rollovers.

Enhancements to Tire–Soil Force Calculation Method

To significantly enhance the capability of modeling soil-tripped rollovers, the research team proposes developing a customized tire–soil force calculation module using results from a series of tire–soil interaction testing and finite-element analyses. This updated module will be based on the true response of the tire furrowing in soil and replace the currently used friction ellipse

model. The objective of the tire–soil response testing and simulation is to determine the soil furrowing forces due to variations in the following:

- Tire slip angle.
- Tire speed.
- Weight on the tire during furrowing.
- Tire size.

In these tests and simulations, tire–soil interaction will be determined by measuring or calculating the lateral and longitudinal forces at the wheel spindle as a function of the distance traveled by the tire on soil.

Using the test and simulation data, the research team will generate force–distance plots for various combinations of tire slip angles, speeds, sizes, and weights. These plots will be coded into the tire–soil force calculation module as lookup tables. A mathematical formulation of soil furrowing forces, which will be based on empirical data from tire–soil testing and further enhanced through use of finite-element analyses, will be used to apply customized soil furrowing forces to the vehicle. During simulation, the tire–soil force calculation module will interact with CarSim at each time step. Whenever the vehicle is traveling on a soil terrain, this module will determine the soil furrowing forces from the force-displacement lookup tables using the tire's instantaneous slip angle, speed, vertical load, and size. The module will also track the distance the tire has sideslipped on the soil so that an appropriate force can be applied from the force–distance plots.

Use of this force calculation method for incorporating soil furrowing forces will be a significant enhancement to rollover modeling on roadside slopes where soil furrowing effects are known to be a prevalent cause of vehicle rollovers.

Figure 12 illustrates the steps for implementing the tire–soil interaction into CarSim. First, the tire–soil interaction experiments will be conducted, and forces at the tire spindle will be recorded via a triaxial load cell. Because performing tests for a large number of tire–soil interaction conditions is cost prohibitive, this testing will be somewhat limited. After performing these tests for a limited number of conditions, the research team will use finite-element analysis to develop a validated model of tire–soil interaction. Using this validated model, the research team will perform further simulations to determine the tire–soil response for a greater number of tire–soil interaction conditions and variables. Finally, the data from the tests and simulations will be used to develop the new empirical model for the tire–soil interaction and will be coded into the force calculation module that interacts with CarSim to apply the soil furrowing forces.
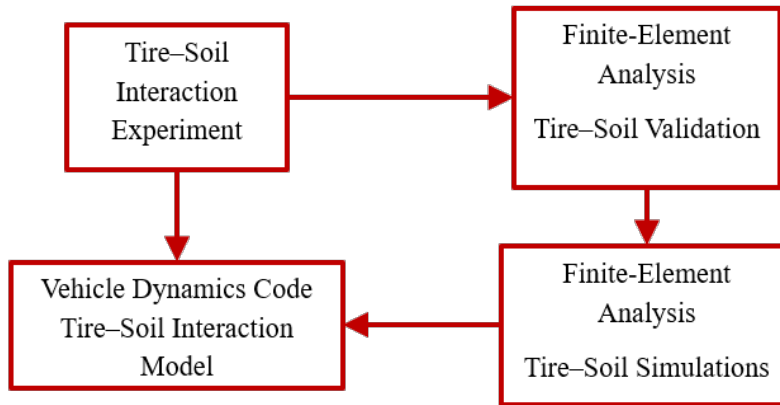
Figure 12. Flowchart. Tire–soil interaction enhancement.

Tire–Soil Test Setup and Parametric Investigation

This section presents a proposed testing method to develop a more generalized tire–soil model that accounts for variables such as soil type, slip angle, speed, tire size, and weight. The output of the experiment will be used to improve rollover prediction when simulating roadside encroachments.

The test setup will consist of a single tire attached to the back of a larger tow vehicle straddling a soil pit under specified conditions. The single tire will be loaded with the appropriate weight and dragged across the soil pit. The tire assembly will be customizable to allow variations in the slip angle and vertical load (i.e., weight) applied to the tire during the test. To get a realistic response of the tire–soil interaction, the tire in the test will be loaded with weights to account for the partial weight of a full vehicle that the tire would be supporting as it sideslipped. The speed of the tire through the soil pit will be controlled by the tow vehicle. As the tire moves through the soil pit at a specified sideslip angle, a triaxial load cell will determine the forces resulting from the tire–soil interaction. The distance traveled through the soil will also be recorded using high-speed cameras. The forces and the distance traveled will be synchronized to allow researchers to cross-plot the forces and distance traveled. This method will result in obtaining the desired force–distance response of the tire on the soil for a variety of slip angles, vehicle speeds, vehicle weights, and tire sizes.

This proposed test method has many advantages. It allows researchers to collect data on the soil furrowing force from a single tire setup instead of using full-scale vehicle tests, which can be cost prohibitive. Furthermore, it isolates the dynamic testing to focus on the tire–soil interaction, allowing researchers to make changes to the desired variables with greater ease and precision. The remainder of this section details the test assembly designed by the research team of phase I.

Figure 13 shows the test assembly, which can be attached behind or to the side of a larger tow vehicle. The figure illustrates the general test setup, mass placement, and pulling direction of the tire. The tire in this figure has been loaded with a 1,300-lb mass, which represents approximately one-quarter of the mass of a pickup truck and can be varied in testing to determine the response

for different vehicle sizes if needed. To ensure zero camber condition for the tire and keep the weights vertical during the test, the research team designed a tire-alignment system, as shown in figure 13 and figure 14.
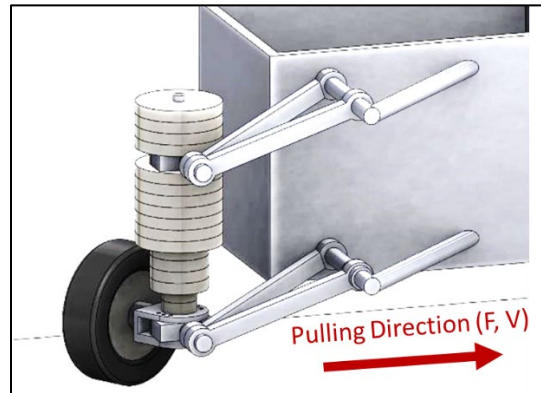
Source: FHWA.

Figure 13. Illustration. Tire–soil test setup.
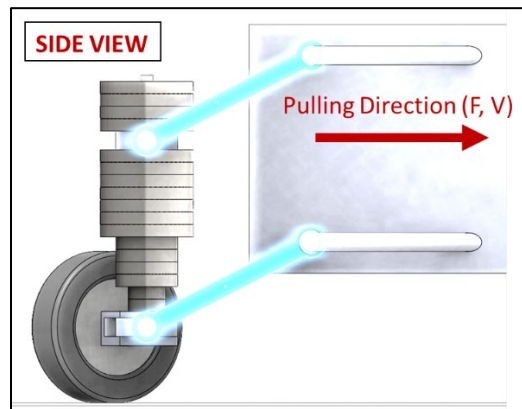
Source: FHWA.

Figure 14. Illustration. Vertical alignment of the mass using the upper and lower control-arm assembly.

Figure 15 through figure 19 illustrate various tire and mass attachment parts and assemblies. The attachment assembly allows slip angle adjustments to the tire ranging from 0 to 90 degrees in 10-degree increments. The 0- and 90-degree angles simulate tracking and nontracking conditions, respectively. The slip angle can be adjusted and locked for each test so that it remains constant during the test.
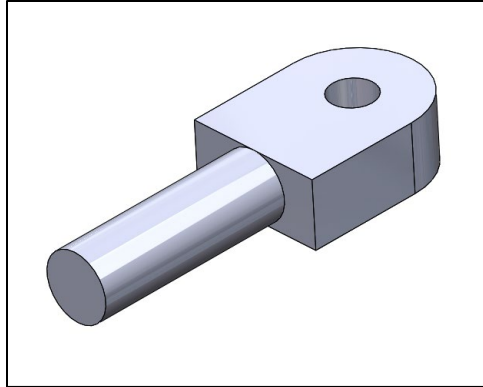
Figure 15. Illustration. Tire and mass attachment part—top of the vertical alignment pivot plate and rod.
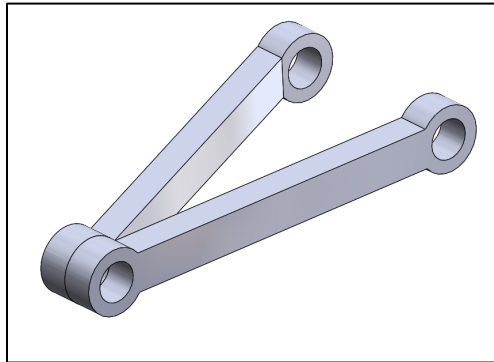
Figure 16. Illustration. Tire and mass attachment part—vertical alignment control arms.
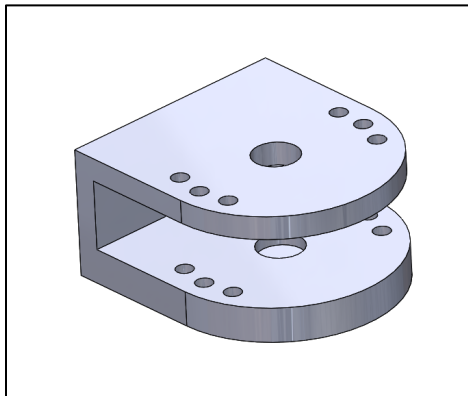
Figure 17. Illustration. Outer part of the slip angle mechanism.
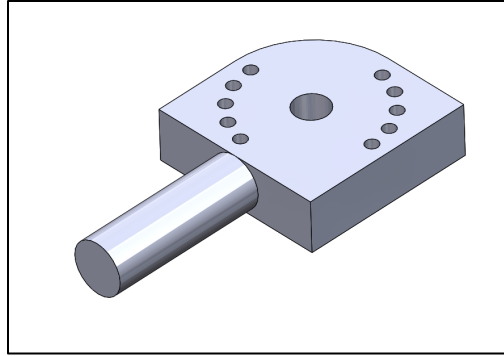
Source: FHWA.

Figure 18. Illustration. Inner part of the slip angle mechanism.
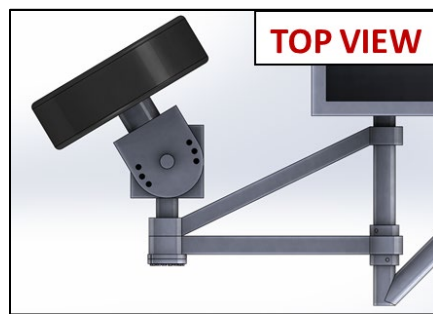
Source: FHWA.

Figure 19. Illustration. Assembly of the slip angle mechanism.

To measure the forces at the wheel's spindle, the research team will use a triaxial load cell between the spindle and wheel. The load cell has the capability to measure forces in the three spatial axes as a function of time. This force–time response is one of the key parameters to record. During each test, high-speed cameras will be placed to record the movement of the tire on the soil. These cameras will be synchronized with the force transducer data, allowing the research team to record the distance–time characteristics for each test. By recording these two responses, the research team will be able to generate the force–distance response of the tire as it furrows on soil.

The research team analyzed the static stability of the setup and developed a simplified finite-element model (figure 20) to evaluate the range of stresses in the tire and mass attachment assembly. The applied mass was 1,300 lb, and steel material was used for the assembly parts. A soil furrowing force of 3,900 lb, which was three times the vertical load on the tire, was conservatively applied to the wheel. Under the applied static loads, the stresses and strains were within the elastic range of the material. The overall test assembly was determined to be stable.
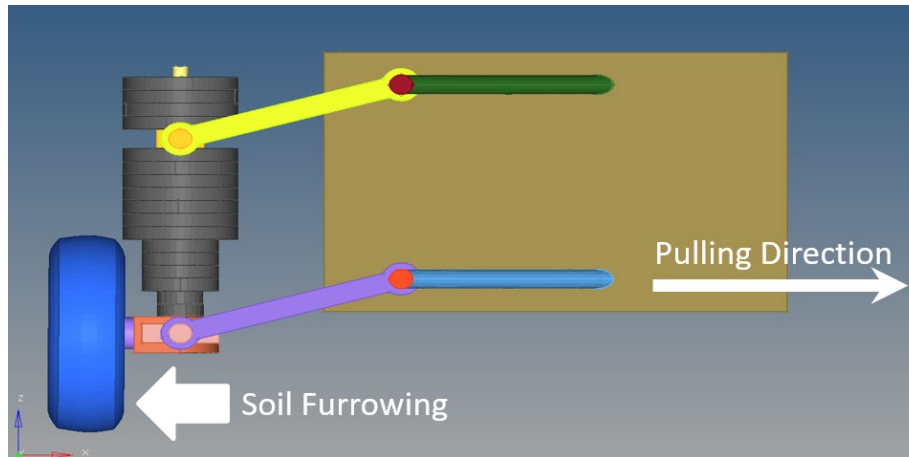
Figure 20. Illustration. Static analysis of the tire–soil test assembly.

For the test soil surface, the research team will construct an approximately 4-ft-wide, 2-ft-deep, and 60-ft-long test pit. The test pit will be backfilled with select engineered fill. On the approach end of the test pit, the research team will place a 20-ft-long steel plate that will be anchored to the concrete pavement surrounding the test pit. The tire test assembly will be slightly raised from the ground so that the test tire does not scrub the pavement as the tow vehicle approaches the test pit. Once the tow vehicle reaches the steel plate, the tire test assembly will be lowered onto the plate. The surface of the plate will be greased to minimize friction between the tire and the steel plate. Sliding the first 20 ft on the steel plate will allow the tire assembly to stabilize before entering the test pit.

The research team proposes performing the testing program with the following test parameters:

- Two tire types: pickup truck and large passenger sedan.
- Two speeds: 55 and 40 mph.
- Four sideslip angles: 90, 70, 50, and 30 degrees.

These 16 tests cover a broad range of vehicle sideslip conditions, and the data collected from these tests will be used to develop validated finite-element models of the tire–soil interaction. These validated simulation models will then be used to simulate additional combinations of vehicle speeds and sideslip angles, thus providing more data for use in developing the tire–soil force calculation algorithm for applying soil furrowing forces in the vehicle dynamics simulations.

To reduce cost and increase the number of tests that can be performed each day, the research team will construct two parallel soil pits. While the soil in one of the pits is being reset after a test, another test can be performed in the second pit. The budget for this task covers 3 d of testing, in which it is expected that the desired 16 tests can be performed.

Tire–Soil Interaction Simulation

To increase the range of variables for which the behavior of tire–soil interaction can be determined, the research team proposes supplementing the test data with data generated using detailed finite-element simulations. The research team will develop finite-element models of tire–soil interaction similar to the test setup. The models will be validated using the parameters and responses from testing. Once validated, the models will be used to conduct simulations of more variations of the parameters being investigated. This validation will generate additional data that can be used for developing the tire–soil force calculation algorithm to apply soil furrowing forces in the vehicle dynamics simulations.

Current tire models in public-domain vehicle models do not have the fidelity needed to simulate tire–soil interaction with reasonable accuracy. Therefore, the research team will enhance these tire models to accurately capture the interaction. The research team has developed a high-fidelity light pickup truck tire model using geometric scanning and material testing of the actual tire and calibrated the model using an FMVSS 139 plunger and bead unseating tests. Figure 21 shows the pickup truck tire and its corresponding finite-element model. Figure 22 shows one of the validation exercises of the tire model using an FMVSS 139 plunger test and simulation.[65]

© 2017 TTI.

Figure 21. Illustration. Dueler H/T 684 III tire and corresponding finite-element model.[65]
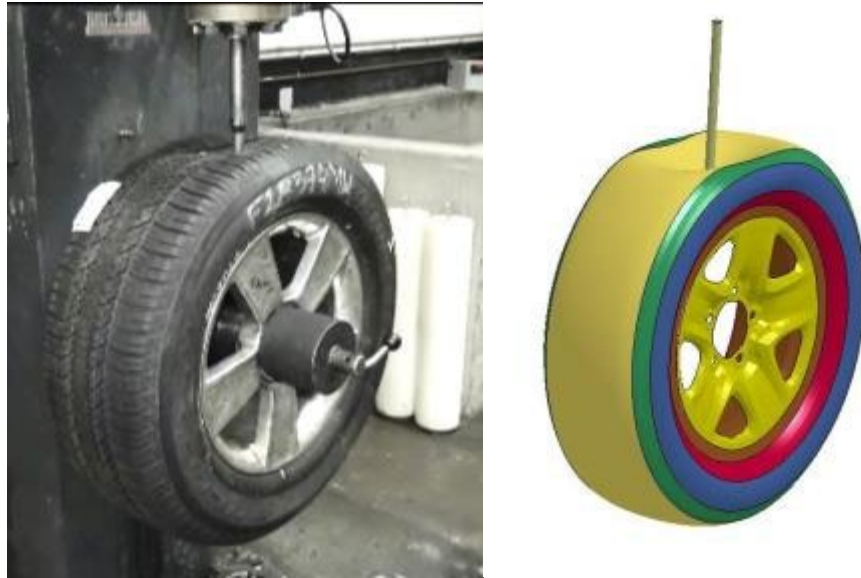
Figure 22. Illustration. Comparison of the experiment and simulation of the plunger test of the tire.[65]

Once the tire models have been enhanced to have sufficient fidelity, the research team will simulate the tire–soil interaction test. The results of the experimental tire tests will be used to develop a validated model of the tire–soil interaction for a particular tire. Once the model has been validated, the research team will simulate additional cases of tire–soil interaction for which a test response is not available. These additional simulations will enhance the response range of the forces and moments at the wheel spindle for additional tire–soil interaction parameters. Figure 23 shows a sample simulation of the tire interacting with soil. In this case, the tire is dragged through a soil block using the prescribed motion with a 90-degree sideslip. This simulation uses the current high-fidelity tire model and the discrete spheres modeling technique to represent the soil in the finite-element simulation. The simulations performed in phase II will be similar.
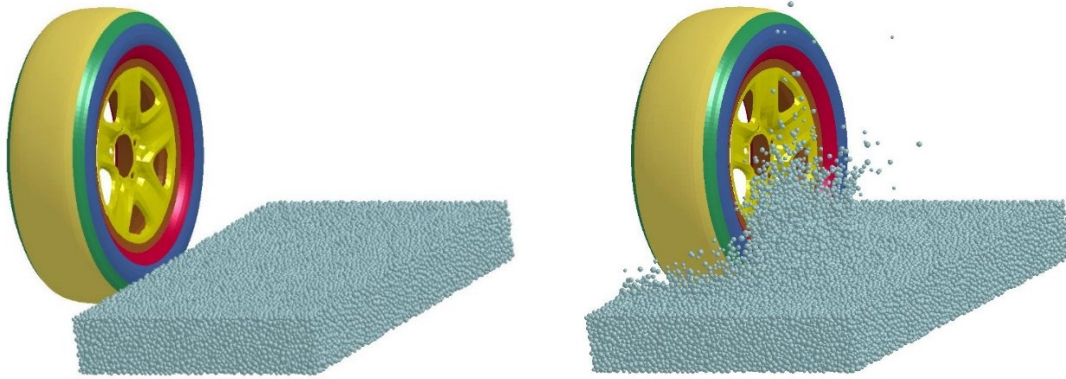
Figure 23. Illustration. Tire furrowing into soft soil using finite-element simulation with discrete spheres.

Once sufficient tire–soil interaction data have been generated from testing and simulation, they will be used to make an empirical formulation representing soil furrowing forces in the vehicle dynamics simulations. This formulation will be implemented as a user-defined module that interfaces with the vehicle dynamics software during simulation run time and applies appropriate soil furrowing forces to the wheel's spindle. Being able to apply soil furrowing forces in this manner will significantly enhance the accuracy and state of the art for simulating vehicle rollover on roadside slopes with soft soils.

SIMULATION INTERFACE MANAGER

Developing comprehensive design guidelines requires researchers to include a large number of design and encroachment variables. Furthermore, an appropriate range of each variable should be included to understand the influence of these design variables and their interdependence on each other. For this reason, millions of simulations must be performed. Developing input files for this many cases, performing each simulation manually, and analyzing the results is not possible without some automation. To automate this process, researchers have developed the Simulation Interface Manager (SIM). The SIM interfaces with CarSim during simulation run times and performs many functions. The SIM is available for use in phase II of this project and will serve as a significant enhancement over the simple use of vehicle dynamics software without an automation tool. Figure 24 shows a high-level flowchart of the SIM program. The functions performed by the SIM are described briefly in the following sections.
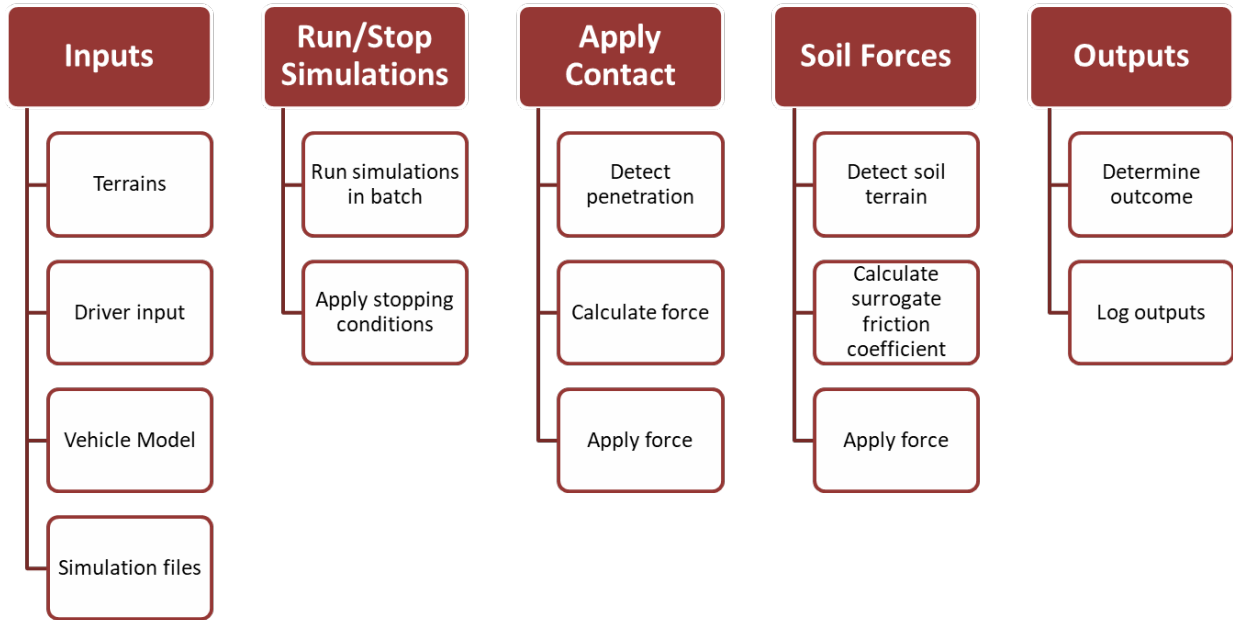
© 2014 TTI.

Figure 24. Flowchart. High-level flowchart of the SIM.

Input Generation

The SIM has the capability to generate all input files needed for each simulation case analyzed using the vehicle dynamics software. In this project, the research team anticipates analyzing more than 12 million cases. For each of these cases, the research team will need to generate terrain inputs, driver inputs, and simulation inputs that combine the terrain, vehicle, and driver inputs. All these input data will be difficult and time consuming to generate manually. However, the SIM can generate these data with minimal input from the user, resulting in significant cost and time savings and making the input-generation process less prone to human error.

Simulation Starting and Stopping

The SIM interacts with CarSim and can perform the simulations in loop without the need for user intervention. It manages each simulation's run time and terminates the simulation based on various termination criteria, such as if the vehicle returns to the road, travels too far, rolls over, and so forth.

Tire–Terrain Contact Implementation

During each simulation, the SIM checks whether the vehicle has penetrated the terrain. If penetration is detected, the program applies terrain contact forces to the vehicle. Any enhancements to the tire–terrain contact will be implemented to improve this aspect of the SIM.

Soil Furrowing Forces

The SIM is also capable of calculating the soil furrowing forces. When appropriate, the program applies soil furrowing forces to the vehicle during the simulation run time. Any enhancements to the tire–soil force calculation method will be implemented to improve this aspect of the SIM.

Output Generation

Similar to input generation, the task of recording and extracting relevant outcomes from the millions of simulation cases can be daunting. The SIM automates this process by generating output logs for all simulation cases and recording the key simulation outcomes for further use in data analysis.

Changes Anticipated for Phase II

As mentioned, some modifications to the SIM will be needed in phase II of this project. These modifications will involve implementing the new tire–soil force calculation module to replace the currently used friction ellipse model. To improve upon the existing contact algorithm, some changes to the vehicle-body-to-terrain contact algorithm will be needed after more validation data are generated during phase II. Other changes to the SIM will also be needed to generate outputs in a format suitable for the data analytics program.

CHAPTER 6. SIMULATION VARIABLE EVALUATION AND SELECTION

To develop design guidance that offers the potential for reducing rollover risk, it is necessary to understand how different roadway and roadside design variables influence rollover probability during a vehicle encroachment. This effort requires an extensive simulation matrix that considers a wide range of variables. For example, encroachment variables include encroachment speed and angle, vehicle type, driver inputs, and vehicle orientation (i.e., tracking or nontracking). This chapter presents the process followed to evaluate and select ranges and values for key variables affecting rollover crashes and support the development of a comprehensive simulation for phase II of this research. This process considered data from literature, analyses of crash data, and various vehicle encroachment simulations using CarSim. Researchers have performed sensitivity analyses on multiple encroachment variables using CarSim and developed and analyzed frequency distributions for selected encroachment variables using the NCHRP Project 17-22 database.[59]

ENCROACHMENT CONDITIONS

Various combinations of vehicle orientations (i.e., tracking or nontracking), driver inputs (i.e., braking and/or steering), and encroachment conditions (i.e., speed and angle) are possible during roadside encroachments. To construct the encroachment conditions matrix, which is a subset of the overall encroachment simulation matrix proposed for phase II, the research team investigated different parameters, including steering rate, vehicle sideslip angle, encroachment angle, encroachment speed, and yaw rate. The following sections detail this process.

Steering Rate

A complex factor in modeling rollover crashes is the steering and braking inputs applied by the driver leading up to the rollover event. Driver inputs include appropriate perception–reaction time and various braking and steering maneuvers considered appropriate based on whether the vehicle is tracking or nontracking at the moment of encroachment. The steering rate for a panic-steer maneuver back toward the roadway was determined based on NHTSA's Fishhook maneuver guidelines.[66] The research team used the recommended steering rate of 720 degree/s to develop a maximum steer of 360 degrees after a prescribed perception–reaction period.

To evaluate the sensitivity of steering rate as part of the driver input definition, a steering rate sensitivity assessment matrix was developed (table 9) and the cases were simulated in CarSim. This matrix includes two vehicles (small passenger car and pickup truck), three maximum steer angles (270, 360, and 450 degrees), and two steering rates (450 and 720 degree/s). For each simulation, a constant encroachment speed of 65 mph and angle of 20 degrees was used. A 1-s perception–reaction time was used for the simulations based on literature.[10]

Table 9. Design variables for steering rate sensitivity analysis.

Vehicle Type	Case No.	Panic Steering: Max Steer Angle (°)	Panic Steering: Steer Rate (Degree/s)
MASH small car design vehicle	1	270	450
MASH small car design vehicle	2	360	720
MASH small car design vehicle	3	450	450
MASH small car design vehicle	4	270	720
MASH small car design vehicle	5	360	450
MASH small car design vehicle	6	450	720
MASH pickup truck design vehicle	7	270	450
MASH pickup truck design vehicle	8	360	720
MASH pickup truck design vehicle	9	450	450
MASH pickup truck design vehicle	10	270	720
MASH pickup truck design vehicle	11	360	450
MASH pickup truck design vehicle	12	450	720

Figure 25 shows the steering wheel input (i.e., steering rate and angle) versus time as applied to the small passenger car (cases 1 through 6 in table 9). Figure 26 shows a screenshot of the superimposed vehicles from the different simulation cases. As shown in the screenshot and the plots of the vehicle CG presented in figure 27, no significant differences in vehicle trajectories exist for any simulation case from the POD to the time the vehicles return to the road.
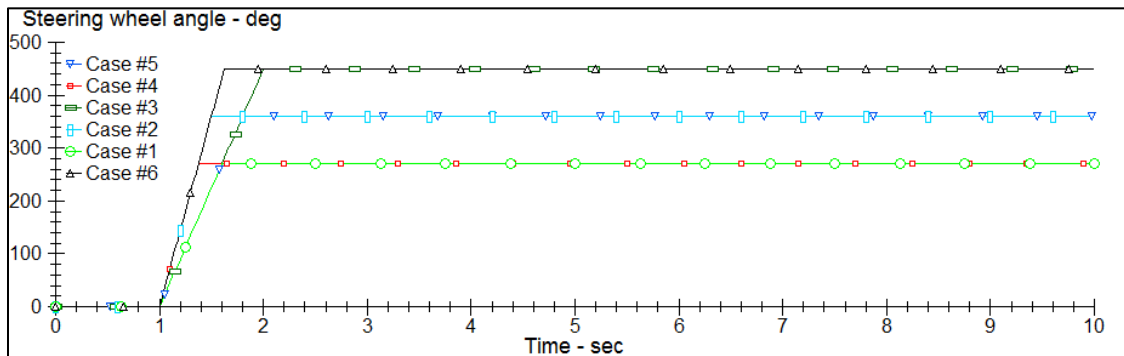
Source: FHWA.

Figure 25. Graph. Steering wheel angle input for MASH small car design vehicle.

Figure 26. Screenshot. Steering rate sensitivity analysis in CarSim (MASH small car design vehicle cases).
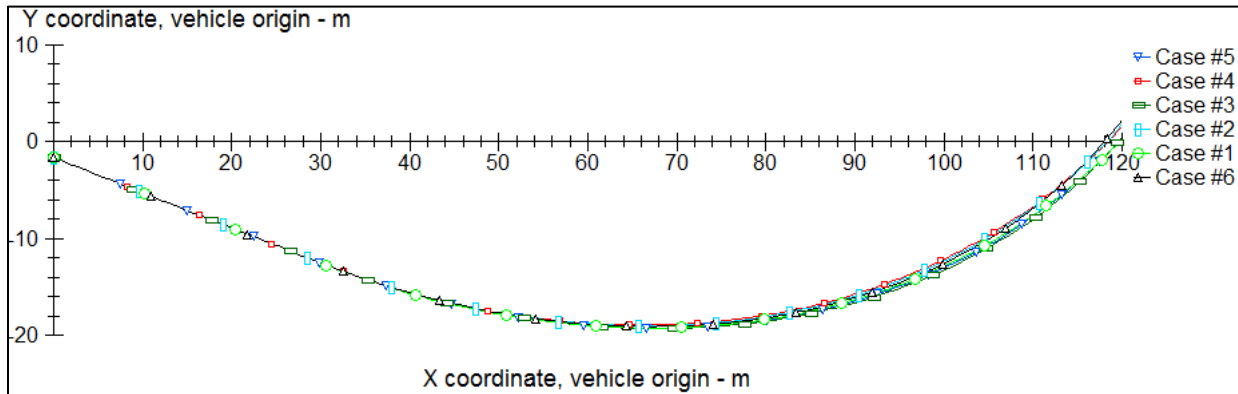
Figure 27. Graph. CG trajectory for MASH small car design vehicle.

Figure 28 shows that identical steering wheel inputs were applied to the pickup truck simulation cases, and figure 29 shows the resulting vehicle trajectory plots. No significant differences in vehicle trajectories were observed for the pickup truck simulation cases from the POD to the time the vehicles returned to the road.
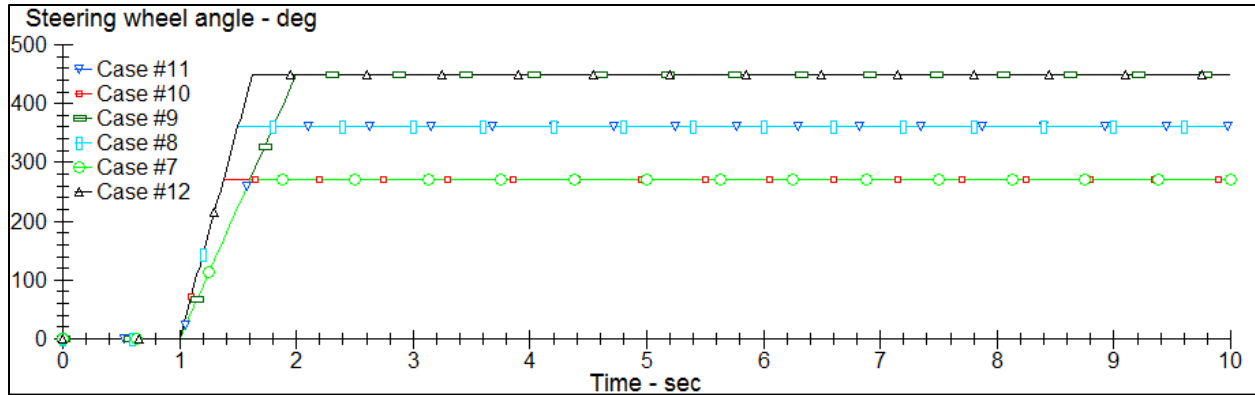
Source: FHWA.

Figure 28. Graph. Steering wheel angle input for MASH pickup truck design vehicle.
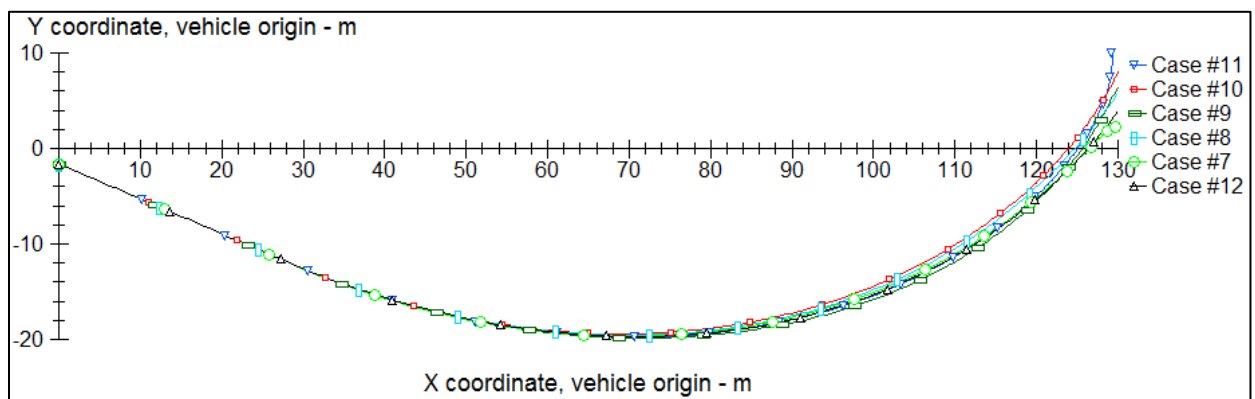
Source: FHWA.
1 m = 3.2808 ft.

Figure 29. Graph. CG trajectory for MASH pickup truck design vehicle.

Vehicle response is not sensitive to the maximum steering angle value used in the encroachment simulations or the steering rate used to reach the maximum steering angle. Therefore, it is not necessary to vary these parameters in the simulation matrix. The proposed maximum steering angle of 360 degrees applied at a steering rate of 720 degree/s appears adequate for representing a panic-steering driver input for the range of vehicles proposed for the simulation matrix.

Sideslip Angle

When a vehicle encroaches onto the roadside, its orientation as it leaves the traveled way can be described as tracking or nontracking. In a tracking encroachment, the heading direction is aligned with its departure direction and the rear tires track the path of the front tires. In a nontracking encroachment, the vehicle's departure direction differs from its heading direction.

In a study of rural two-lane roads, most vehicles that rolled over on side slopes and in ditches were nontracking as they left the roadway.[3] Thus, properly representing nontracking vehicles in the phase II simulation matrix will be important to accurately capture vehicle response and predict rollover probability for different roadway and roadside design configurations.

72

One of the key parameters used to define the characteristics of a nontracking encroachment is the sideslip angle (θ_{SS}), which is defined as the angle between the vehicle's heading direction and departure direction, as depicted in figure 30. The θ_{SS} relates to the direction of motion of the vehicle as opposed to its heading angle (θ_H) or the steering angle of the vehicle's tires. The selection of θ_{SS} to represent nontracking vehicles in the simulation matrix is not obvious because of the broad range of slip angles that can occur as a vehicle departs the roadway. The process of selecting slip angles for the nontracking vehicles in the simulation matrix involved analyzing θ_{SS} frequency distribution derived from crash data and a sensitivity study using vehicle dynamics simulations.
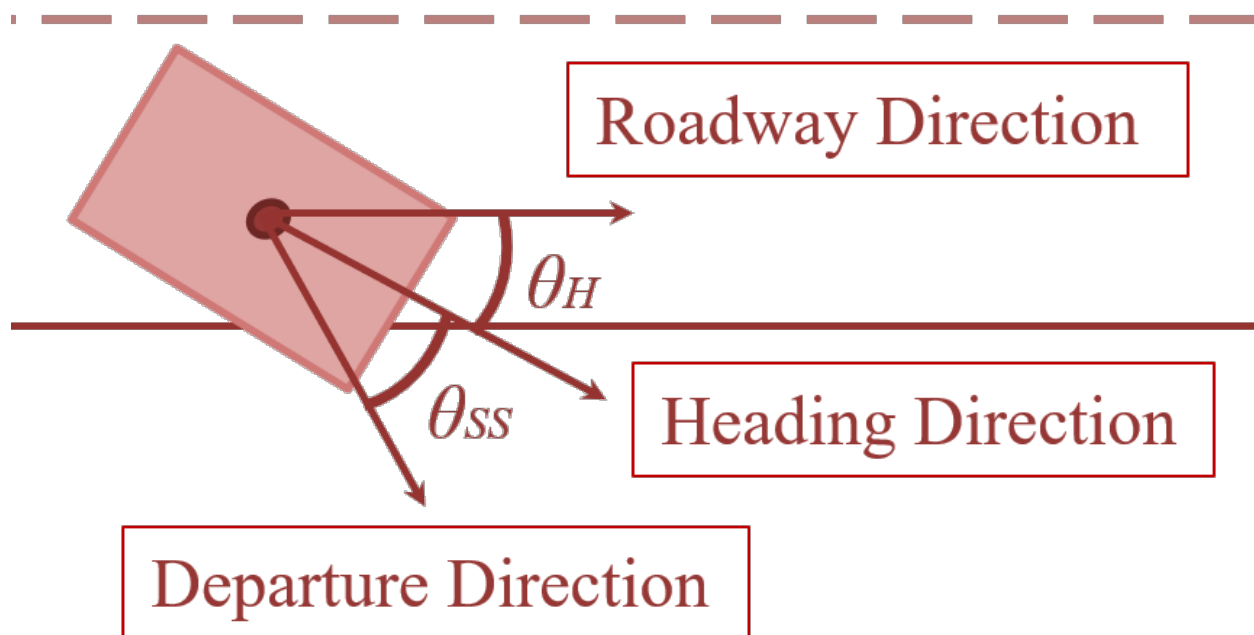
Source: FHWA.

Figure 30. Illustration. Representation of θ_{SS} and θ_H.

NCHRP Project 17-22 Database Study

The NCHRP Project 17-22 database currently contains 890 SVROR crashes sampled from the NASS CDS between 1997 and 2001 (with 16 cases included for 2004).[58] Clinical analyses of the selected roadway-departure crash cases were performed to reconstruct key encroachment parameters, including sideslip angle, encroachment angle, and encroachment speed, at the POD from the traveled way. A total of 815 cases were selected for the sideslip angle study based on availability of the desired data.

Sideslip angle frequency distributions were developed from the admissible NCHRP Project 17-22 dataset. Separate distributions were extracted for different roadway configurations (i.e., straight, right curve, and left curve). Sideslip angles for these roadway configurations were

further segregated by side of departure (i.e., right or left). The mean and standard deviation (STD) were computed for each frequency distribution.

For the straight road category, there were a total of 510 cases, 276 cases (54 percent) with a right-side encroachment and 234 cases (46 percent) with a left-side encroachment. Figure 31 shows the total sideslip angle frequency distribution for straight roadways. The distribution is fairly symmetric, with a mean of −1 degree. Note that the sideslip angle in the NCHRP Project 17-22 database is positive in the clockwise (CW) direction (i.e., CW is positive).
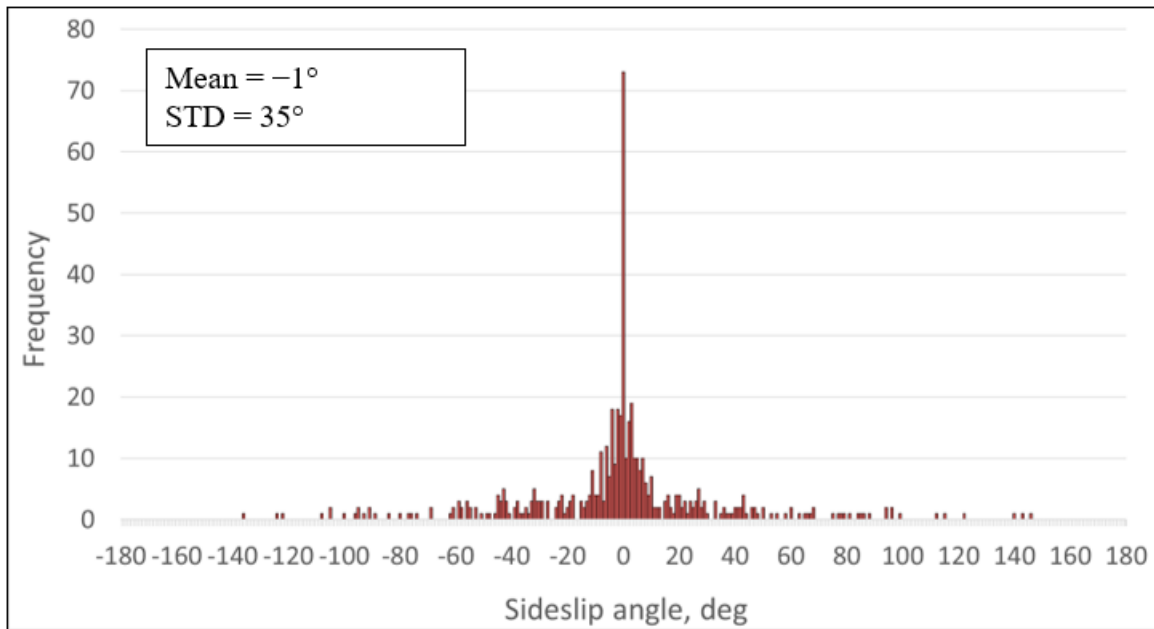
Source: FHWA.

Figure 31. Bar chart. Sideslip angle frequency distribution for encroachments off straight roadways (510 cases).

As figure 32 and figure 33 illustrate, the sideslip angle distributions for both the right- and left-side encroachments on straight roadways are similar in shape, mean, and STD. Note that the −11-degree mean of the sideslip angle for right-side encroachments is a mirror image of the 11-degree mean for left-side encroachments. These distributions indicate that a simulation analysis designed to evaluate right-side encroachments would also be applicable to left-side encroachments. This conclusion eliminates the need for representing encroachment on both sides of the roadway in the phase II simulation matrix.
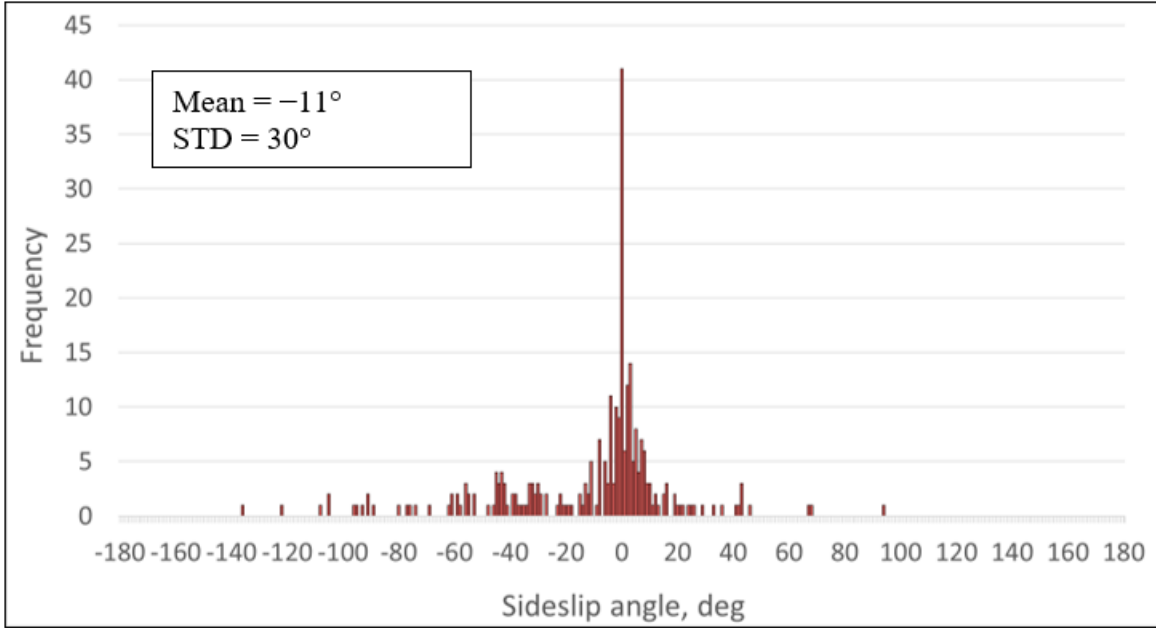
Source: FHWA.

Figure 32. Bar chart. Sideslip angle frequency distribution for right-side encroachments off straight roadways.
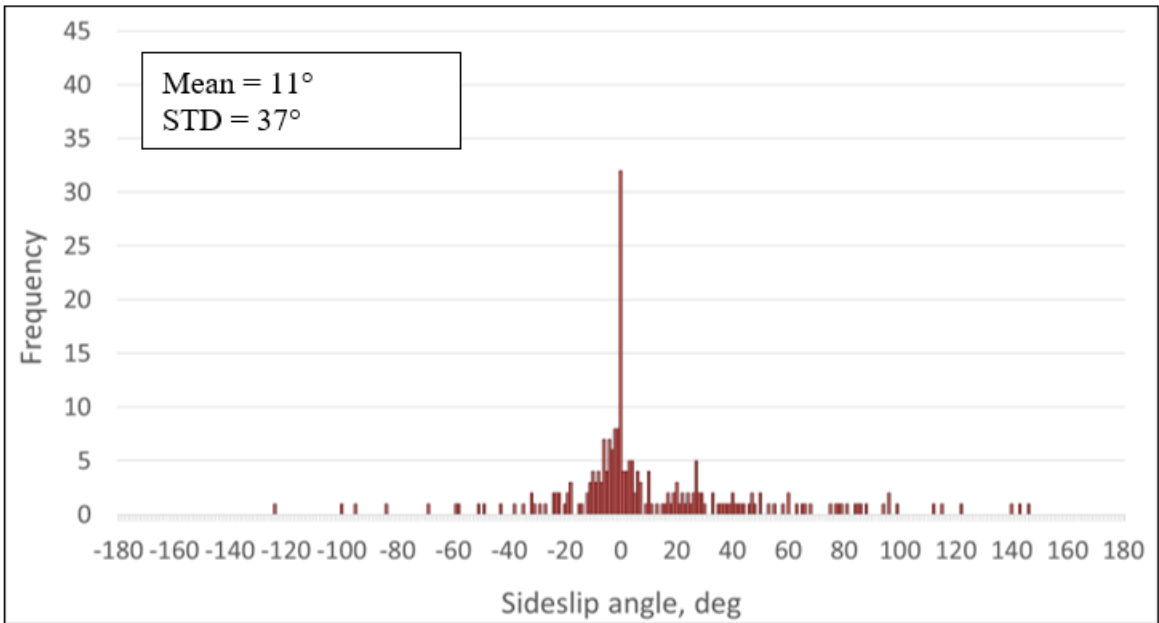
Source: FHWA.

Figure 33. Bar chart. Sideslip angle frequency distribution for left-side encroachments off straight roadways.

Curved roadways were divided into right and left curves for investigating sideslip angles. A total of 152 cases had an encroachment that occurred on a roadway with a right curve. Figure 34 presents the associated sideslip angle frequency distribution.

75
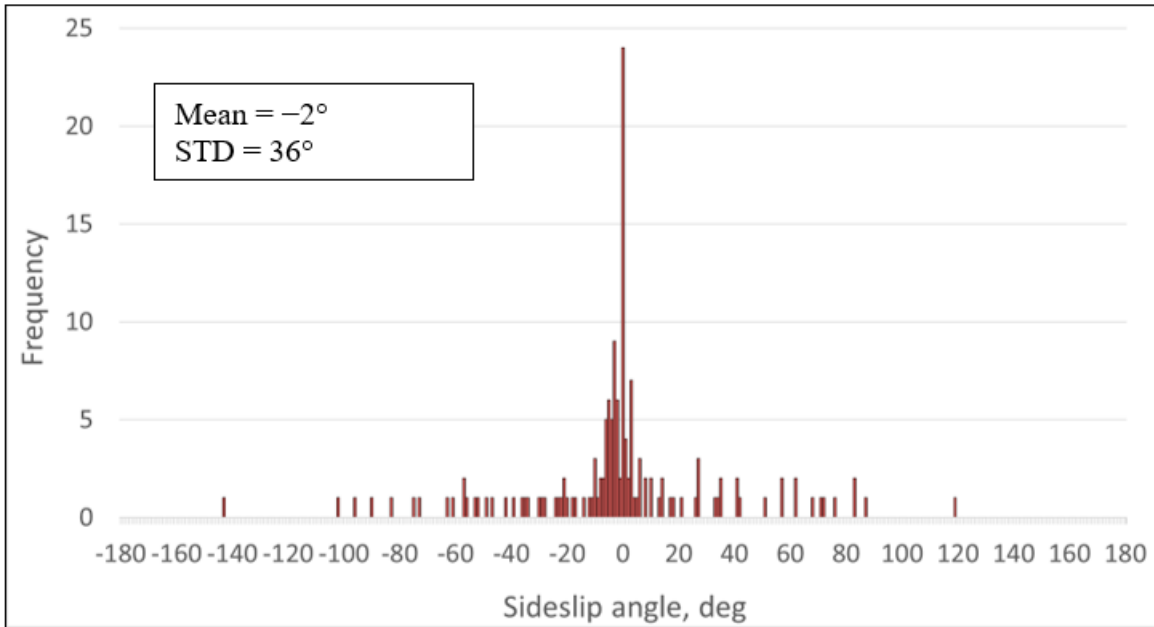
Source: FHWA.

Figure 34. Bar chart. Sideslip angle frequency distribution for encroachments off roadways with a right curve (152 cases).

Sideslip angles associated with roadways with a right curve were further divided into frequency distributions based on the side of roadway departure. As shown in figure 35 and figure 36, respectively, 55 cases (36 percent) had a right-side encroachment and 97 cases (64 percent) had a left-side encroachment. It is clear from these distributions that left-side encroachments are predominant on roadways with a right curve and that these encroachments occur on the outside of the curve. This finding makes sense from a physics standpoint (centrifugal force associated with overdriving the curve) and from the perspective of a distracted motorist (maintaining a straight line path as the roadway curves to the right). The frequency distribution for left-side encroachments is more well defined and has a mean of 5 degrees. The higher percentage of left-side encroachments on roadways with right curves indicates a predisposition to encroach on the outside of the curve. This finding was further investigated for roadways with left curves.
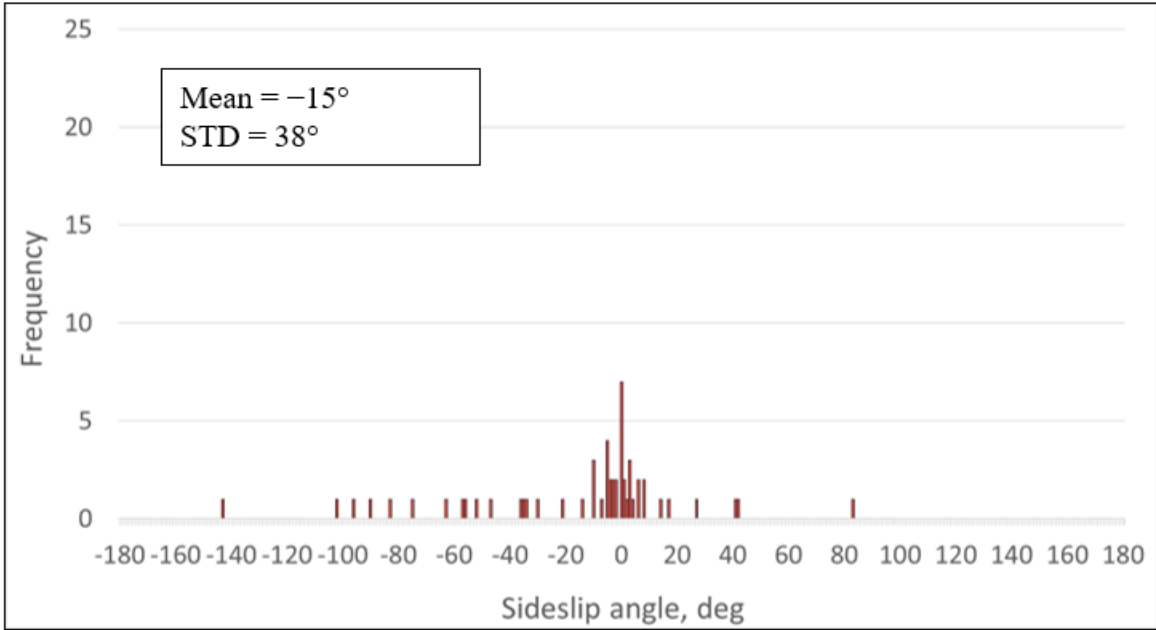
Source: FHWA.

Figure 35. Bar chart. Sideslip angle frequency distribution for right-side encroachments off roadways with a right curve.
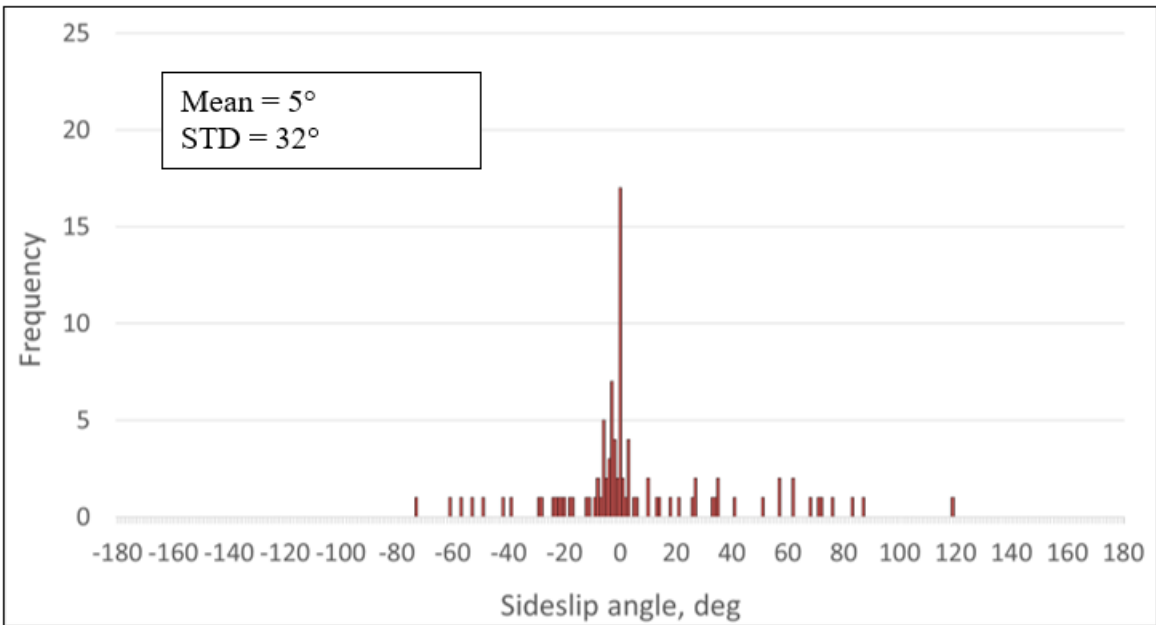
Source: FHWA.

Figure 36. Bar chart. Sideslip angle frequency distribution for left-side encroachments off roadways with a right curve.

A total of 153 cases had an encroachment that occurred on a roadway with a left curve. Figure 37 presents the associated sideslip angle frequency distribution. The sideslip angles associated with roadways with a left curve were similarly divided into frequency distributions based on the side

77

of roadway departure. As shown in figure 38 and figure 39, respectively, 105 cases (69 percent) had a right-side encroachment and 48 cases (31 percent) had a left-side encroachment.
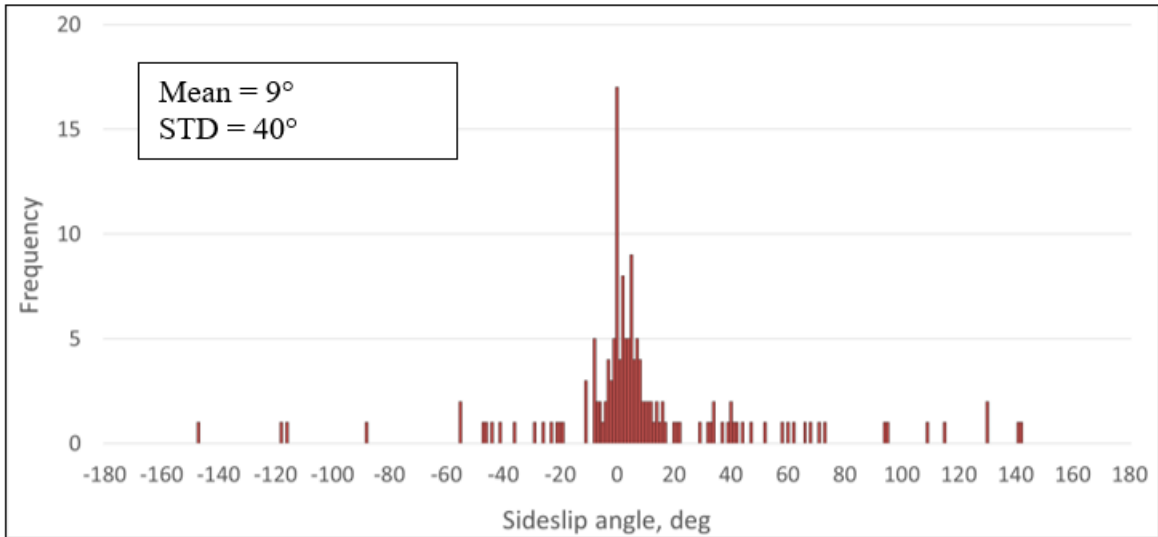
Source: FHWA.

Figure 37. Bar chart. Sideslip angle frequency distribution for encroachments off roadways with a left curve (153 cases).
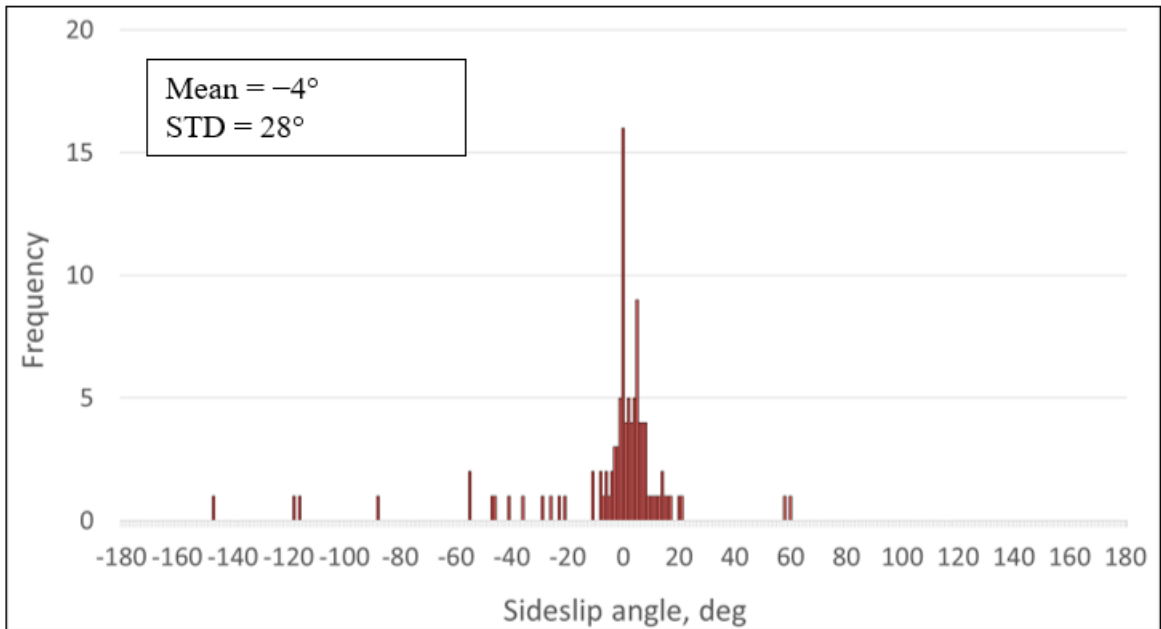
Source: FHWA.

Figure 38. Bar chart. Sideslip angle frequency distribution for right-side encroachments off roadways with a left curve.
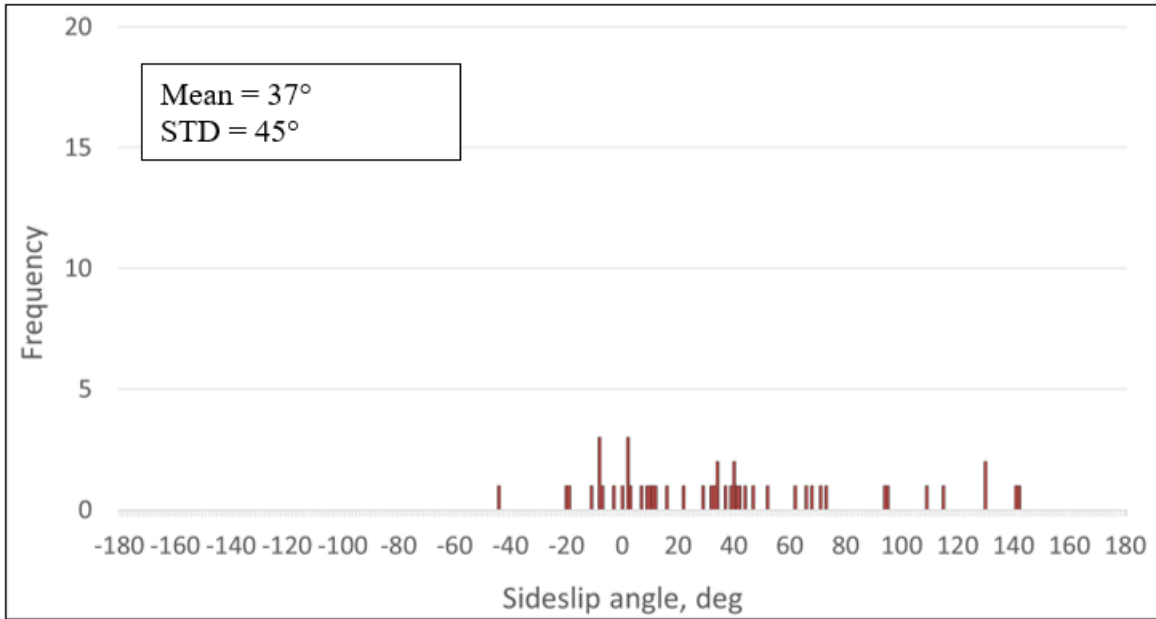
Source: FHWA.

Figure 39. Bar chart. Sideslip angle frequency distribution for left-side encroachments off roadways with a left curve.

Similar to the case for roadways with a right curve, the encroachments on the outside of the curve (i.e., right-side encroachments) were predominant on roadways with a left curve. The frequency distribution for the right-side encroachments is much better defined and has a mean of −4 degrees. This mean sideslip angle is essentially a mirror image of the mean sideslip angle associated with left-side encroachments on the outside of right curves. Note that the sideslip angle frequency distribution for left-side encroachments on roadways with a left curve is somewhat randomly distributed, indicating no clear trends or characteristics that might be of interest to phase II simulation efforts.

The significantly higher percentage of encroachments on the outside of both left and right curves makes the characteristics of these encroachments a primary interest for the curved roadway configurations that are recommended as a point of emphasis in phase II simulations. The two distributions, shown in figure 36 and figure 38 for the outside of right and left curves, respectively, are essentially mirror images of each other as they are similar in shape, mean, and STD.

The research team used the information presented in this section to develop recommendations for characterizing the vehicle orientation associated with nontracking encroachments on curved roadways, which will be an emphasis of the phase II simulations.

The research team proposes using two nontracking vehicle orientations to represent the range of nontracking vehicle encroachments observed in the crash data. The first orientation will have a sideslip angle of 5 degrees, which is representative of the mean sideslip angle for encroachments occurring on the outside of both left and right curves. The second orientation will have a sideslip angle of 15 degrees. Inspection of the distributions shown in figure 36 and figure 38 for the

outside of right and left curves, respectively, shows that this sideslip angle is roughly associated with the outside edge of the primary portions of the distributions. Thus, these two sideslip angles will reasonably capture the range indicated in the frequency distributions of the crash data.

Vehicle Dynamics Simulation Study

Vehicle sideslip can be implemented in a vehicle encroachment simulation by defining a velocity vector for the vehicle not aligned with the heading direction of the vehicle. In CarSim, this can be accomplished by prescribing lateral velocity (V_y) and longitudinal velocity (V_x) components.[8] Figure 40 illustrates how the velocity vector of the vehicle (**V**) can be represented by these velocity components to define θ_{SS}.
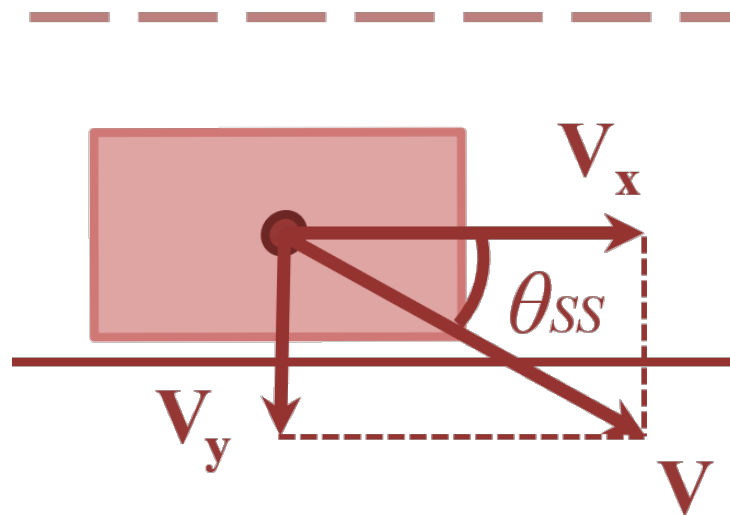
Source: FHWA.

Figure 40. Illustration. CarSim velocity components.

To study the effect of θ_{SS} on encroachment trajectory, six encroachment cases with θ_{SS} ranging from 0 to 25 degrees in 5-degree increments were simulated using CarSim. An initial velocity of 50 mph and a heading angle of 0 degrees were used for all simulation cases. A steering degree of freedom allowed the vehicle to follow its preferred path without prescribed driver input, which approximates a driver who has fallen asleep or is in some manner impaired or incapacitated. The cases, which are summarized in table 10, have characteristic velocity components calculated using the equations shown in figure 41.

Table 10. Sideslip simulation study matrix.

Case No.	θ_{SS} (°)	V_x (mph)	V_y (mph)
1	0	+50	0
2	5	+49.51	−4.31
3	10	+48.95	−8.61
4	15	+48.01	−12.86
5	20	+46.70	−17.00
6	25	+45.05	−21.00

$$\begin{cases} V_x^2 + V_y^2 = V^2 \\ \tan(\theta_{SS}) = \dfrac{V_y}{V_x} \end{cases}$$

Figure 41. Equation. Vehicle velocity components and sideslip angle.

Figure 42 shows the resulting vehicle trajectories for sideslip simulation cases. The extent of the vehicle's lateral travel increases as the sideslip angle increases. Figure 43 shows that the sideslip angle decreases during the encroachment until the vehicle resumes a tracking mode. The rate of change for the slip angle is similar for all cases. Clearly, the sideslip angle can significantly alter the path of the vehicle by allowing it to encroach farther off the traveled way. Additionally, the sideslip angle can induce additional vehicle yaw or rotation during the encroachment. These factors can lead to a more critical vehicle response and potential soil furrowing as the vehicle interacts with the terrain. The nontracking encroachment conditions incorporated into the simulation matrix will enable evaluating these factors, particularly if the tire–soil interaction model is funded and implemented in the simulation.
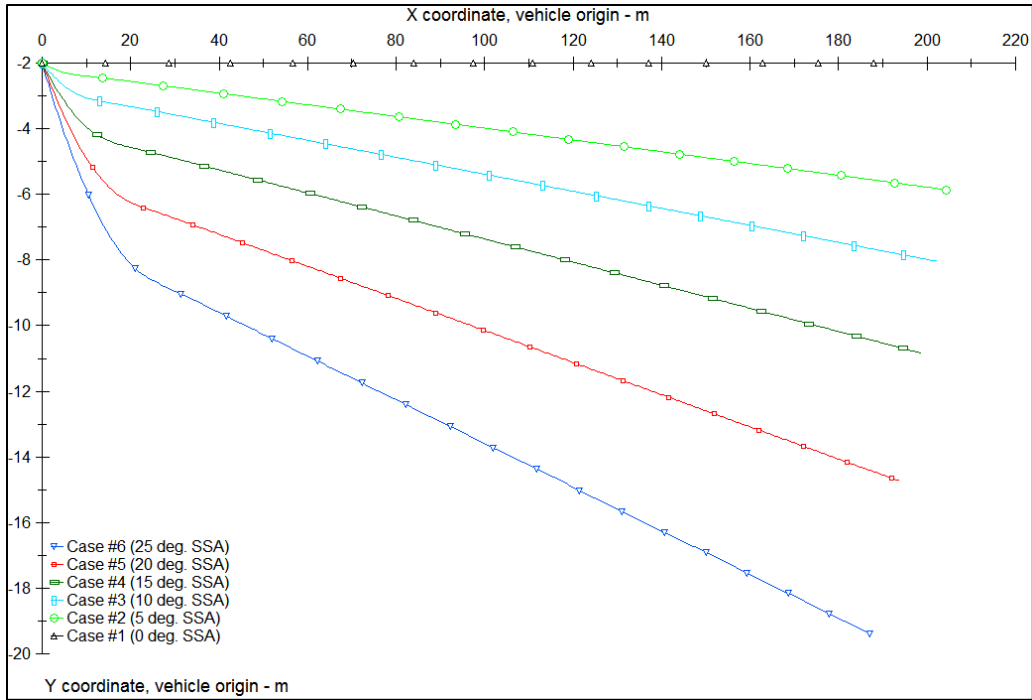
Source: FHWA.
1 m = 3.2808 ft.

Figure 42. Graph. Vehicle trajectories for sideslip angle simulation study.
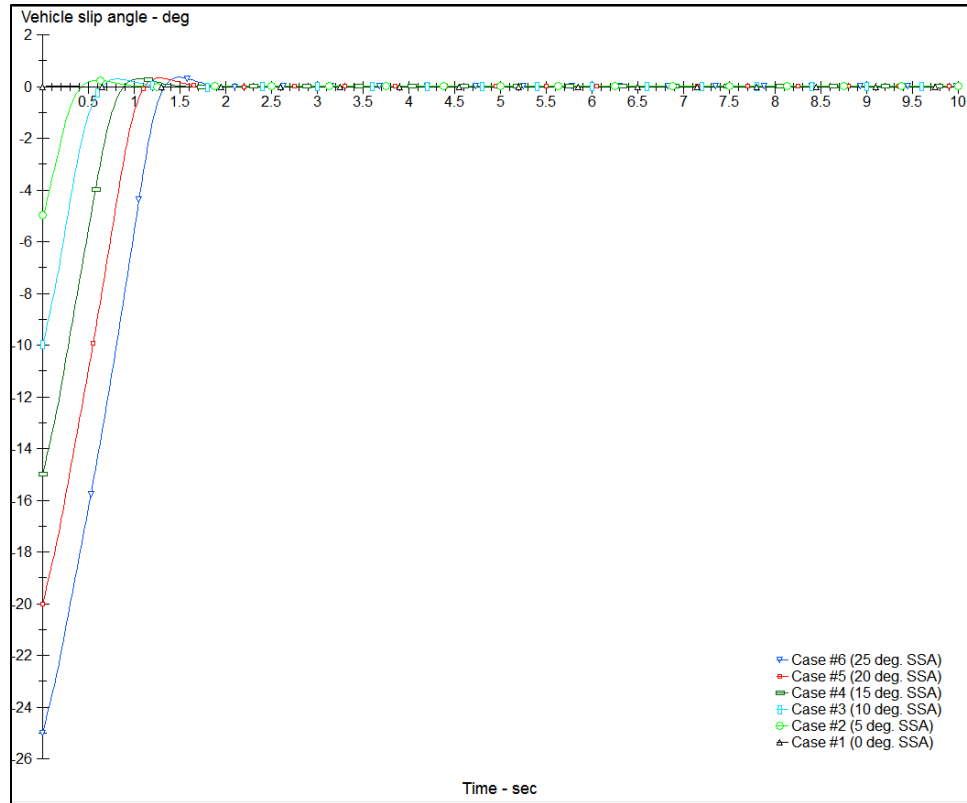
Source: FHWA.

Figure 43. Graph. Vehicle sideslip angle versus time for sideslip simulation study.

Encroachment Angle

The encroachment angle at the POD from the traveled way is a key parameter in any simulation study of roadside encroachments. For a given vehicle, encroachment speed, and driver input, an increase in encroachment angle permits greater lateral extent of movement off the roadway, which presents an opportunity for the encroaching vehicle to have more significant interaction with the roadside terrain (e.g., ditch backslope) and can increase the risk of rollover.

The encroachment angle of the vehicle at the POD was examined using reconstructed crash data from the NCHRP Project 17-22 database.[58] The objective of the study was to guide the range of selected encroachment angles used in the simulation matrix.

In a tracking departure, the encroachment angle (θ_{EN}) is the angle between the roadway and the departure direction of the vehicle. In a nontracking departure, such as the example illustrated in figure 30, θ_{EN} is measured as the sum of θ_{SS} and θ_H. θ_{EN} frequency distributions were developed for both straight and curved roadways. The curved roadways were divided into right and left curves, and each distribution was further divided into right- and left-side encroachments.

Figure 44 and figure 45 show the encroachment angle frequency distributions for right- and left-side encroachments off straight roadway segments, respectively. The encroachment angle is primarily distributed between 0 and 40 degrees for both right- and left-side encroachments. The encroachment angles corresponding to two STDs off the mean are 30 and 38 degrees for

83

right- and left-side encroachments, respectively. Based on inspection of these distributions, a maximum encroachment angle of 30 degrees seems reasonable. Note that each encroachment angle value will be assigned a weight factor based on the frequency distribution. Thus, it is not necessary to fully cover the range of the frequency distribution with the selected simulation values.
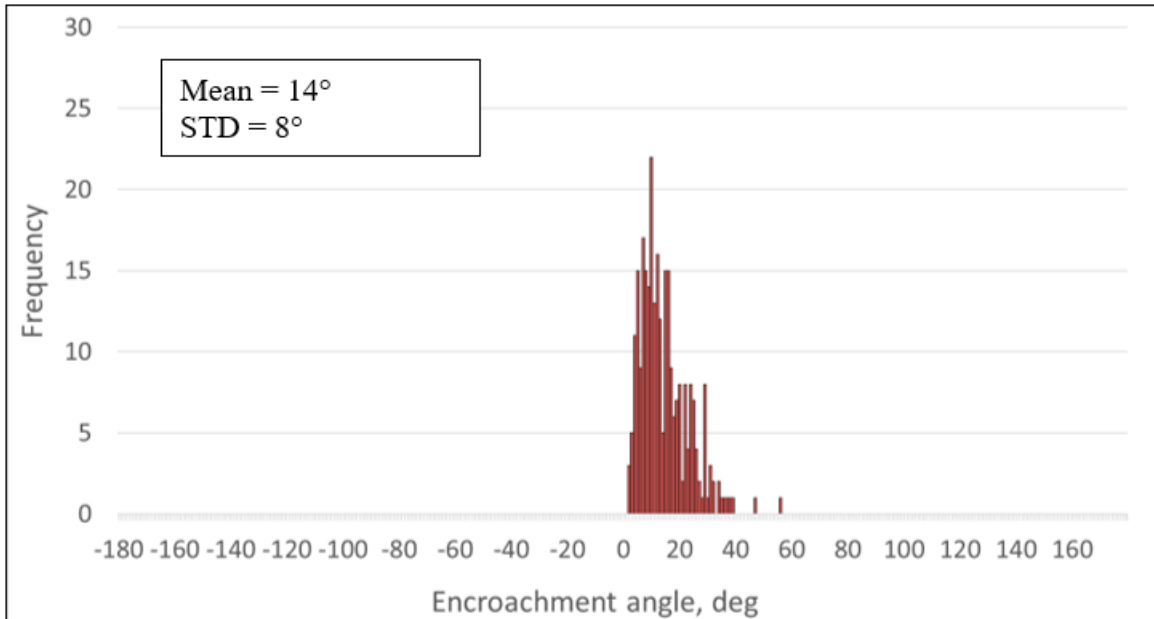
Source: FHWA.

Figure 44. Bar chart. Encroachment angle frequency distribution for right-side encroachments off straight roadways.
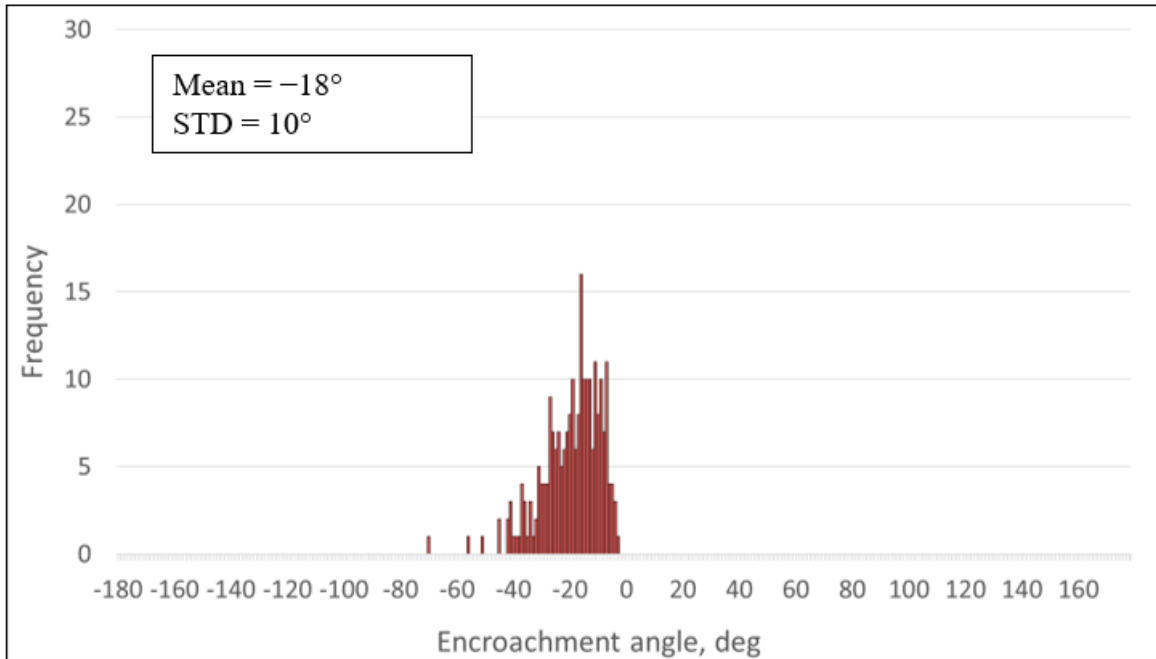
Source: FHWA.

Figure 45. Bar chart. Encroachment angle frequency distribution for left-side encroachments off straight roadways.

Figure 46 and figure 47 show the encroachment angle frequency distributions for right- and left-side encroachments on roadways with a right curve, respectively. The encroachment angles corresponding to two STDs off the mean are 31 and 36 degrees for right- and left-side encroachments, respectively. Thus, once again, a maximum encroachment angle of 30 degrees appears to reasonably cover the range of encroachment angles associated with encroachments off roadways with a right curve.
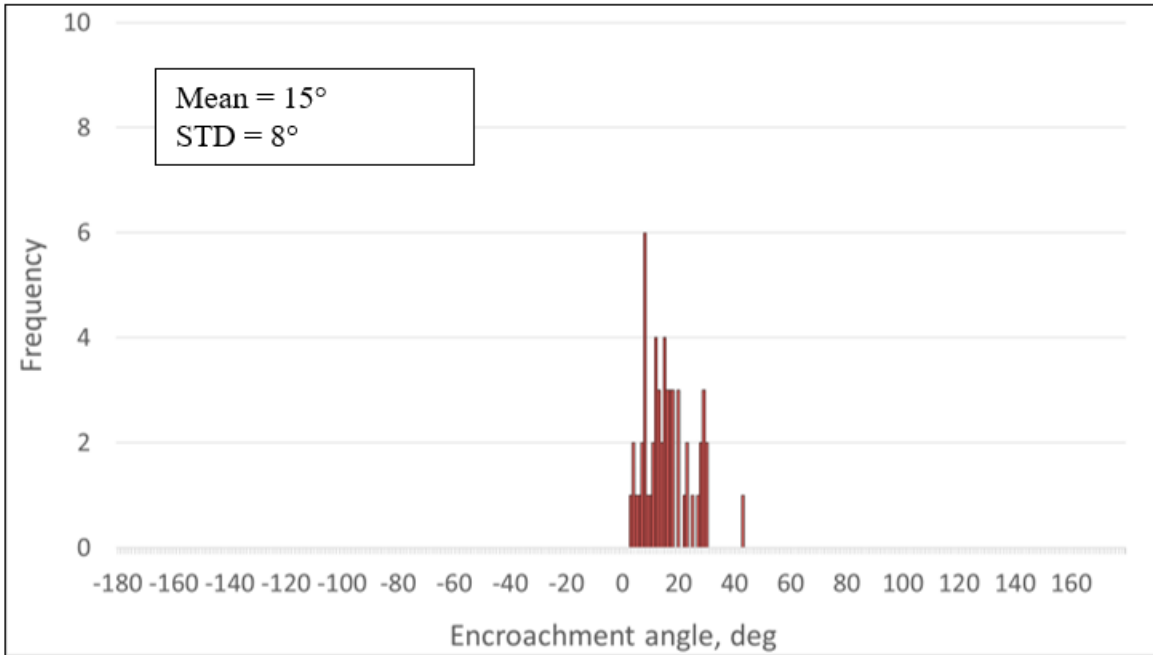
Source: FHWA.

Figure 46. Bar chart. Encroachment angle frequency distribution for right-side encroachments off roadways with a right curve.
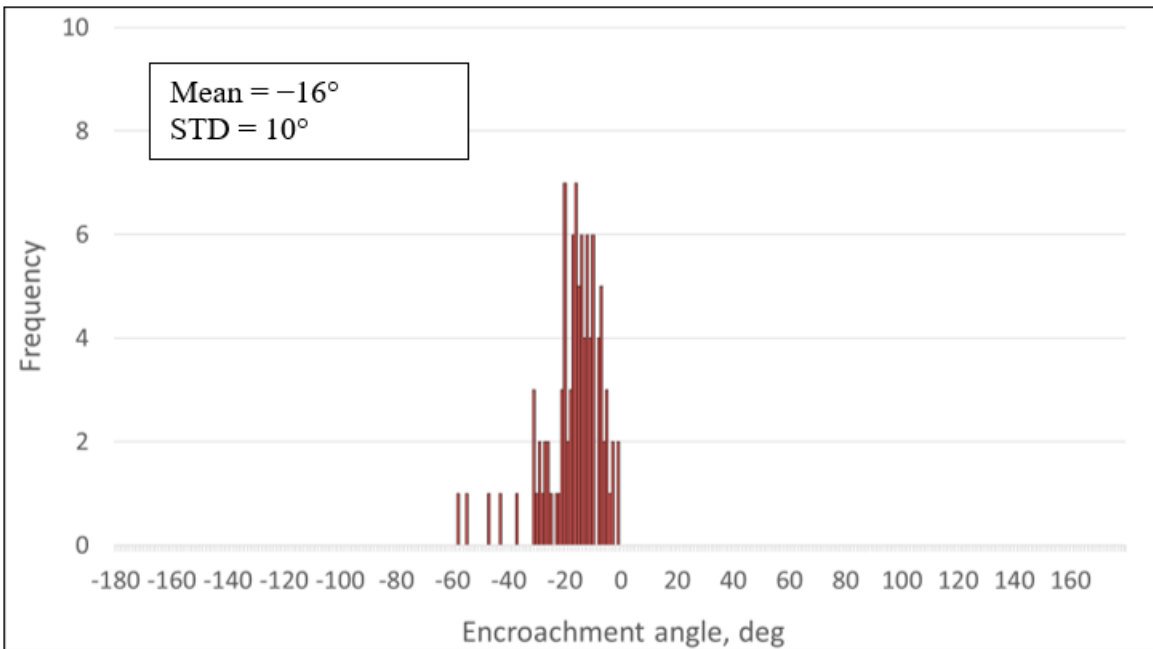
Source: FHWA.

Figure 47. Bar chart. Encroachment angle frequency distribution for left-side encroachments off roadways with a right curve.

Finally, the encroachment angle frequency distributions for right- and left-side encroachments off roadways with a left curve are shown in figure 48 and figure 49, respectively. The

86

encroachment angles corresponding to two STDs off the mean are 26 and 40 degrees for right- and left-side encroachments, respectively. Note that the distribution associated with left-side encroachments on a left curve is based on a relatively small sample size. A maximum encroachment angle of 30 degrees appears reasonable for right-side encroachments off roadways with a left curve, which is intended to be a focus of the phase II simulations.
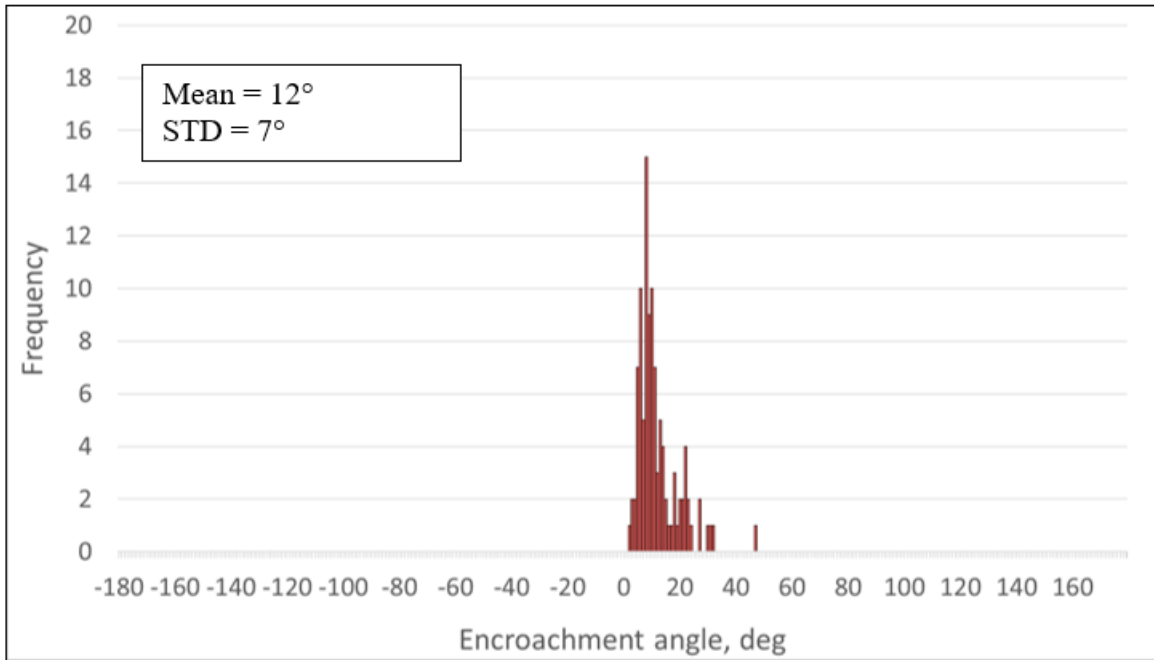
Source: FHWA.

Figure 48. Bar chart. Encroachment angle frequency distribution for right-side encroachments off roadways with a left curve.
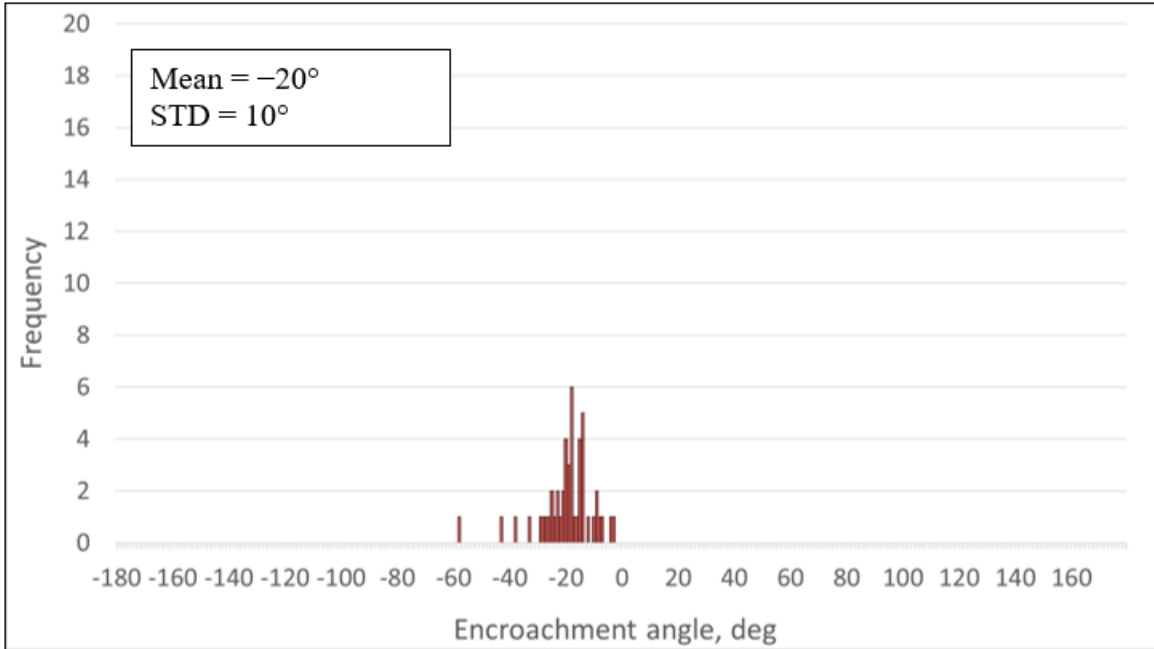
Source: FHWA.

Figure 49. Bar chart. Encroachment angle frequency distribution for left-side encroachments off roadways with a left curve.

The proposed encroachment angle values for the phase II simulation matrix are 10, 20, and 30 degrees. Each value will be assigned a weight factor or probability based on the frequency distribution. The weight factor for a simulated encroachment angle of 10 degrees will be the percentage of encroachment angles in the frequency distribution with values less than or equal to 15 degrees. Similarly, the weight factor assigned to the encroachment angle of 20 degrees will be the percentage of encroachment angles falling between 15 and 25 degrees. Finally, the weight factor for the 30-degree encroachment angle will be the percentage of encroachment angles exceeding 25 degrees.

Encroachment Speed

The encroachment speed at the POD from the traveled way is another key parameter in simulation studies of roadside encroachments. For a given vehicle, encroachment angle, and driver input, an increase in encroachment speed permits greater lateral extent of movement off the roadway, which presents an opportunity for the encroaching vehicle to have more significant interaction with the roadside terrain (e.g., ditch backslope) and can increase the risk of tripping and rollover.

The encroachment speed of the vehicle at the POD was examined using the NCHRP Project 17-22 database.[58] The encroachment speeds in the 17-22 database were reconstructed from a clinical review of crash cases using scene diagrams, crash narratives, scene photographs, and supplemental roadway and roadside data. The objective of evaluating these encroachment speeds was to guide the range of selected encroachment speeds to be used in the phase II simulation matrix.

Figure 50 and figure 51 show the frequency distributions of encroachment speed associated with rollover and nonrollover cases, respectively. These distributions support the premise that rollovers are associated with higher encroachment speed. The mean encroachment speed for the rollover cases is 55.2 mph, whereas the mean encroachment speed for the nonrollover cases is only 43.8 mph. As mentioned, a higher encroachment speed results in greater lateral extent of encroachment, which typically exposes the encroaching vehicle to more terrain features and possible trip mechanisms. Also, from a physics standpoint, higher speeds provide an increased likelihood of generating the trip forces required to induce vehicle rollover.
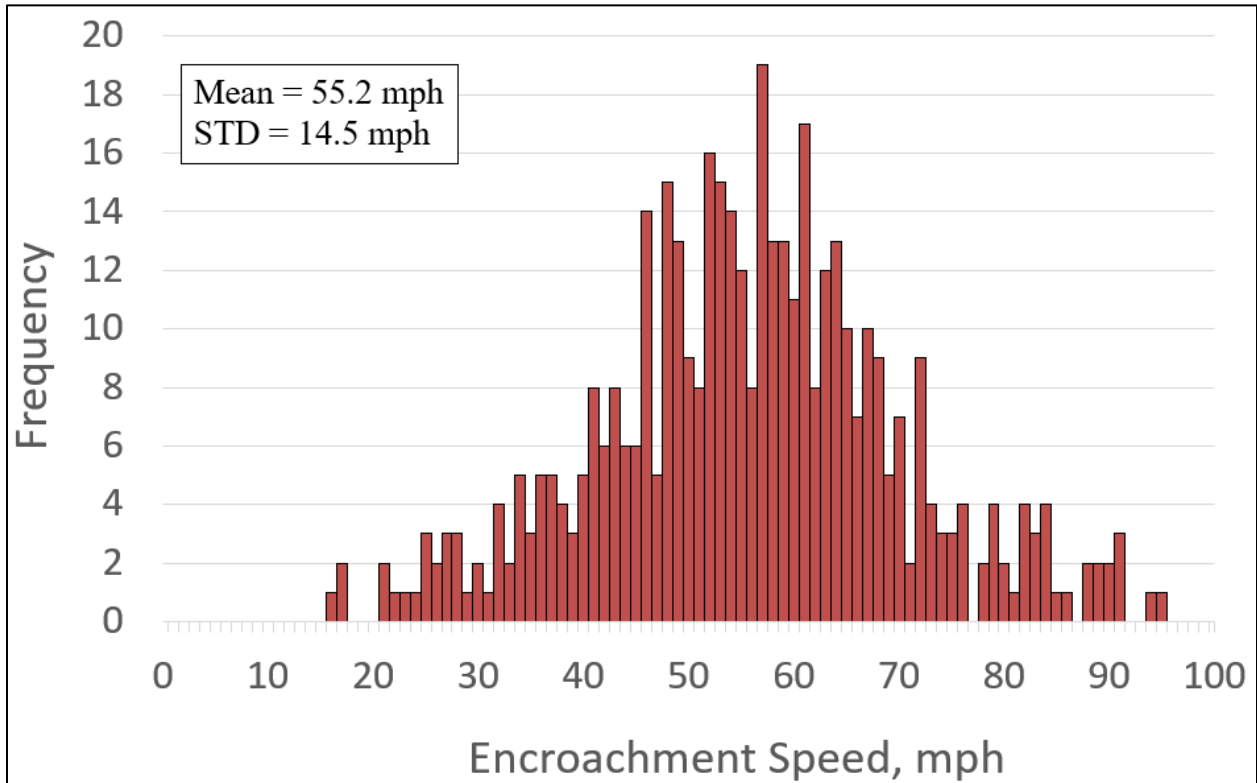
Source: FHWA.

Figure 50. Bar chart. Encroachment speed frequency distribution for rollover cases.
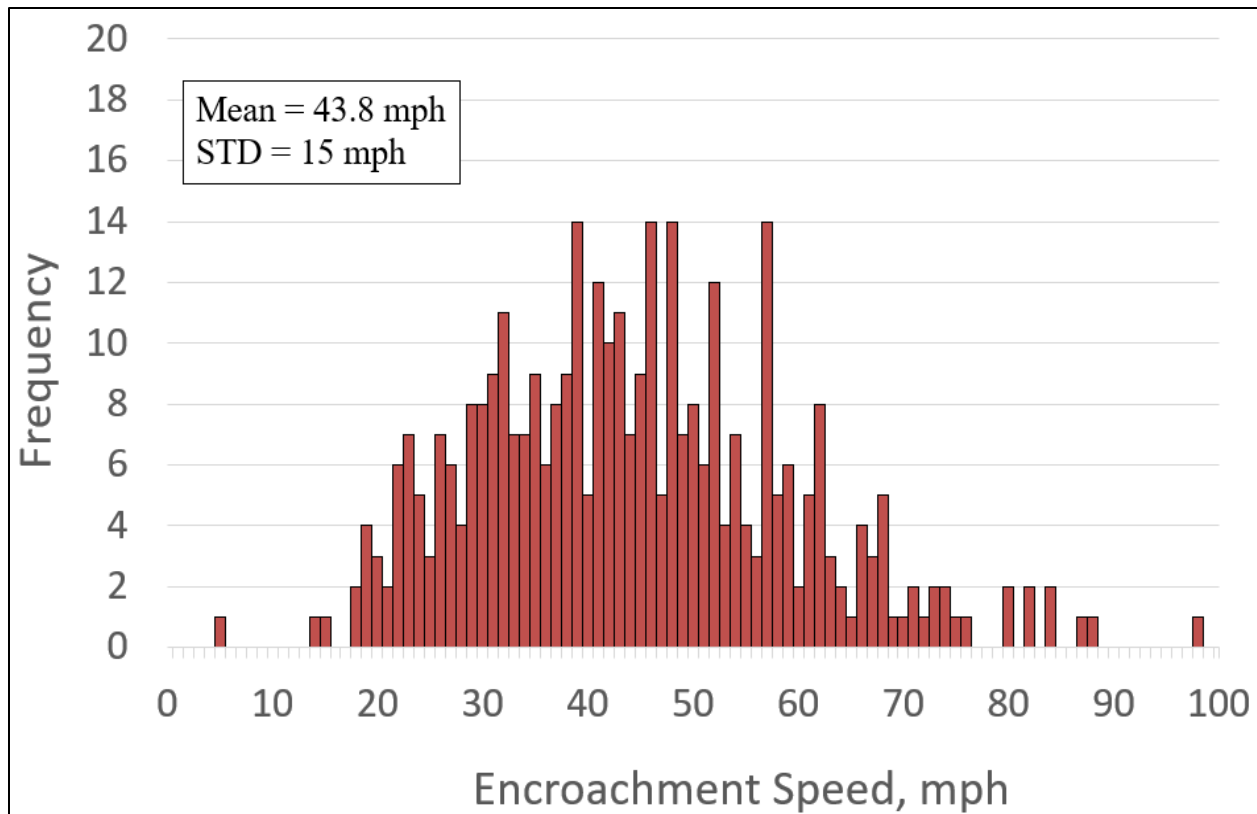
Source: FHWA.

Figure 51. Bar chart. Encroachment speed frequency distribution for nonrollover cases.

The proposed encroachment speed values for the phase II simulation matrix are 45, 55, 65, and 75 mph. A weight factor will be developed for each of these encroachment speeds based on the combined frequency distribution (rollovers and nonrollovers). The research team believes these values will reasonably cover the frequency distribution.

Yaw Rate

One of the parameters associated with nontracking encroachments is yaw rate. When a driver loses control of a vehicle, the vehicle is typically nontracking and can have a yaw rate that results in rotation or spin out of the vehicle. A yaw rate value of 15 degree/s has been used in previous studies of roadside encroachment simulations.[10,12] The research team developed a simulation matrix of nine cases to investigate the sensitivity of vehicle trajectory to the applied yaw rate. Each simulation case was defined by a prescribed encroachment speed, encroachment angle, and sideslip angle. For each case, three different vehicle yaw rates were considered—0, 15, and 30 degree/s—which resulted in a matrix of 27 total encroachment simulations. The yaw rates were applied counterclockwise (CCW) to represent a driver losing control of the vehicle while trying to return to the roadway after a right-side encroachment. Table 11 details each nontracking simulation case. The matrix includes three different encroachment angles (−20 CW, 0, and 20 degrees CCW) and three different sideslip angles (10, 20, and 30 degrees).

90

Table 11. Matrix of yaw rate sensitivity study.

Encroachment Angle (°)	Sideslip Angle (°)	Forward Velocity Component (mph)	Lateral Velocity Component (mph)	Vehicle No.	Yaw Rate (Degree/s)	Set No.
0	10	+48.95	−8.61	1	0	1
0	10	+48.95	−8.61	2	15	1
0	10	+48.95	−8.61	3	30	1
0	20	+46.70	−17.00	1	0	2
0	20	+46.70	−17.00	2	15	2
0	20	+46.70	−17.00	3	30	2
0	30	+43.04	−24.85	1	0	3
0	30	+43.04	−24.85	2	15	3
0	30	+43.04	−24.85	3	30	3
+20 CCW	10	+48.95	−8.61	1	0	4
+20 CCW	10	+48.95	−8.61	2	15	4
+20 CCW	10	+48.95	−8.61	3	30	4
+20 CCW	20	+46.70	−17.00	1	0	5
+20 CCW	20	+46.70	−17.00	2	15	5
+20 CCW	20	+46.70	−17.00	3	30	5
+20 CCW	30	+43.04	−24.85	1	0	6
+20 CCW	30	+43.04	−24.85	2	15	6
+20 CCW	30	+43.04	−24.85	3	30	6
−20 CW	10	+48.95	−8.61	1	0	7
−20 CW	10	+48.95	−8.61	2	15	7
−20 CW	10	+48.95	−8.61	3	30	7
−20 CW	20	+46.70	−17.00	1	0	8
−20 CW	20	+46.70	−17.00	2	15	8
−20 CW	20	+46.70	−17.00	3	30	8
−20 CW	30	+43.04	−24.85	1	0	9
−20 CW	30	+43.04	−24.85	2	15	9
−20 CW	30	+43.04	−24.85	3	30	9

To illustrate the vehicle behavior obtained in the simulations, the outputs for two simulation sets, 2 and 8, are presented. Figure 52 illustrates the positions of the vehicles during the three encroachments that make up set 2. As the vehicles recovered to the roadway, there was no significant difference between their position or orientation with the two non-zero yaw rates. Figure 53 shows the nearly identical trajectory for the vehicles with the two non-zero yaw rates. They also had a similar maximum lateral travel distance.

A. Car 1 at 0 degree/s, car 2 at 15 degree/s CCW, and car 3 at 30 degree/s CCW at 0 s.

B. Car 1 at 0 degree/s, car 2 at 15 degree/s CCW, and car 3 at 30 degree/s CCW at 1 s.

C. Car 1 at 0 degree/s, car 2 at 15 degree/s CCW, and car 3 at 30 degree/s CCW at 2 s.

Figure 52. Illustrations. Yaw rate sensitivity simulation of set 2.
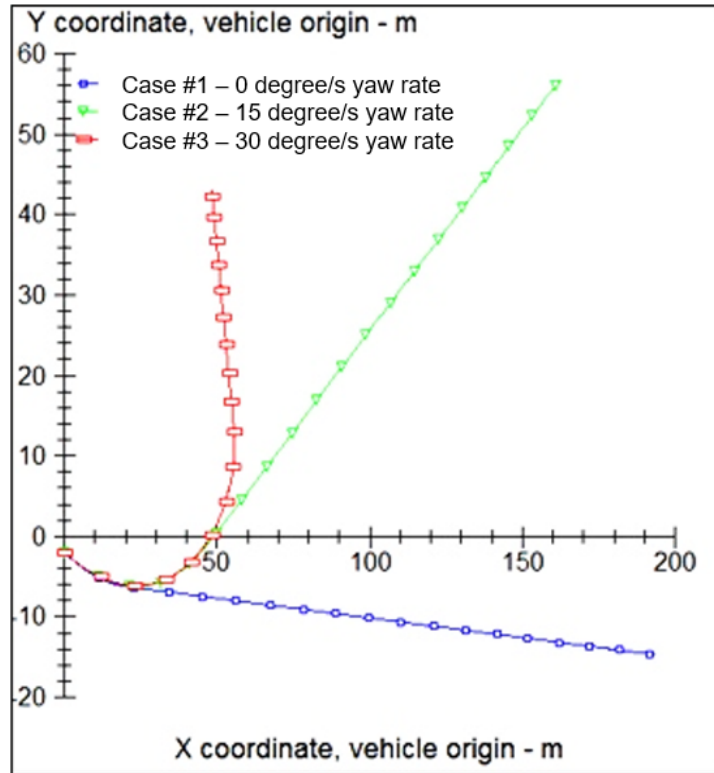
Source: FHWA.
1 m = 3.2808 ft.

Figure 53. Graph. Set 2 vehicle trajectories.

Figure 54 illustrates the positions of the vehicles at different times during the three encroachments that make up set 8. There was no significant difference between the position or orientation of the vehicles with the two non-zero yaw rates until they began to return to the traveled way after reaching their maximum lateral extent of movement. Figure 55 shows that the trajectory of these yawed vehicles was essentially identical through the initial stages of the encroachment and beyond the point of maximum lateral movement.
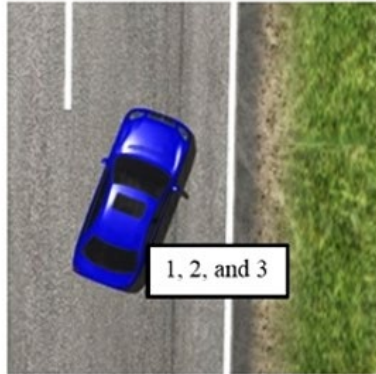
Source: FHWA.

A. Car 1 at 0 degree/s, car 2 at 15 degree/s CCW, and car 3 at 30 degree/s CCW at 0 s.
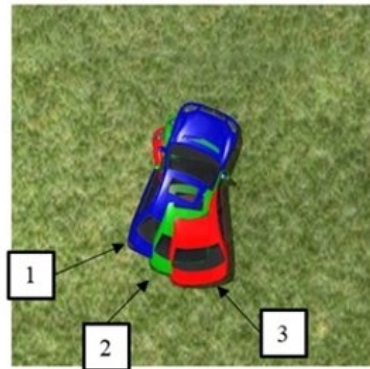
Source: FHWA.

B. Car 1 at 0 degree/s, car 2 at 15 degree/s CCW, and car 3 at 30 degree/s CCW at 1 s.
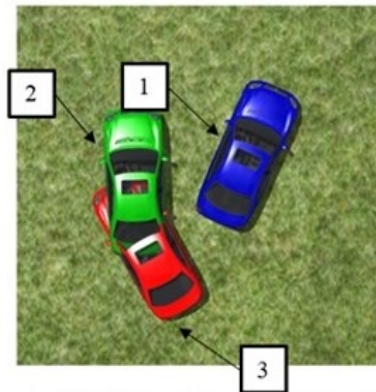
Source: FHWA.

C. Car 1 at 0 degree/s, car 2 at 15 degree/s CCW, and car 3 at 30 degree/s CCW at 2 s.

Figure 54. Illustrations. Yaw rate sensitivity simulation of set 8.
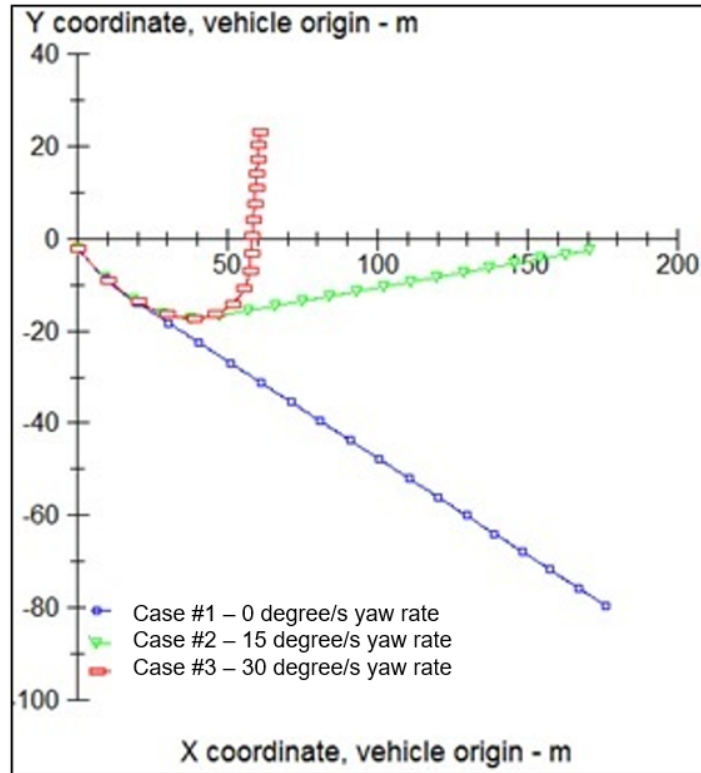
Source: FHWA.
1 m = 3.2808 ft.

Figure 55. Graph. Set 8 vehicle trajectories.

The results of the yaw rate sensitivity simulations (sets 1 through 9) show identical vehicle trajectories with the two initial non-zero yaw rates up to and beyond the maximum lateral travel distance. This finding indicates that the encroachment trajectory is not sensitive to yaw rate within the range evaluated. Thus, the research team retained the yaw rate value of 15 degree/s in the phase II simulation matrix for nontracking simulation cases designed to have a prescribed yaw rate.

Tracking and Nontracking Scenarios for the Simulation Matrix

Based on the variable studies conducted, the research team developed the following conclusions and recommendations:

- Steering rate does not have a significant effect on overall vehicle trajectory, and a value of 720 degree/s with a maximum steer angle of 360 degrees appears to be adequate for representing a panic return-to-road steer maneuver.

- Sideslip angle frequency distributions indicate a much higher encroachment rate on the outside of curves. The similarity of the sideslip angle frequency distributions on the outside of left and right curves indicates that a simulation analysis designed to evaluate right-side encroachments on a roadway with a left curve would also be applicable to left-side encroachments on a roadway with a right curve. The research team proposes

95

using two nontracking vehicle orientations (with sideslip angles of 5 and 15 degrees) to represent the range of nontracking vehicle encroachments observed in the crash data.

- Encroachment angle frequency distributions indicate that a maximum encroachment angle of 30 degrees is reasonable for the phase II simulation matrix. The research team proposes using encroachment angle values of 10, 20, and 30 degrees.

- Encroachment speed distributions for rollover and nonrollover cases show a significantly higher mean encroachment speed for rollover cases. The research team recommends encroachment speed values of 45, 55, 65, and 75 mph for the simulation matrix.

- A yaw rate of 15 degree/s, found in previous studies, was deemed to still be relevant to the current vehicle fleet based on simulations defined by prescribed encroachment speed, encroachment angle, and sideslip angle.

Recommended driver inputs include appropriate perception–reaction time and various braking and steering maneuvers based on whether the vehicle is tracking or nontracking at the POD. Table 12 presents driver input scenarios, divided into tracking and nontracking vehicle encroachments, based on the encroachment condition studies presented in the Encroachment Angle and Encroachment Speed sections in this chapter. The freewheeling condition (case 1.1) models an asleep or somehow impaired or incapacitated driver. For other tracking vehicle encroachments, the driver is modeled as distracted and subsequently becoming aware of the vehicle encroachment. A 1-s perception–reaction time is used before any direct driver input. Once aware of the encroachment, the driver tries to correct the vehicle path by panic steering (case 1.2), panic braking (case 1.3), or panic steering and braking (case 1.4). For nontracking impacts with a shallow sideslip angle (i.e., 5 degrees), the driver is modeled as having perceived an imminent encroachment situation and the same options—panic steering (case 2.1), panic braking (case 2.2), and panic steering and braking (case 2.3)—are used but without the 1-s perception–reaction time. For nontracking encroachments with a more significant sideslip angle (i.e., 15 degrees), the driver is modeled as already having reacted to an imminent encroachment on the roadway, which resulted in a sideslipping vehicle. Thus, no perception–reaction time is added, and the driver input is either constant steering back toward the roadway (case 3.1), constant braking (case 3.2), or constant steering and braking (case 3.3).

Table 12. Vehicle orientation and driver inputs.

Case	Tracking or Nontracking	PR Time (s)	θ_{SS} (°)	Yaw Rate (Degree/s)	Condition	Description
1.1	Tracking	1	<1	0	Freewheeling	No driver input
1.2	Tracking	1	<1	0	Panic steering	360° CCW steer angle at a rate of 720 degree/s CCW
1.3	Tracking	1	<1	0	Panic braking	15 MPa braking pressure linearly developed over 0.5 s
1.4	Tracking	1	<1	0	Panic steering and braking	Combined panic steering and braking
2.1	Nontracking	0	$1 \leq \theta_{SS} < 15$	0	Panic steering	360° CCW steer angle at a rate of 720 degree/s CCW
2.2	Nontracking	0	$1 \leq \theta_{SS} < 15$	0	Panic braking	15 MPa braking pressure linearly developed over 0.5 s
2.3	Nontracking	0	$1 \leq \theta_{SS} < 15$	0	Panic steering and braking	Combined panic steering and braking
3.1	Nontracking	0	≥15	15 CCW	Constant steering	360° constant CCW steering
3.2	Nontracking	0	≥15	15 CCW	Constant braking	Constant 15 MPa braking pressure
3.3	Nontracking	0	≥15	15 CCW	Constant steering and braking	Combined constant steering and braking

1 MPa = 145.038 psi.
PR = perception–reaction.

VEHICLE SELECTION AND MODELING

This section describes how the research team selected vehicle makes and models to use when conducting the vehicle dynamics analyses in phase II. A brief overview of the proposed model development process is also presented.

Vehicle Selection

The research team selected the following five vehicle classes by placing an emphasis on developing design guidelines that account for and are applicable to a range of vehicle classes currently on the Nation's roads based on their characteristics and with consideration of sales:

- Small passenger sedan.
- Large passenger sedan.
- SUV.
- Pickup truck.
- Minivan.

The research team recommended a vehicle make and model for each vehicle class to be modeled and subsequently used in the vehicle dynamics simulation analyses in phase II. The research team selected the vehicle makes and models primarily using 2016 U.S. vehicle-sale data, with some consideration given to crash data analysis conducted under NCHRP Project 17-55 that identified vehicles most likely to roll over on slopes.[12] Each vehicle that appeared in the sales data was classified into a specific vehicle category using the Insurance Institute for Highway Safety vehicle-classification method specified by its Highway Loss Data Institute.[3]

For the small passenger sedan, the Nissan® Versa was selected because it had 65.9-percent higher sales than the next highest sales of a small car model in the year 2016. For the large passenger sedan, the Honda® Accord was selected (even though the Toyota® Camry had the highest sales) because it had the most rollovers on slopes in the NCHRP Project 17-55 crash data analysis and its sales were only about 12-percent less than the Toyota Camry.[12] For the SUV, the Ford® Explorer was selected because it had the highest sales and the most rollovers on slopes in the crash data analysis. For the pickup truck, the Ford F-series was selected because it had about 43-percent higher sales than the next pickup truck. It is recommended that the minivan make and model be selected based on sales volume.

Vehicle Modeling

One of the tasks in phase II will be developing the vehicle dynamics models of the vehicles selected for the simulation analysis. Researchers have developed vehicle models for various vehicle types in the past.[10,12] This section presents a brief description of the vehicle-development process using a small car model as an example.

The vehicle-development process started with an evaluation of the preset vehicle models included in the CarSim library. The research team performed this evaluation to select a base model in the vehicle library that most closely resembled the vehicle being modeled. The evaluation was based on factors like vehicle mass, weight distribution, dimensions

(i.e., wheelbase, wheel center height, and vehicle length), CG location, and various engine specifications. The research team determined that CarSim's Class-B car model (figure 56) was the closest to the passenger car, so it was selected as the base model for further development.

Figure 56. Illustration. Class-B vehicle model used as the base model for developing the desired small car model.

To develop a representative model of the small car, the research team made changes to the base vehicle model, including modifying the sprung mass, unsprung mass, suspension geometry, suspension spring and damper properties, bump-stop locations and travel distance, vehicle moments of inertia, steering parameters, tire sizes, and overall body dimensions. Various dimensions and properties of the vehicle were directly measured using an exemplar vehicle. Because the research team was unable to perform the special testing required to determine vehicle roll, pitch, and yaw moments of inertia, these values were taken from the Expert AutoStats® software database, which is commonly used in the crash-reconstruction field. The moments of inertia in this software are approximate and based on analytical calculations.[67]

In addition to measuring various dimensions and properties of the vehicle, the research team also determined coordinates of seven hard points (i.e., relatively stiff structural locations) under the vehicle. If these hard points come into contact with the terrain, significant ground-to-vehicle forces that can influence the trajectory of the vehicle may occur. The SIM has an algorithm for modeling contact between the terrain and vehicle during an encroachment simulation and uses these hard points to apply contact forces to the vehicle if ground penetration is detected during the simulation.

The vehicle-modeling methodology discussed in this section is recommended when developing vehicle models for future simulation efforts.

HORIZONTAL-CURVATURE CONDITIONS

Design characteristics of the roadway can influence vehicle rollover probability. Among the leading roadway factors are the presence of horizontal curves and their associated superelevation. A study of rural two-lane roads found that about one-third of all slope rollover crashes and one-half of all slope rollover fatalities take place on curves.[3] As such, the research team recommends that phase II investigate roadways with horizontal curves.

Highway design elements should, as far as economically practical, be designed to provide safe, continuous operation at a speed likely to be observed under normal conditions for that roadway. This approach can be achieved by using design speed as an overall design control. The design of roadway curves should be based on an appropriate relationship between design speed and curvature and their joint relationships with superelevation and side friction.[49] The following discussion is based on design guidance of horizontal curves in AASHTO's Green Book.[49]

A simple curve has four primary variables: radius, design speed, side friction factor, and superelevation. From the laws of mechanics, the basic formula that governs vehicle operation on a curve is as shown in the equation in figure 57.

$$\frac{0.01e+f}{1-0.01ef} = \frac{v^2}{gR} = \frac{0.067V^2}{R} = \frac{V^2}{15R}$$

Figure 57. Equation. Relationship between vehicle speed and horizontal-curve properties.

Where:
e = rate of roadway superelevation (percent).
f = side friction (demand) factor.
v = vehicle speed (ft/s).
g = gravitational constant (32.2 ft/s^2).
V = vehicle speed (mph).
R = radius of the curve (ft).

Based on Chapter 3 section 3.3.2, General Considerations, in the Green Book, limiting values for superelevation rate (e_{max}) and side friction demand (f_{max}) have been established for curve design.[49] For e, there are practical upper limits to consider on a horizontal curve, such as climate, constructability, adjacent land use, and frequency of slow-moving vehicles. For f, the upper limit is the friction at the point of an impending tire skid. The friction value used for a design is typically substantially less than the coefficient of friction at an impending skid. Based on Chapter 3 section 3.3.3, Design Considerations, in the Green Book, the maximum superelevation rate common for highways use is 10 percent (although 12 percent is used in some cases).[49] Superelevation rates above 8 percent are used only in areas without snow and ice. Therefore, superelevation rates of 4 to 8 percent in 2-percent increments are recommended for defining curved roadways in the phase II simulation matrix.

Table 13 presents the minimum curve radii for a design using limiting values of superelevation and friction. Curve radii ranging from 1,200 to 2,800 ft seem to capture typical design practices for high-speed roadways ($\geq$50 mph). However, tighter curve radii and/or curves that are underdesigned for the design speed of the roadway can be particularly problematic in terms of both roadside encroachment frequency and rollover probability. Curve radius is related to degree of curvature using the equation shown in figure 58.

Table 13. Minimum radius for design of rural highways, urban freeways, and high-speed urban streets using limiting values of *e* and *f*.

Design Speed (mph)	Maximum *e* (%)	Limiting Values of *f*	Total (*e*∕100 + *f*)	Calculated Radius (ft)	Rounded Radius (ft)
15	4.0	0.175	0.215	70.0	70
20	4.0	0.170	0.210	127.4	125
25	4.0	0.165	0.205	203.9	205
30	4.0	0.160	0.200	301.0	300
35	4.0	0.155	0.195	420.2	420
40	4.0	0.150	0.190	563.3	565
45	4.0	0.145	0.185	732.2	730
50	4.0	0.140	0.180	929.0	930
55	4.0	0.130	0.170	1,190.5	1,190
60	4.0	0.120	0.160	1,505.0	1,505
15	6.0	0.175	0.235	64.0	65
20	6.0	0.170	0.230	116.3	115
25	6.0	0.165	0.225	185.8	185
30	6.0	0.160	0.220	273.6	275
35	6.0	0.155	0.215	381.1	380
40	6.0	0.150	0.210	509.6	510
45	6.0	0.145	0.205	660.7	660
50	6.0	0.140	0.200	836.1	835
55	6.0	0.130	0.190	1,065.0	1,065
60	6.0	0.120	0.180	1,337.8	1,340
65	6.0	0.110	0.170	1,662.4	1,660
70	6.0	0.100	0.160	2,048.5	2,050
75	6.0	0.090	0.150	2,548.4	2,510
80	6.0	0.080	0.140	3,057.8	3,060
15	8.0	0.175	0.255	59.0	60
20	8.0	0.170	0.250	107.0	105
25	8.0	0.165	0.245	170.8	170
30	8.0	0.160	0.240	250.8	250
35	8.0	0.155	0.235	348.7	350
40	8.0	0.150	0.230	465.3	465
45	8.0	0.145	0.225	502.0	500
50	8.0	0.140	0.220	760.1	760
55	8.0	0.130	0.210	963.5	965
60	8.0	0.120	0.200	1,204.0	1,205
65	8.0	0.110	0.190	1,487.4	1,485
70	8.0	0.100	0.180	1,820.9	1,820
75	8.0	0.090	0.170	2,213.3	2,215
80	8.0	0.080	0.160	2,675.6	2,675
15	10.0	0.175	0.275	54.7	55
20	10.0	0.170	0.270	99.1	100
25	10.0	0.165	0.265	157.8	160
30	10.0	0.160	0.260	231.5	230
35	10.0	0.155	0.255	321.3	320
40	10.0	0.150	0.250	428.1	430
45	10.0	0.145	0.245	552.9	555
50	10.0	0.140	0.240	696.8	696
55	10.0	0.130	0.230	879.7	880
60	10.0	0.120	0.220	1,094.6	1,095

Design Speed (mph)	Maximum *e* (%)	Limiting Values of *f*	Total (*e*∕100 + *f*)	Calculated Radius (ft)	Rounded Radius (ft)
65	10.0	0.110	0.210	1,345.8	1,345
70	10.0	0.100	0.200	1,838.8	1,840
75	10.0	0.090	0.190	1,980.3	1,980
80	10.0	0.080	0.180	2,378.3	2,380

$$Degree\ of\ curvature = \frac{5729.59}{Curve\ Radius\ in\ ft}$$

Figure 58. Equation. Degree of curvature.[49]

Table 14 presents curve radii associated with different degrees of curvature.

Table 14. Horizontal curve radius associated with degree of curvature.

Degree of Curvature	Curve Radius (ft)
1	5,730
2	2,865
3	1,910
4	1,432
5	1,146
6	955
7	819
8	716
9	637
10	573

As part of their analysis of 7 yr of crash data from 1999 to 2005 in the State of Washington, van Schalkwyk and Washington determined rates of ROR crashes for different categories of horizontal degrees of curvature.[68] Figure 59 shows the ROR crashes and severe crash rates for different degrees of roadway curvature. The results indicate that an increase in degree of curvature generally corresponds to an increase in crash and severe crash rates. Crash rates appear to increase steadily beyond a degree of curvature of 2 but begin a more substantial increase at a degree of curvature of 9 and greater.
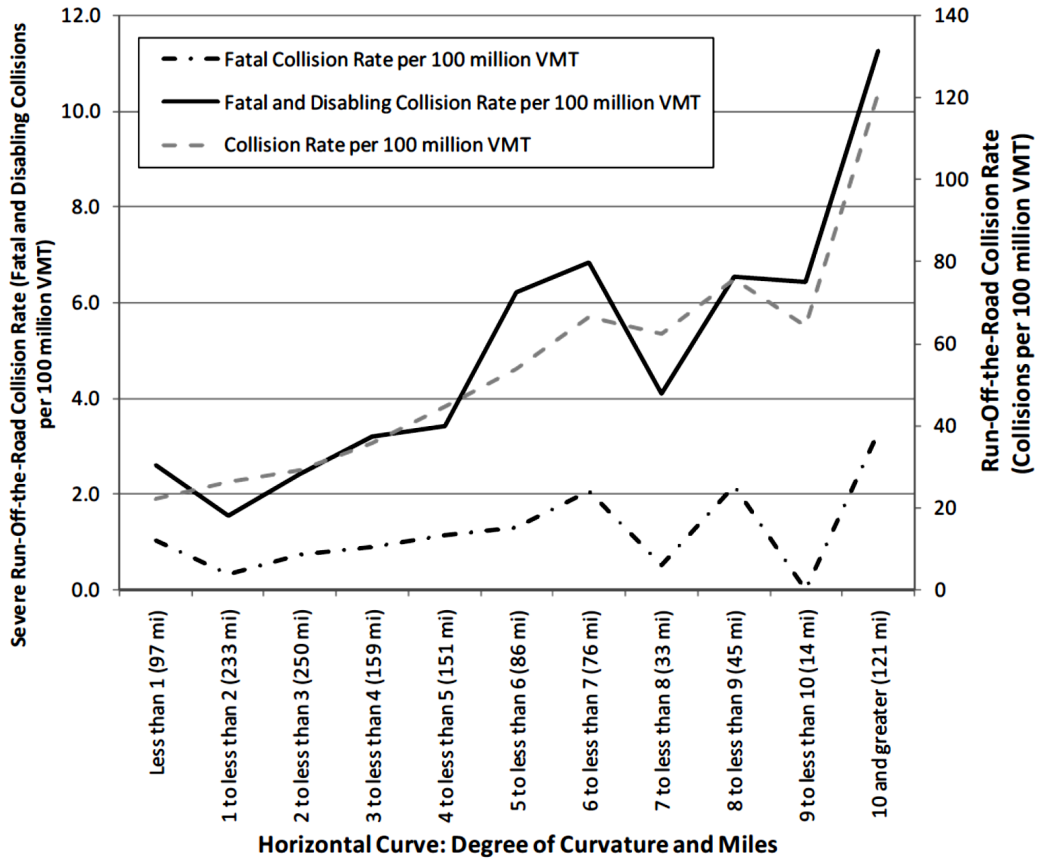
© 2008 Washington State Department of Transportation.
VMT = vehicle miles traveled.

Figure 59. Graph. ROR crash rates for different degrees of horizontal curvature.[(68)]

Based on this information, the research team recommends a broad range of curvatures for evaluation, with an emphasis on higher degrees of curvature because those are associated with higher crash rates. The horizontal curves proposed for study in phase II are curves with a degree of curvature of 4.0, 5.5, 7.0, 8.0, 9.0, and 10.0 degrees.

CHAPTER 7. DATA ANALYTICS

INTRODUCTION

Data analytics has shown great promise and usefulness in many sciences and industries where a large amount of data (a.k.a., big data) must be analyzed for trends, sensitivities, and probabilistic prediction of desired responses. Advanced algorithms, approaches, and tools have been developed in response to the exponential growth of data in many fields, including transportation. The research team recommends using data analytics to analyze desired vehicular responses as functions of roadway and roadside variables. The research team recommends constructing an extensive database of desired responses, design variables, and encroachment conditions via massive simulation runs and then constructing a higher-order metamodel (e.g., response surface). The constructed metamodel can be used for probabilistic analyses to develop sensitivities, trends, and probabilities via Monte Carlo (MC) simulations.

METAMODELING

A neural network (NN) is a computing architecture that consists of massively parallel interconnections of simple neurons. Engineers are interested in NNs for problem-solving. NNs can adapt to changes in data, learn the characteristics of input signals, and perform filtering operations that are beyond the capabilities of conventional linear filtering techniques because of their nonlinear nature. NNs can be used for pattern classification by defining nonlinear regions in the feature space. They can also overcome limitations of conventional computers because of their ability to learn and their parallel architecture.

NNs can be divided into three basic categories: feedforward, feedback, and self-organizing.[69,70] Each category is based on a different philosophy and obeys different principles. Feedforward NNs contain one or more layers of nonlinear processing elements or units. The elements belonging to neighboring layers are connected by sets of synaptic weights. These neural architectures are called feedforward because the output of each layer feeds the next layer of elements. The Perceptron and Adaline are the earliest feedforward neural architectures. Multilayered NNs include one or more layers of hidden elements between the input and output layer (figure 60).[71] A feedforward NN may be seen as a system transforming a set of input patterns into a set of output patterns; this type of NN can be trained to provide a fit of a measured or calculated desired response to a given input. The NN achieves the fit by adapting its synaptic weights during the learning phase based on learning rules that minimize the difference between the NN's fit and the desired response. These rules are set by the user of the NN. Training feedforward NNs requires a set of input and output patterns. This type of learning is called supervised learning, as explained in the previous sentences.
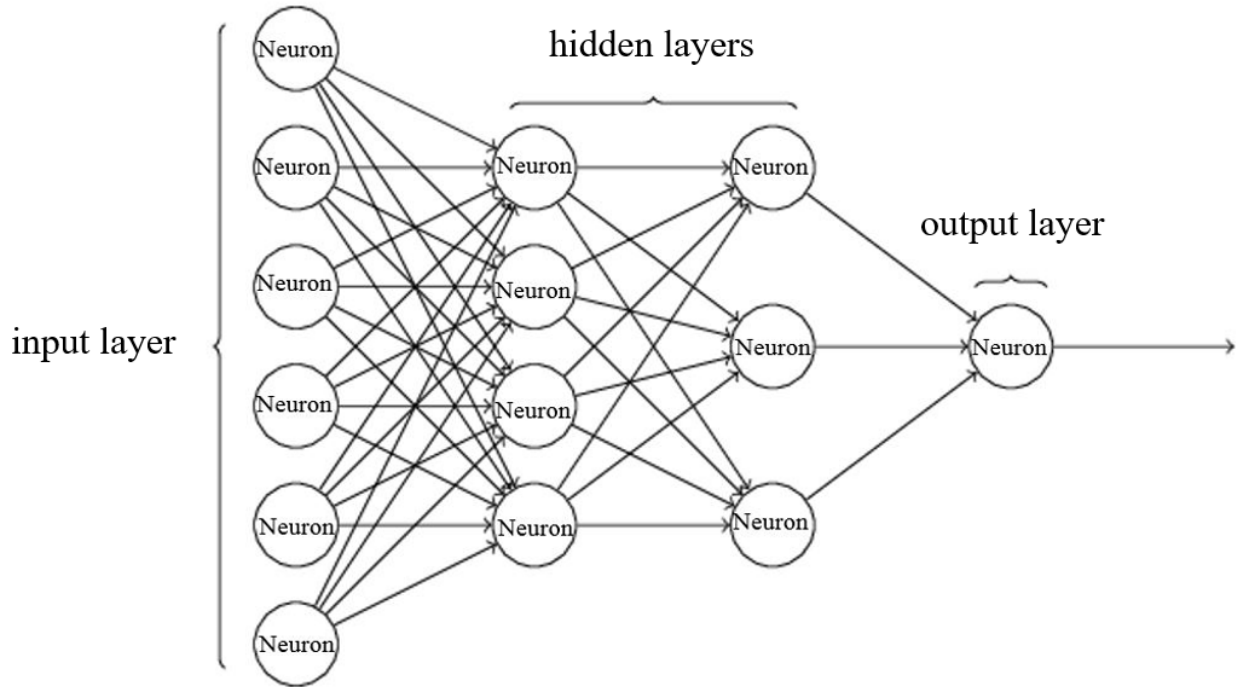
Figure 60. Illustration. NN.[(71)]

MC SIMULATION

The MC method is a statistical approach to the study of differential equations, or more generally, of integral-differential equations that occur in various branches of natural sciences.[(72)] The MC method provides approximate solutions to various mathematical problems by performing statistical sampling experiments using extensive computational evaluations of such equations.[(73)] This method applies to problems with no probabilistic content and those with innate probabilistic structure.

The MC method uses a random selection of independent variables (i.e., design variables) to select the point where the desired function or performance will be evaluated. These evaluations give a more accurate representation of the overall desired response once a large number of evaluations are conducted to prevent clustering and bias. A simple example would be determining the probability of heads or tails by conducting large number of coin flip experiments. The MC method becomes more expensive and increases in complexity as the number of variables increases. The descriptive statistics, reliability information on all constraints, number of times a specific constraint was violated during the simulation, probability of violating the bounds, confidence region of probability, and reliability analysis for each constraint can be computed for all responses. Therefore, the MC method can be used to simulate the uncertainty of variables using random samples given the variable distribution.

COMBINING THE MC METHOD WITH METAMODELS

To overcome the cost of brute-force MC analysis, researchers in the field of optimization developed a number of analysis methods where MC analyses would be performed on the

metamodel. This approach starts by constructing the metamodel using a sample set that is significantly less than the massive set of samples needed for the brute-force MC analysis but still sufficient to construct a metamodel with the desired accuracy. The reduction of the sampling size depends on the complexity of the problem at hand, the nature of the metamodel, and the number of the iterations needed to reach the optimum solution. Once the sample set is obtained, MC would randomly sample the constructed response surface.

The process for incorporating the combined MC and response surface approach is shown in figure 61, which represents the overall flow of the data analytics process. Existing codes, such as CarSim and the SIM, are used to generate the outcomes (i.e., responses) of vehicular encroachments. Vehicle type, encroachment conditions (e.g., speed and angle), and selected roadway and roadside design variables are all considered. The metamodel chosen is the NN, which can capture higher nonlinear responses better than other approximations, such as linear approximation. Roll angle probability and lateral travel responses can be determined using MC simulation of the constructed NN.
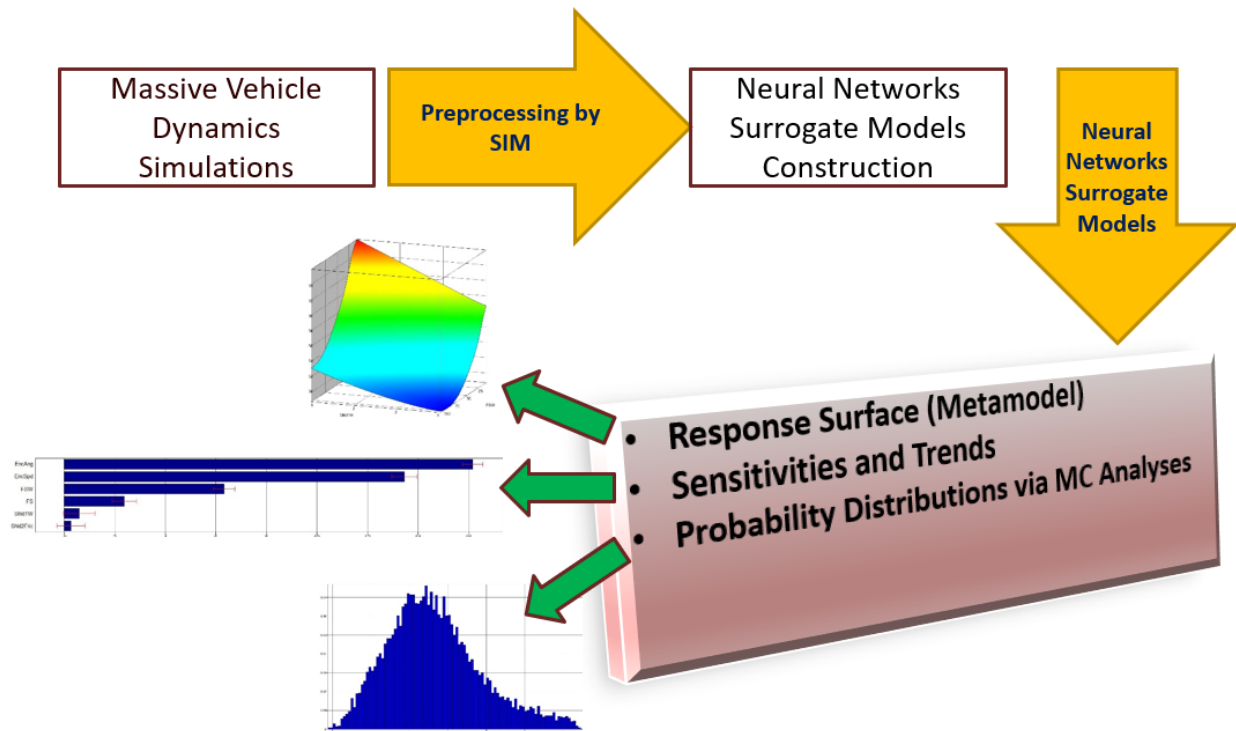
Source: FHWA.

Figure 61. Flowchart. Recommended data analytics flowchart using metamodel and MC.

The program used for building the response surface and conducting the MC simulation was LS-OPT.[74] LS-OPT is a program that allows the user to define the design process, explore the design space, and compute optimal designs according to user-specified constraints and objectives. Additionally, LS-OPT offers seven types of response surfaces: polynomial, sensitivity, feedforward NN, radial basis function network, kriging, support vector regression,

and user-defined. LS-OPT has a built-in MC analysis tool that can be used for both brute-force MC and combined MC–metamodel analyses. The research team investigated different response surfaces for this project and ultimately chose the feedforward NN because it has the highest accuracy given the metrics of interest.

The research team constructed an example of using the data analytics approach with LS-OPT using the following variables: shoulder width, foreslope ratio, and foreslope width. The encroachment conditions were speed and angle. The specific values of the roadside variables used are listed in table 15. The vehicle model was a pickup truck. The research team extracted this dataset from data generated under NCHRP Project 17-55 using vehicle dynamics simulation.

Table 15. Design variable ranges.

Design Variable	Description	Values
Shld1W	Shoulder width (ft)	1, 2, 3, 4
FS	Foreslope ratio (H:V)	10:1, 6:1, 4:1, 3:1, 2:1
FSW	Foreslope width (ft)	8, 16, 32, 105
EncSpd	Encroachment speed (mph)	25, 35, 45, 55, 65, 75
EncAng	Encroachment angle (degree)	5, 10, 15, 20, 25, 30
Shld2Fric	Shoulder friction	0.75

Figure 62 and figure 63 show the response surfaces for the vehicular maximum roll angle and maximum extent of lateral travel, respectively. Only independent variables for a given response are shown because of the higher dimensionality of the surface and visual limitation of 3D surfaces to the human eye. These response surfaces provide information about how each variable influences rollover probability and the interaction between the variables.
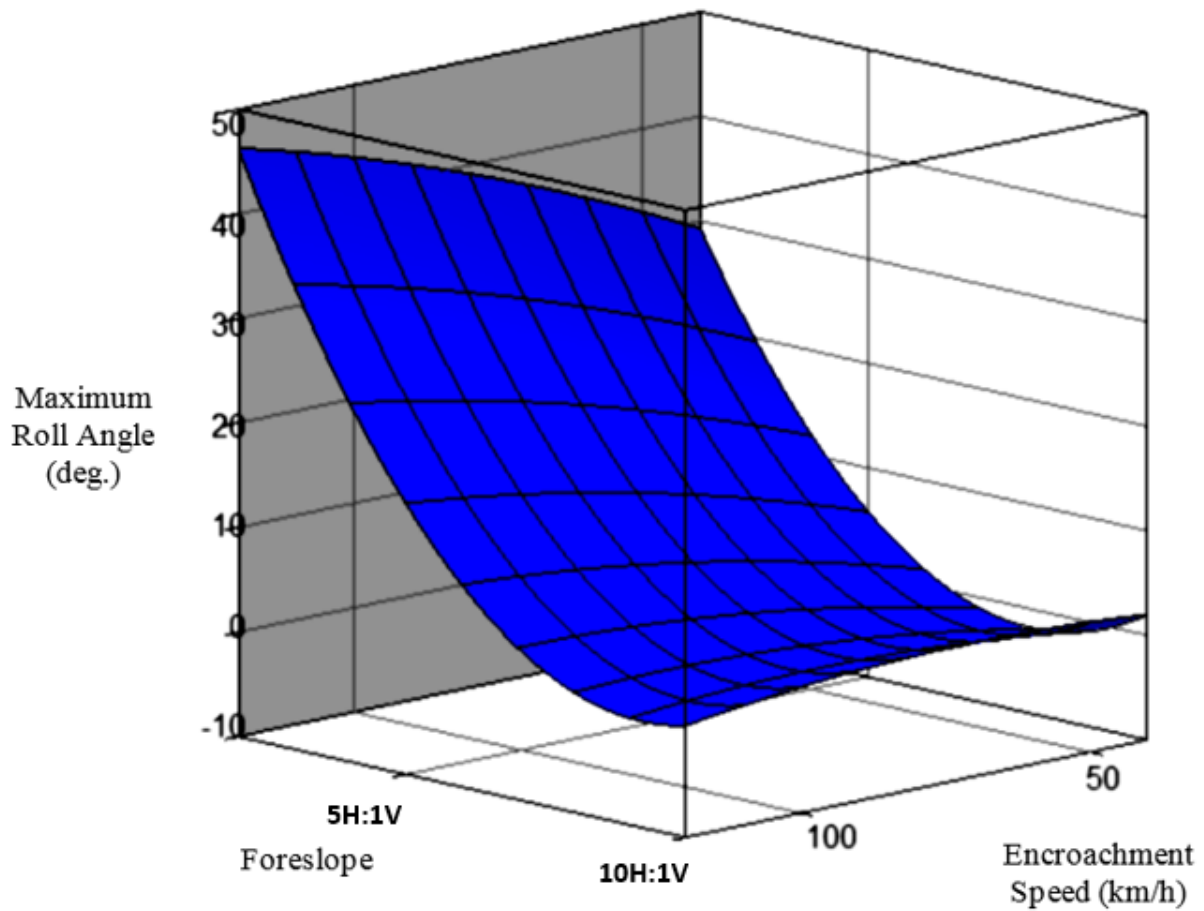
Figure 62. Illustration. Maximum roll angle response surface as a function of the foreslope ratio and encroachment speed.
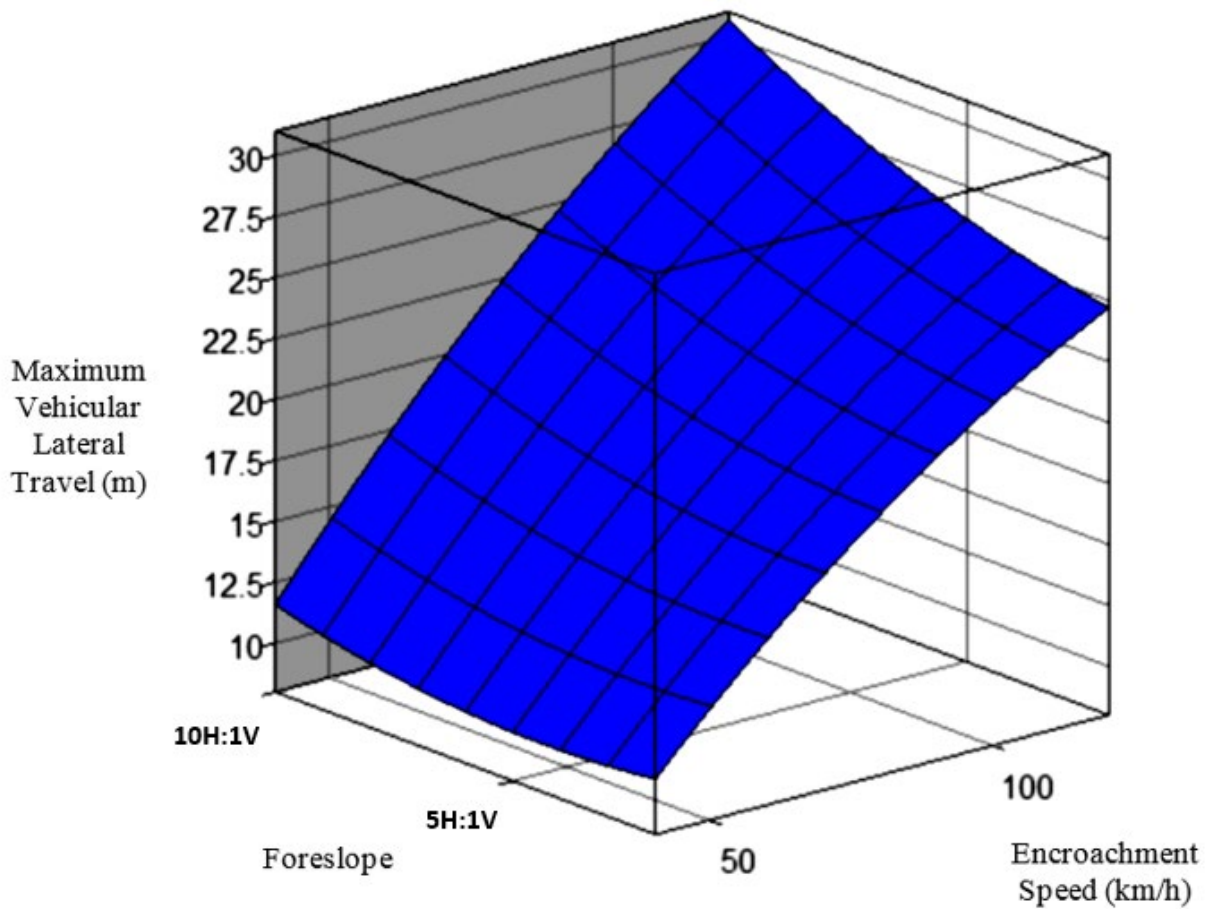
Figure 63. Illustration. Maximum extent of lateral travel response surface as a function of the foreslope ratio and encroachment speed.

Figure 64 shows the quality of the maximum lateral extent of travel response surface. The metrics used to assess the quality of these surfaces are the root mean square error (ε_{RMS}) and the coefficient of determination (R^2). The surface level of accuracy is good when R^2 is close to 1 and ε_{RMS} is close to zero. Practical values depend on the problem at hand and desired accuracy. R^2 and ε_{RMS} are calculated using the equations in figure 65 and figure 66, respectively.
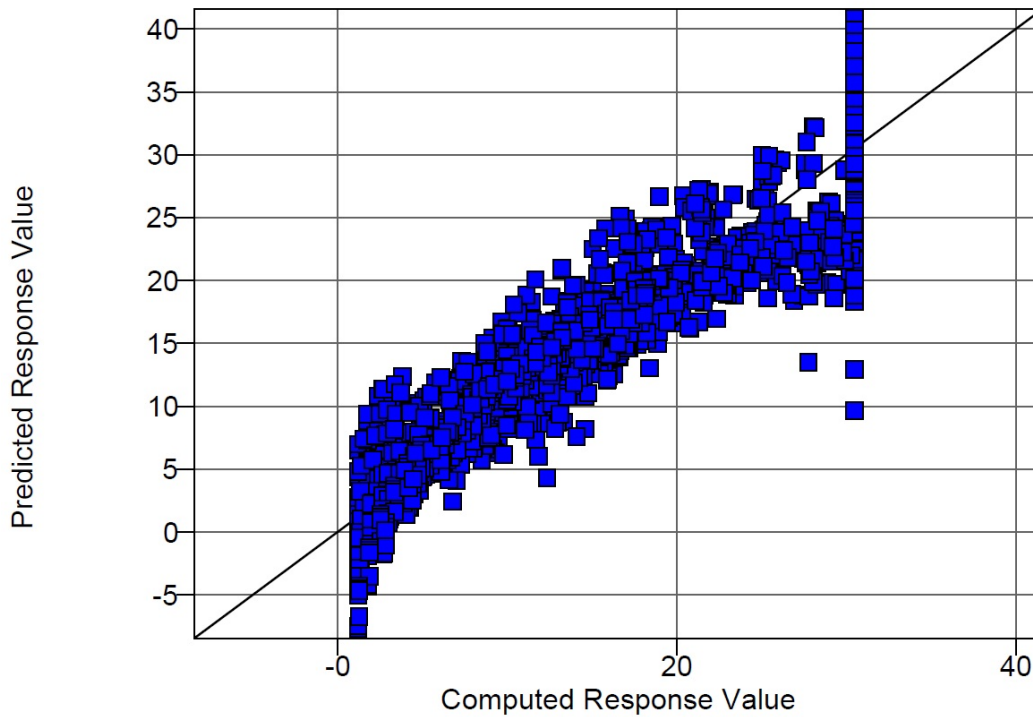
Source: FHWA.

Figure 64. Graph. Quality of lateral travel response surface.

$$R^2 = \frac{\sum_{i=1}^{P}(\hat{y_i} - \bar{y}_i)^2}{\sum_{i=1}^{P}(y_i - \bar{y}_i)^2}$$

Figure 65. Equation. R^2.

Where:
P = number of design points.
y_i = predicted response.
$\bar{y}_i$ = mean of responses.
$\hat{y}_i$ = actual response.

$$\varepsilon_{RMS} = \sqrt{\frac{1}{P}\sum_{i=1}^{P}(y_i - \hat{y}_i)^2}$$

Figure 66. Equation. ε_{RMS}.

111

SENSITIVITIES, TRENDS, AND RISK MEASURES OUTPUT

This section gives an example of how the MC method can be used for studying sensitivities, trends, and risk measures. Once MC analyses are conducted on the metamodel of interest, many measures can be used to understand the relationship between design variables and the response of interest. Two common sensitivities measures are presented in this section: the analysis of variance (ANOVA) measure and the global sensitivity measure.

The ANOVA of the polynomial metamodel method is presented as a demonstration. Figure 67 shows a bar chart of ANOVA results for a sample of design and response variables. The bars show which design variables have the most influence on the response (in this case, the maximum roll angle). The ANOVA value and confidence interval are represented by solid bars and vertical lines, respectively. When the confidence interval is small, the contribution of that variable is significant. Figure 68 illustrates this concept.
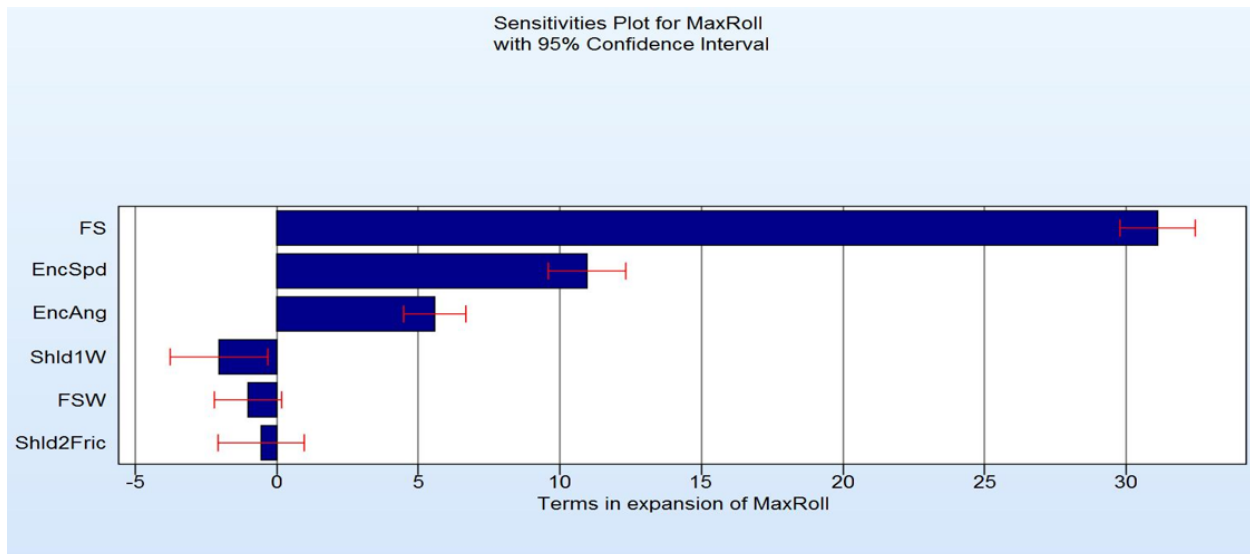
Source: FHWA.

Figure 67. Bar chart. ANOVA for the maximum roll angle.
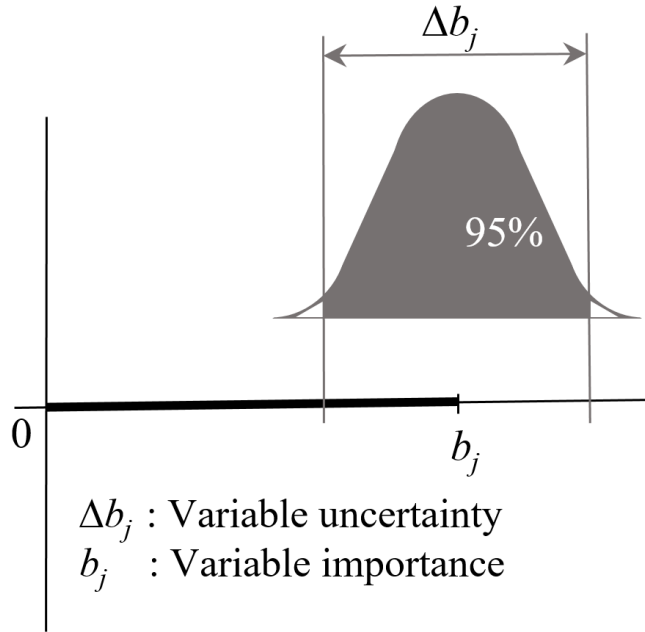
Source: FHWA.
Δb_j = variable uncertainty; b_j = variable importance.

Figure 68. Illustration. ANOVA value with 100*(1 − alpha)% confidence level.

In this analysis example, the foreslope ratio had the most substantial contribution to the maximum roll angle and a high confidence level. Shoulder width and shoulder friction had the smallest contribution to the maximum roll angle and the lowest confidence levels.

The global sensitivity measure is also known as the stochastic sensitivity analysis or Sobol's analysis. The variance of the response may be written using the Sobol's indices approach shown in figure 69.

$$f(x_1, \ldots, x_n) = f_0 + \sum_{i=1}^{n} f_i(x_i) + \sum_{i=1}^{n} \sum_{j=i+1}^{n} f_{ij}(x_i, x_j) + \ldots + f_{1,2,\ldots,n}(x_1, \ldots, x_n)$$

Figure 69. Equation. Response variance.

Where:
  f_i = response measure of interest.
  x_i, x_j = design variables of interest.

Figure 70 and figure 71 show the results from global sensitivities analysis for the maximum roll angle and maximum extent of lateral travel, respectively. For the maximum roll angle, the foreslope ratio had the greatest percentage of influence on the response and encroachment speed had the second largest influence. For the maximum lateral extent of travel, encroachment angle had the greatest percentage of influence and encroachment speed had the second largest influence.

Global Sensitivities Plot for MaxRoll
Mean = 10.6278, Total variance = 32.1372, Noise variance = 76.4458
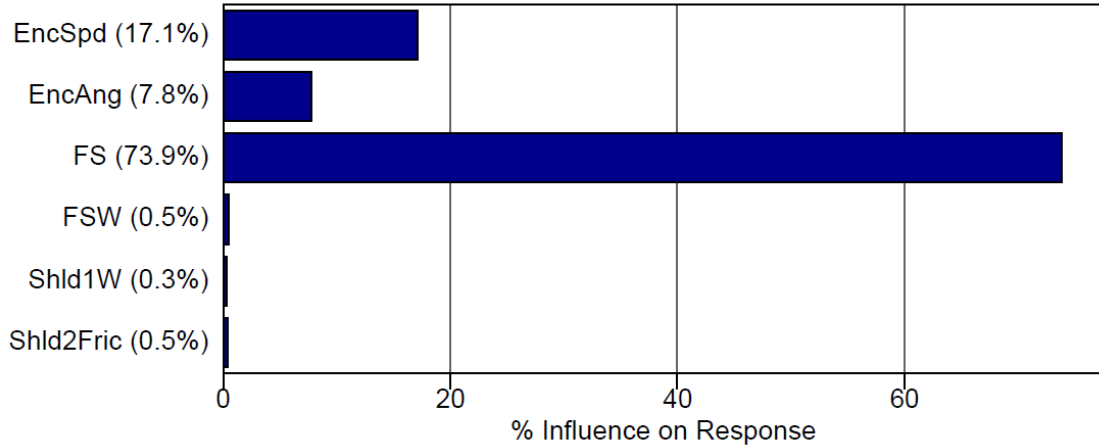
Source: FHWA.

Figure 70. Bar chart. Sensitivity of the maximum roll angle response on the design variables and encroachment conditions.

Global Sensitivities Plot for MaxLatTrav
Mean = 17.0197, Total variance = 43.0659, Noise variance = 10.6608
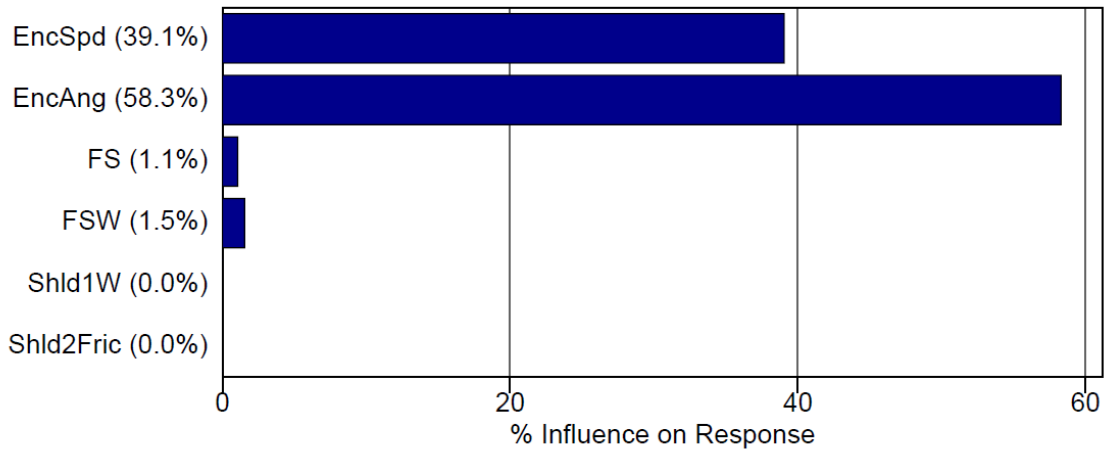
Source: FHWA.

Figure 71. Bar chart. Sensitivity of the maximum lateral extent of travel response on the design variables and encroachment conditions.

114

Both sensitivity measures can help when trying to understand what variables have the most influence on a desired response. This information can be valuable when developing design guidelines and selecting the most effective safety treatments for a given roadway configuration by allowing researchers to focus on the design variables that have a larger effect on the response.

Another important feature of the MC simulation of the metamodel is the ability to determine probabilities of attaining a certain response value given a set of distributions of design and encroachment parameters. For example, the MC simulation can calculate the probability of the maximum roll angle not exceeding 30 degrees given a specific road curvature, a posted speed, a vehicular speed, roadside design elements, and encroachment angle distributions. The designer can change the maximum roll angle threshold and let the MC analysis calculate the associated probability. Alternatively, the technique can be used to change the values of different roadside design elements to reduce rollover probability.

In summary, the research team recommends data analytics for phase II of this research because it will give the research team and designer a discriminate assessment of the effect that roadway and roadside design variables have on a given safety metric (e.g., rollover probability). The approaches and tools described in this section will greatly enhance the ability to analyze large datasets generated through large-scale vehicle dynamics simulations, such as those described in chapter 6 of this report. Data analytics offers innovative methods and techniques for understanding and interpreting trends and relationships that exist between roadway and roadside design variables of interest. The data analytics approach will enable developing more meaningful and effective design guidance.

CHAPTER 8. SUMMARY AND CONCLUSIONS

One of the tasks of phase I was to review previous research related to vehicle rollovers. The purpose of this review was to understand the state of the art in rollover modeling and simulation to better develop a comprehensive plan for further study of rollover causation factors that would lead to developing design guidelines to reduce rollovers.

The research team performed an extensive literature review (chapter 2). Relevant past and ongoing research studies were reviewed and summarized. Information gleaned from this review was used to identify key factors that influence rollovers, capabilities and limitations of existing simulation analysis tools, and recommendations for advancing the next generation of rollover modeling and simulation.

During the literature review, the research team placed special emphasis on reviewing research performed by Glennon et al.[4] However, any research relating rollovers to various roadway and roadside design elements was critically reviewed to assess current relevance. The work by Glennon et al. in the 1980s was based on a small number of vehicle dynamics simulations. Most of the recommendations resulting from this research were general in nature and based on limited data. As described in chapter 2, the research by Glennon et al. was limited in scope and did not account for many variables that can now be considered using today's simulation technologies and computational capabilities.[4]

One of the initial objectives at the beginning of this project was to recreate some of the work performed by Glennon et al. to verify results, particularly any recommendations related to the design of horizontal curves. However, the review concluded that this effort would be of little value for mitigating the rollover problem. Glennon et al.'s research guidance was based on a 1971 vehicle model, few roadway and roadside variables and configurations, and extremely limited encroachment conditions. The research team further concluded that using currently available state-of-the-art simulation tools and technology would enable a far more comprehensive study that would provide more specific design guidance for a much broader range of design variables. This approach would, therefore, offer a better opportunity to achieve a meaningful reduction in rollover crashes.

As noted in chapter 2, several ongoing research studies (e.g., NCHRP Project 16-05 and NCHRP Project 17-55) are developing roadside design guidance with the objective of reducing rollovers associated with vehicle encroachments onto roadside slopes and ditches. These studies have used some of the latest simulation technologies and are investigating a large number of encroachment and roadside design variables. However, these studies primarily focused on straight roadways. Although some guidance has been developed under these projects to assist with roadside design on curves, the scope of this guidance is somewhat limited.

Given that rollover crashes on roadways with horizontal curves are underresearched yet significantly overrepresented in crash data, the research team concluded that this area would significantly benefit from more comprehensive research. For example, a study of rural two-lane roads found that about one-third of all slope rollover crashes and one-half of all slope rollover fatalities took place on curves.[3] Therefore, the focus of the current and future phases of this

project became the development and execution of a next-generation simulation analysis strategy to investigate design factors that influence rollovers on roadways with horizontal curves and the development of design guidance for mitigating these rollovers.

The research team recommends performing a comprehensive computer simulation study as the next phase of this research. The computer simulation approach permits a detailed analysis of vehicle kinematics for a wide range of variables for which data are not otherwise available. The results could be used to determine the influence of various design variables on vehicle stability and develop relationships between these variables that could not otherwise be obtained.

The research team determined a multirigid-body vehicle dynamics simulation to be the best tool for developing comprehensive design guidance intended to reduce rollovers on curves. There are several benefits to using vehicle dynamics simulation, including the ability to incorporate a large number of roadway and roadside design variables, shorter computational time requirements, the ability to simulate long event durations associated with roadside encroachments, and the ease of creating multiple new vehicle models using available or readily obtainable vehicle measurements and properties. In comparison, finite-element modeling is severely limited in the number of simulations that can be performed because of the significantly higher complexity and computational time requirements for each simulation. Further, only a limited number of finite-element vehicle models are available in the public domain, and the development of new vehicle models is an expensive and time-consuming task.

As discussed in chapter 3, vehicle dynamics simulations provide a comparable and sometimes improved level of accuracy for determining vehicle kinematics during a roadside encroachment. The availability of a database of base vehicle models, subsystems, and new vehicle features, such as ABS braking and advanced suspension properties, and the ability to apply reliable steering and braking inputs and batch a large number of simulation cases were key reasons for recommending the vehicle dynamics simulation method.

Although current simulation tools offer the opportunity for in-depth investigation of numerous factors and variables that influence vehicle rollover, as noted in chapters 3 and 4, underlying approximations that limit the accuracy of rollover prediction during complex roadside encroachments still exist. The most significant of these limitations is the current technique for modeling tire–soil interaction. Realistic tire–soil interaction can be critical when assessing the response of a vehicle encroaching on the roadside, particularly one that is nontracking. In the previously referenced study of rural two-lane roads, the researchers found that most vehicles that rolled over on side slopes and ditches were skidding (or nontracking) as they left the roadway.[3] Moreover, there are limitations to incorporating vehicle-body-to-terrain contact in these simulations. The existing method of incorporating this contact in the simulation is rudimentary, and its validation and robustness can be improved.

One of the main objectives of phase I was to develop a detailed plan for enhancing vehicle rollover simulation capabilities to truly support the next generation of rollover research. In pursuit of this objective, the research team identified several key areas where meaningful improvements can be made and described plans for achieving these improvements in chapter 4. The primary areas in need of significant improvement in predictive accuracy of rollover modeling are the development and incorporation of a more sophisticated tire–soil interaction

model to capture soil furrowing forces and the enhancement and validation of a vehicle-body-to-terrain contact model. Experimental testing and finite-element simulation techniques can be used to obtain the necessary data to develop and validate these models. Enhancing the simulation and modeling tools in the manner proposed in this report will have lasting benefits for future research and support the next generation of rollover modeling and roadside encroachment simulation.

As part of the proposed strategy to support the next generation of rollover research, the research team developed a recommended simulation matrix of design and encroachment variables intended to develop guidelines for reducing rollovers on curved road segments. Chapter 5 presented the recommended parameters, along with their range of values and rationale for selection. Because of the complexity of the rollover problem and large number of encroachment and design variables that can influence it, the proposed simulation matrix consists of more than 14 million discrete encroachment simulations, each of which will have a generated outcome. This is an unprecedented number of simulations and an order of magnitude greater than any used in previous or ongoing projects. The analysis of this many variables using this many vehicle dynamics simulations will be a daunting but critical task. Such a study will be successful only if researchers can comprehensively analyze the resulting data to support the development of meaningful design guidelines that can be implemented to mitigate the rollover problem.

Another key aspect of the recommended strategy in support of next-generation rollover research is the use of data analytics to understand the influence and interaction of key roadway and roadside design variables on rollover probability. As described in chapter 6, data analytics offers innovative methods and techniques for understanding and interpreting the trends and relationships that will be captured within this large volume of data. Data analytics has become extremely useful because of the increased demand to analyze big data and affordability of computational resources. The recommended phase II research will generate a massive number of simulation outputs, so it is logical to implement an approach that uses data analytics compared to a traditional brute-force analysis method.

Finally, the results of the phase II simulation analyses will be used to identify design variables sensitive to rollover encroachment outcomes. This information will form the basis for developing relationships between roadway and roadside design variables and rollover probability. For example, it will be possible to establish relationships between roadway curvature, speed, and embankment slope ratios, among others. These relationships will form the basis for updating and expanding current guidance for designing roadway and roadside cross sections to lower the probability of rollover crashes on roads with horizontal curves.

REFERENCES

1. NHTSA. (n.d.). "Crashworthiness Data System." (Website). Available online: https://www.nhtsa.gov/national-automotive-sampling-system-nass/crashworthiness-data-system, last accessed July 4, 2020.

2. Muller, D. (2019). "Light Trucks Are Now a Record 69 Percent of the U.S. Market," *Automotive News*, January 7, 2019. Available online: https://www.autonews.com/sales/light-trucks-take-record-69-us-market, last accessed July 4, 2020.

3. Viner, J.G. (1995). "Rollovers on sideslopes and ditches." *Crash Analysis & Prevention*, *27*(4), pp. 483–491, Elsevier, Amsterdam, Netherlands.

4. Glennon, J.C., Neuman, T.R., and Leisch, J.T. (1983). *Safety and operational considerations for design of rural highway curves*, Report No. DOT-FH-11-9575, Federal Highway Administration, Washington, DC.

5. AASHTO. (2006). *Roadside Design Guide*, American Association of State Highway and Transportation Officials, Washington, DC.

6. Bligh, R.P., Miaou, S.-P., and Mak, K.K. (2004). *Determination of safe/cost-effective roadside slopes and associated clear distances*, NCHRP 17-11, Transportation Research Board, Washington, DC.

7. MSC Adams/Chassis version 2. (2002). (Computer software). MSC Software Corporation, Newport Beach, CA. Available online: https://www.mscsoftware.com/product/adams-car, last accessed July 21, 2020.

8. CarSim version 8.2.1. (2012). (Computer software). Mechanical Simulation Corporation, Ann Arbor, MI.

9. James Jr. M.E. and Ross Jr., H.E. (1974). *HVOSM User's Manual*, Texas Transportation Institute, College Station, TX.

10. Sheikh, N., Miaou, S.-P., and Bligh, R.P. (2012). *Guidelines for cost-effective safety treatment of roadside ditches*, NCHRP 16-05, Transportation Research Board, Washington, DC.

11. Bligh, R. (2010). *Placement of traffic barriers on roadside and median slopes*, NCHRP Project 22-22, Transportation Research Board, Washington, DC.

12. Sheikh, N.M., Bligh, R.P., Miaou, S.-P., and Cakalli, S. (2018). *Guidelines for slope traversability*, NCHRP 17-55, Transportation Research Board, Washington, DC.

13. MacAdam, C.C., Fancher, P.S., Hu, G.T., and Gillespie, T.D. (1980). *A computerized model for simulating the braking and steering dynamics of trucks, tractor-semitrailers, doubles, and triples combinations: User's manual—PHASE 4*, Report No, PB80-227994, Highway Safety Research Institute, Detroit, MI.

14. Google Scholar. (2020). "Google Scholar." (Website). Available online: https://scholar.google.com/, last accessed July 4, 2020.

15. Engineering Village. (2019). "Engineering Village." (Website). Available online: https://www.engineeringvillage.com/home.url, last accessed July 4, 2020.

16. TRB. (2019). "Transport Research International Documentation (TRID)." (Website). Available online: https://trid.trb.org/, last accessed July 4, 2020.

17. Zegeer, C.V., Stewart, R., Council, F., and Neuman, T.R. (1994). "Crash relationships of roadway width on low-volume roads." *Transportation Research Record*, *1445*, pp. 160–168, Transportation Research Board, Washington, DC.

18. Lord, D., Brewer, M.A., Fitzpatrick, K., Geedipally, S.R., and Peng, Y. (2011). *Analysis of roadway departure crashes on two-lane rural roads in Texas*, Report No. FHWA/TX-11/0-6031-1, Federal Highway Administration, Washington, DC.

19. Stine, J.S., Hamblin, B.C., Brennan, S.N., and Donnell, E.T. (2010). "Analyzing the influence of median cross-section design on highway safety using vehicle dynamics simulations." *Accident Analysis and Prevention*, *42*(6), pp. 1169–1777, Elsevier, Amsterdam, Netherlands.

20. Mak, K.K., and Sicking, D.L. (2003). *NCHRP Report 492: Roadside Safety Analysis Program (RSAP)—Engineer's Manual*, Transportation Research Board (TRB), Washington, DC.

21. Peng, Y., Geedipally, S.R. and Lord, D. (2012). "Effect of roadside features on single-vehicle roadway departure crashes on rural two-lane roads." *Transportation Research Record*, *2309*, pp. 21–29, Transportation Research Board, Washington, DC.

22. Sabbaghian, M.H., Kordani, A.A., Kallebasti, B.T., and Attari, A. (2015). "Effect of shoulder width and drop-off on vehicle rollover and shoulder crossover using vehicle dynamics simulations." Presented at the 5th International Symposium on Highway Geometric Design, Vancouver, Canada.

23. Lee, J. and Mannering, F. "Impact of roadside features on the frequency and severity of run-off roadway crashes: an empirical analysis." *Crash Analysis & Prevention*, *34*(2), pp. 149–161, Elsevier, Amsterdam, Netherlands.

24. Molan, A.M. and Kordani, A.A. (2014). "Multi-body simulation modeling of vehicle skidding and roll over for horizontal curves on longitudinal grades." Presented at the Transportation Research Board 93rd Annual Meeting, Washington, DC.

25. Hildebrand, E., Lougheed, P., and Hanson, T. (2007). "Relating roadside collisions to highway clear zone width." *Proceedings of the Canadian Multidisciplinary Road Safety Conference, XVIII*, Montreal, Canada.

26. Gross, F., Jovanis, P.P., Eccles, K., and Chen, K. (2009). *Safety evaluation of lane and shoulder width combinations on rural, two-lane, undivided roads*, Report No. FHWA-HRT-09-031, Federal Highway Administration, Washington, DC.

27. Hu, W. and Donnell, E.T. (2011). "Severity models of cross-median and rollover crashes on rural divided highways in Pennsylvania." *Journal of Safety Research*, *42*(5), pp. 375–382, Elsevier, Amsterdam, Netherlands.

28. Miaou, S. (2013). "Some limitations of the models in the highway safety manual to predict run-off-road crashes." *Transportation Research Record*, *2377*, pp. 38–48, Transportation Research Board, Washington, DC.

29. AASHTO. (2010). *Highway Safety Manual*, 1st ed. Vol. 1–3, AASHTO, Washington, DC.

30. Chou, C.C., McCoy, R.W., and Le, J. (2005). "A literature review of rollover test methodologies." *International Journal of Vehicle Safety*, *1*(1–3), pp. 200–237, Inderscience Publishers, Geneva, Switzerland.

31. Chou, C.C., Wagner, C.D., Yang, K.H., King, A.I., Hu, J., Hope, K., Arepally, S. (2008). "A review of math-based CAE tools for rollover simulations." *International Journal of Vehicle Safety*, 3(3), pp. 236–275, Inderscience Publishers, Geneva, Switzerland.

32. TNO. (1996). *MADYMO V5.2 user's manual 3-D*, TNO Road Vehicle Research Institute, Amsterdam, Netherlands.

33. Hallquist, J.O. (2014). *LS-DYNA keyword user's manual, version 971*, Livermore Software Technology Corporation, Livermore, CA.

34. Shu-ju, W., Yi-shan, P., Guo-sheng, Z., and Hai-tao, C. (2015). "Analysis of the rollover crash worthiness of the bus body structure based on ECE R66 regulation." *Journal of Highway and Transportation Research and Development* (English Edition), *9*(4), pp. 99–101, American Society of Civil Engineers, Reston, VA.

35. Parent, D.P., Kerrigan, J.R., and Crandall, J.R. (2011). "Comprehensive computational rollover sensitivity study, Part 1: influence of vehicle pre-crash parameters on crash kinematics and roof crush." *International Journal of Crashworthiness*, *16*(6), Taylor and Francis, Oxfordshire, UK.

36. Mongiardini, M., Grzebieta, R.H., Mattos, G.A., and Bambach, M.R. (2016). "Computer modelling of vehicle rollover crash tests conducted with the UNSW Jordan Rollover System." *International Journal of Crashworthiness*, *21*(3), Taylor and Francis, Oxfordshire, UK.

37. Marur P.R. and Namdeo, S. (2007). "Techniques for reducing computational time in vehicle rollover simulations." *International Journal of Vehicle Safety*, *2*(4), Inderscience Publishers, Geneva, Switzerland.

38. Linstromberg, M., Scholpp, G., and Scherf, O. (2005). "Test and simulation tools in a rollover protection development process." Presented at the Siemens Restraint Systems GmbH, ESV Conference, Washington, DC.

39. Garrott W.R. and Heydinger, G.J. (1992). *An investigation, via simulation, of vehicle characteristics that contribute to steering maneuver induced rollover*, SAE Technical Paper 920585, SAE International, Warrendale, PA.

40. Czechowicz M. and Mavros, G. (2014). "Analysis of vehicle rollover dynamics using a high-fidelity model." *Vehicle System Dynamics*, *52*(5), pp. 608–636, Taylor and Francis, Oxfordshire, UK.

41. Taheri, S., Sandu, C., Taheri, S., Pinto, E., and Gorsich, D. (2015). "A technical survey on terramechanics models for tire-terrain interaction used in modeling and simulation of wheeled vehicles." *Journal of Terramechanics*, 57, pp. 1–22, Elsevier, Amsterdam, Netherlands.

42. Taheri, S., Sandu, C., and Taheri, S. (2014). "Development and implementation of a hybrid soft soil tire model (HSSTM)." Presented at the 18th International Conference of the ISTVS, Seoul, Korea.

43. Naranjo, S., Sandu, C., Taheri, Sa., and Taheri, Sh. (2014). "Experimental testing of an off-road instrumented tire on soft soil." *Journal of Terramechanics*, *56*, pp. 119–137, Elsevier, Amsterdam, Netherlands.

44. Day, T.D. (2005). *Simulation of tire interaction with curbs and irregular terrain*, WP-2005-6, Engineering Dynamics Corporation, Beaverton, OR.

45. Bekker, M.G. (1969). *Introduction to terrain-vehicle systems*, University of Michigan Press, Ann Arbor, MI.

46. Fukushima, T., Shitamichi, M., Torigaki, T., Sokusai, H., Nishi, M., and Miyachi, T. (2013). "Parameter identification of sled test method to simulate vehicle soil trip rollover dynamic accurately by numerical simulation considering soil-vehicle interaction." *SAE International Journal of Transportation Safety*, *1*(2), pp. 334–351, SAE International, Warrendale, PA.

47. Graham, J. (2011). *Median cross-section design for rural divided highways*, NCHRP 22-21, Transportation Research Board, Washington, DC.

48. Hu, P.S. and Reuscher, T.R. (2004). *Summary of travel trends: 2001 national household travel survey*, U.S. Department of Transportation, Washington, DC.

49. AASHTO. (2011). *A policy on geometric design of highways and streets*, 6th Edition, American Association of State Highway and Transportation Officials, Washington, DC.

50. AASHTO. (2016). *Manual for Assessing Roadside Safety Hardware*, American Association of State Highway and Transportation Officials, Washington, DC.

51. Kan, S. (2011). *Development of guidance for the selection, use, and maintenance of cable barrier systems*, NCHRP 22-25, Transportation Research Board, Washington, DC.

52. Segal, D.J. (1976). *Highway vehicle object simulation model—1976 engineering manual - analysis*, Report No. FHWA-RD-76-164, Federal Highway Administration, Washington, DC.

53. NHTSA. (2008). *Traffic safety facts: 2007 data*, DOT HS 810 993, National Center for Statistics and Analysis, Washington, DC.

54. FHWA. (2001). *Roadway shoulder rumble strips*, Technical Advisory T 5040.35, Federal Highway Administration, Washington, DC.

55. Ho, C. and Spence, C. (2008). *The multisensory drivers: implications for ergonomic car interface design*, CRC Press, Boca Raton, FL.

56. NHTSA. (2009). *FARS Analytic Reference Guide, 1975 to 2008*, U.S. Department of Transportation, Washington, DC.

57. NHTSA. (2008). *2007 FARS Coding and Validation Manual*, U.S. Department of Transportation, Washington, DC.

58. Mak, K.K., Sicking, D.L., Coon, B.A., and de Albuquerque, F.D.B. (2009). *Identification of vehicle impact conditions associated with serious ran-off-road crashes*, NCHRP 17-22, Transportation Research Board, Washington, DC.

59. Ferdous, M.R. (2011). *Placement of traffic barriers on roadside and median slopes*, Doctoral dissertation, Texas A&M University, College Station, TX.

60. Ross Jr., H.E. and Post, R.E. (1972). *Comparisons of full-scale embankment tests with computer simulations—Volume One, test results and comparisons*, Report No. 140-7, Texas Transportation Institute, College Station, TX.

61. Weaver, G.D., Marquis, E.L., and Luedecke Jr., A.R. (1971). *Vehicle dynamics on roadway slopes*, Report No. 626A-1, Texas Transportation Institute, College Station, TX.

62. Ross, Jr., H.E. and Post, E.R. (1975). *Dynamic behavior of an automobile traversing selected curbs and medians*, Report No. 140-6, Texas Transportation Institute, College Station, TX.

63. Mak, K.K. and Mason, R.L. (1980). *Accident analysis—breakaway and nonbreakaway poles including sign and light standards along highways. Volume II: Technical Report*, Southwest Research Institute, San Antonio, TX.

64. Grimes, W.D., Balasa, J.A., and Hunter, E.J. (2006). *Analyzing the trip-phase of soft-soil rollovers*. Technical Paper 2006-01-1558, Society of Automotive Engineers World Congress & Exhibition, Warrendale, PA.

65. Abu-Odeh, A, Sadeq, M., Masad, E., Reddy Geedipally, S., and Ko, M. (2017). *Experimental and analytical investigation of the performance of SUV and balloon tires commonly used in Qatar*, Transportation Research Board, Washington, DC.

66. Forkenbrock, G.J., O'Harra, B.C., and Elsasser, D. (2004). *A demonstration of the dynamic tests developed for NHTSA's NCAP rollover rating system—phase VIII of NHTSA's light vehicle rollover research program*, DOT HS 809 705, National Highway Traffic Safety Administration, Washington, DC.

67. 4N6XPRT Systems. (n.d.). "Expert AutoStats." (Website). Available online: http://www.4n6xprt.com/4n6as/, last accessed July 4, 2020.

68. van Schalkwyk, I. and Washington, S.P. (2008). *Cost effective safety improvements on two-lane rural state roads in Washington State*, Report No. WA-RD 695.1, Washington State Department of Transportation, Olympia, WA.

69. Karayiannis, N.B. and Venetsanopoulos, A.N. (1993). "Neural network architectures and learning schemes." *Artificial Neural Networks* in the International Series in Engineering and Computer Science, *209*, Springer, Boston, MA.

70. Karayiannis, N.B. and Venetsanopoulos, A.N. (1993). "Introduction." *Artificial Neural Networks* in the International Series in Engineering and Computer Science, Springer, Boston, MA.

71. Nielsen, M. (2015). "Chapter 1: Using neural nets to recognize handwritten digits." *Neural Networks and Deep Learning*, Determination Press. Available online: http://neuralnetworksanddeeplearning.com/chap1.html, last accessed July 4, 2020.

72. Metropolis, N. and Ulam, S. (1949). "The Monte Carlo Method." *Journal of the American Statistical Association*, *44*(247), pp. 335–341, Taylor and Francis, Oxfordshire, UK.

73. Fishman, G.S. (1996). "Introduction." *Monte Carlo: Concepts, Algorithms, and Applications* in the Springer Series in Operations Research, Springer, New York, NY.

74. Stander, N., Roux, W., Goel, T., Eggleston, T., and Craig, K. (2010). *LS-OPT user's manual version 4.1*, Livermore Software Technology Corporation, Livermore, CA.